CRANFIELD INSTITUTE OF TECHNOLOGY

SCHOOL OF MECHANICAL ENGINEERING

PhD THESIS

Academic Year 1990-1991

D NIKANPOUR

Annular Flow Enhanced Two-Phase Evaporative Heat Exchanger for Space-Based Systems.

Supervisor: Professor P O'Callaghan

December 1991

ABSTRACT

The development of multi-kilowatt space-based systems requires the transport of waste heat loads over long distances in micro-gravity conditions.
In this context two-phase heat transport systems are attractive enabling a high rate of heat transport with low pump powers compared to single phase systems.

In this context the design of a two-phase heat exchanger to transfer heat from a single-phase fluid (water) to a two-phase fluid (Freon 114) is discussed.

Until reliable micro-gravity ($< 10^{-3}g$) test data on the heat transfer and pressure drop in a two-phase flows are available, it is deemed necessary that the design of heat exchangers' passages should promote gravity-independent flow regimes. This would make the design and test data, obtained at ground conditions, applicable in micro-gravity environments.

The design concept investigated hinges on utilising a set of **helical** flow passages (with small cross sectional area) to ensure a predictable flow regime, **annular** flow, up to high vapour qualities (>0.8), in both micro-gravity and one 'g' environments.

The concept was applied to the design of a 5kW helically coiled evaporative heat exchanger for space-based systems, which was subsequently manufactured and tested. Ground tests gave results close to analytical predictions based on computer simulations of the heat transfer and pressure drops in helical flow passages.

Finally design guideline for a two-phase evaporative heat exchanger for space-based systems is provided, along with conclusions and areas to be further researched.

CONTENTS

ACKNOWLEDGEMENTS

NOMENCLATURE

LIST OF FIGURES
LIST OF PLATES
LIST OF TABLES

ACKNOWLEDGEMENTS

I would like to thank the European Space Agency, BAe, and AIT for funding and supporting this study.

Moreover many thanks to my internal and external supervisors Dr.P. O'Callaghan of School of Mechanical Engineering at CIT, and Dr. F. Astrabadi of Aerospace Consultants. Their many useful suggestions, guidance and help during the course of the work was invaluable and much appreciated.
Finally my sincere thanks to all SME faculty and staff members.

NOMENCLATURE

$a = \frac{k}{\rho c}$ thermal diffusivity (m^2/s)

A = cross sectional area (m^2)

B = wall thickness (m)

c = constant pressure specific heat (kJ/kg K)

d = duct hydraulic diameter (m)

D = coil diameter (m)

E_1 = constant used

E_2 = constant used

f = friction factor

g = acceleration due to gravity (m/s^2)

$G = \frac{Q}{A}$ = mass velocity (kg/sm^2)

h = heat transfer coefficient (W/m^2K)

H_i = constant used

L = length of Freon duct (m)

k = thermal conductivity (W/m K)

p = pressure (N/m^2)

pe = permeability (cc cm/cm^2)

q = rate of heat flow (W)

$\dot{q}_c$ = critical heat flux (W/m^2)

Q = mass flow rate (kg/s)

R = thermal resistance per unit length (m K/W)

s = fin thickness (m)

S = suppression factor used in Chen correlation (Tab. 4.4)

SR = slip ratio

T = temperature (°C)

u = mean velocity (m/s)

v = specific volume (m^3/kg)

$x = \frac{Q_g}{Q}$ vapour mass quality

X = Martinelli parameter

$$X = \frac{\left[\frac{dp}{dL}\right]_{liq}}{\left[\frac{dp}{dL}\right]_{g}}$$

where $\left[\frac{dp}{dL}\right]$ is the variation of pressure with the duct length

liq: signifies liquid

g: signifies gas/vapour phase

z = Duct axial co-ordinate

GREEK LETTERS

$\alpha = \frac{A_g}{A}$ = void fraction

β = ratio of gas volume to total volume flow

μ = absolute viscosity (kg/ms)

ν = kinematic viscosity (m^2/s)

ρ = density (kg/m^3)

ϕ^2_f = two-phase frictional multiplier based on pressure gradient for liquid flow

ψ = parameter used in Merilo (ref.50) correlation

λ = latent heat of vaporization (J/kg)

σ = surface tension (N/m)

ΔT_{SAT} = difference between wall temperature and saturation temperature of Freon

ΔP_{SAT} = difference between saturation pressure corresponding to wall temperature and saturation pressure corresponding to bulk temperature of Freon.

ϑ = duct slope with respect to the horizontal

SUBSCRIPTS

a = acceleration

al = aluminum

c = coil

C = convection

f_L = liquid fraction

F = freon

i = corresponding to the ith point

Fr = friction

f_g = vapor fraction

NcB = nucleate boiling

s = straight duct

Sat = saturation

sub.cool = subcooled

TP = two-phase

∞ = external air

t = turbulent

w = wall

w = water

z = static head

SUPERSCRIPTS

i = inlet

e = exit

DIMENSIONLESS NUMBERS

$Fr = \frac{u^2}{gd} = \frac{G^2 v^2}{gd}$ Froud number

$Nu = \frac{hd}{k}$ Nusselt number

$Pr = \frac{\nu}{a} = \frac{\mu c}{k}$ Prandtl number

$Re = \frac{ud}{\nu} = \frac{Gd}{\mu}$ Reynolds number

$We = \frac{G^2 d}{\sigma \varrho}$ Weber number

$D_N = Re(\frac{d}{D})^{\frac{1}{2}}$ Dean number

LIST OF FIGURES

Freon mass flow rate (error bars indicated)

110 Figure 10.2 Variation of pressure drop with Freon mass flow rate (error bars indicated)

LIST OF PLATES

LIST OF TABLES

1.0 INTRODUCTION

The thermal control of low power satellites has been achieved predominantly by conducting the on board heat to a set of radiators; and heat rejection is achieved by passive radiative cooling.
The development of multi-kilowatt space-based systems however requires the transport of waste heat loads over long distances in micro-gravity conditions.

Micro-gravity environment, in the context of space-based systems, can be defined as the on-orbit space environment, where the acceleration levels are less than 10^{-3} times the acceleration levels found on-ground.

Pumped single-phase heat transport systems has become the principal method of high power spacecraft thermal management since the days of the Gemini program (ref.1) to Spacelab and the US Space Shuttle programs. These conventional fluid loop systems transport heat from heat sources to heat sink devices.

As mass and power are at a premium in space-based systems, use of conventional single-phase mechanically pumped fluid loop systems has one major disadvantage. With a continuing demand for larger heat loads to be handled from heat sources to heat sinks, the required mass flow rate must be increased, therefore there is a need for bigger pumps with an unacceptable level of pumping power, mass and noise for space-based systems.

Moreover these types of single-phase systems are designed for a specific combination of instrumentation with a pre-determined thermal load. Therefore, in order to accommodate even smaller changes in the heat load, significant design modifications are required.

Future space platforms will require heat rejection systems that are capable of transporting heat from a widely diversified group of multi-disciplinary instrumentation, and require to be maintained within a narrow isothermal bandwidth. The instrumentation will have a broad spectrum of heat loads, where combined loads will fluctuate as the usage varies. In addition, the physical location of the instruments, during its operational life, may be changed (by up to tens of meters) during on-orbit maintenance and servicing.

Current activities on alternative solutions include the development of super multi-kilowatt heat pipes (ref.2) and research on new conjugating binary mixtures where the specific heat of the working fluid is increased in the operating temperature range, (ref.3).

The interactive effects of on board instrumentation and payloads, with varying heat loads, sharing a common liquid coolant loop can be reduced significantly through the use of a two-phase heat transport system. As a result two-phase systems are capable of removing much larger quantities of heat per unit mass of fluid. In addition they are capable of maintaining a narrow isothermal bandwidth close to the saturation temperature with a small flow rate, hence low mass and power.

In this context two-phase heat transport systems offer an alternative solution enabling a high rate of heat transport with lower pump powers compared with single-phase systems, as well as enabling nearly isothermal operation. These systems take advantage of the large latent heat of vaporization of the working fluid. The fluid evaporates at the heat source by use of equipment mounted cold plates or transferred from another fluid system by use of a dedicated heat exchanger. The vapour is then transported to the heat sink (space radiator), where it is condensed, and the resulting liquid is pumped back, flowing again to the heat sources in a closed cycle.

The total system, or thermal utility as is commonly termed is made-up of three principal elements. The first is a group of heat collecting interfacing devices such as cold plates and heat exchangers which provide a means of vaporization of the working fluid. The second is a system referred to as a thermal bus, capable of transporting excess heat to the third element which constitutes the space radiators.
The thermal bus consists of a two-phase fluid loop and a pumping system. The pump size is determined by the power required to overcome the total frictional pressure drop in the system.

Figure 1.1 Schematic of two-phase fluid loop systems [ref.1]

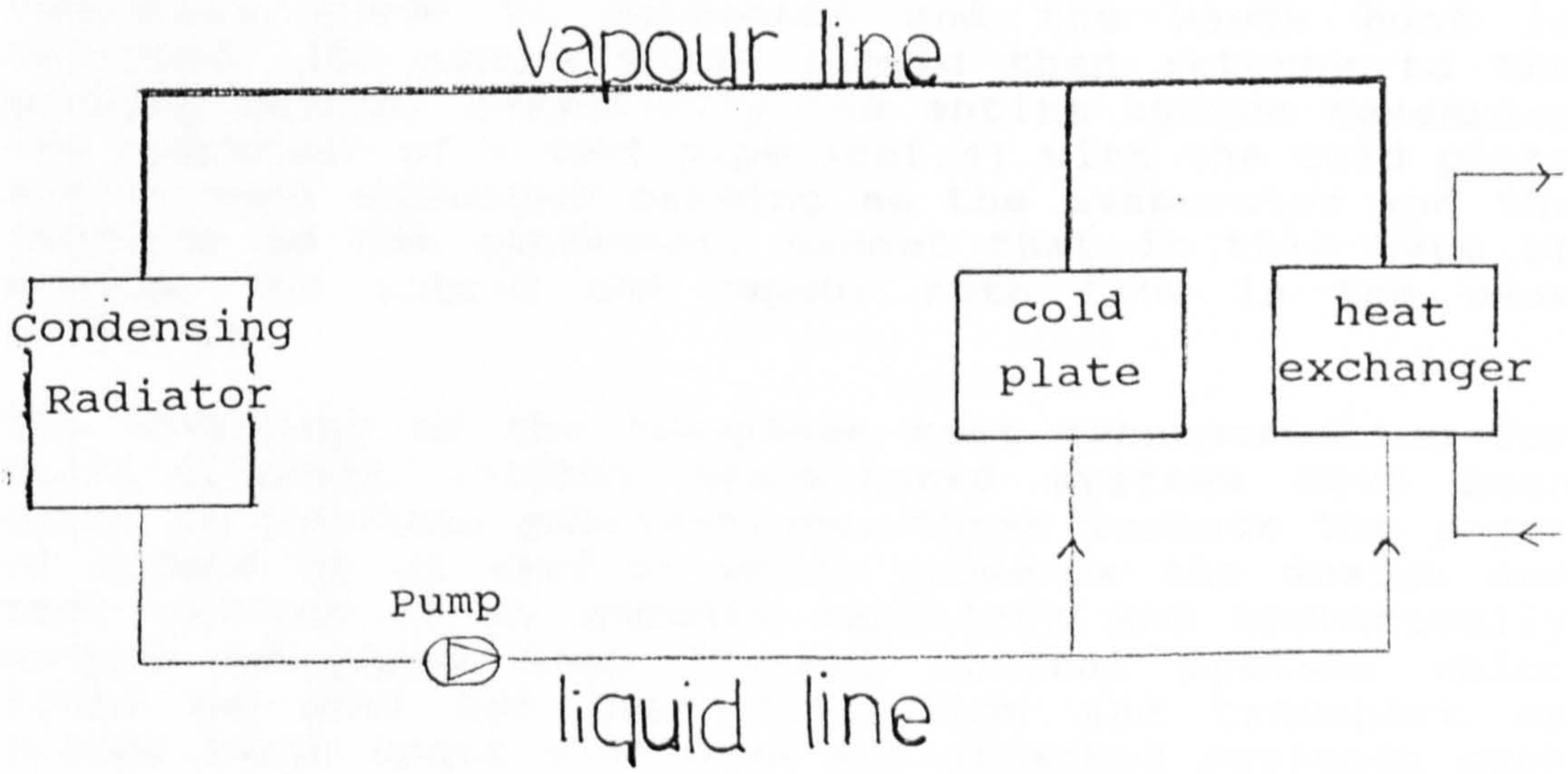

Schematically the fluid loop network shown in Fig. 1.1, indicates the working fluid leaving the pump as saturated liquid and proceeds to the cold plate / heat exchanger which vaporizes the fluid at nearly isothermal conditions, from this point onwards the fluid (liquid-vapour mixture) flows through a set of space radiators where it condenses and the waste heat is rejected. The single-phase liquid then returns to the pumping device. Essentially the entire system resembles the operation of a heat pipe (ref.4) with the cold plate and/or heat exchanger serving as the evaporator and the radiator as the condenser, except that in this type of system, the liquid and vapour both flow in the same direction.

The advantage of the two-phase heat transportation for multi-kilowatt (>10kW) space-based systems have been cited in previous publications. These include the paper of McCabe et al (ref.5) which presents the design and test results of an ammonia capillary and mechanically pumped two-phase loop thermal control systems which could be used for heat collection and transport on future large space platforms and attached payloads such as those of NASA space station. The system consisted of an evaporative section, a condenser section, liquid and vapour transport lines, a mechanical pump and a reservoir. In the evaporator heat was applied to three parallel cold plates which cooled the payload instruments or electronic equipments. Breadboard tests have shown that the cold plate evaporators could also be employed in a capillary pumping mode, when heat was applied to the evaporator, liquid evaporated from a saturated porous (polyethylene) wick connected to the supply reservoir.

Earth based two-phase systems normally rely on gravitational forces in various components to orient the liquid/vapour interfaces. Operation of two-phase systems in the micro-gravity environment of space, where acceleration levels due to gravity are less than 10^{-3} g, will require that other forces (surface tension, centrifugal etc.) be used for liquid/vapour control. Additionally, boiling system behaviour may be radically different under some low gravity conditions, since buoyancy forces are not available to separate the vapour/liquid components.

The study of boiling behaviour under low gravity conditions has been limited to the short time scales available in drop towers with micro 'g' (less than 10^{-3} g) simulation times of less than 5 seconds, and aircraft Keplarian trajectories with times of less than

30 seconds. These time scales however, are not sufficient, under many circumstances, to allow the system to come to steady-state conditions.

Utilization of the Space Shuttle (or future space-vehicles or space stations) for two-phase, low gravity experimentation can assure that steady-state conditions are obtained, and two-phase flow and heat transfer data could be gathered under realistic micro 'g' conditions.

But until such times when consistent and reliable data in micro 'g' two-phase flow boiling become available, the design of such heat exchangers need to be conceived in such ways as to reduce the impact of gravity on its operation. This involves heat exchanger designs which tend to promote a specific internal flow conditions which would then allow performance predictions to be made with a high level of confidence in micro 'g' conditions compared with test data obtained on ground.

Liquid/vapour control experiments under low gravity conditions have been performed for specific applications. Tegart and Kirkland (ref.6) have demonstrated propellant re-supply techniques using Space Shuttle middeck experiments. Screens, wicks and porous plates were successfully used to control the location of the liquid/vapour interface position within a transparent mockup of a propellant tank. Experimentation showed the effectiveness of using these devices to ensure that 100% of the liquid exited the tank in micro 'g' conditions.

Experiments carried out on-board aircraft flying Keplarian trajectories examined the condensing characteristics of non-wetting mercury under low-gravity conditions. Namkoong et al.(ref.7) photographically investigated the condensing phenomena under both one 'g' and zero 'g' conditions and concluded that the flow phenomena were similar for small tubes (0.69cm in diameter) while larger diameter tubes (1.0cm and 1.24cm) showed influences of gravity on flow patterns. Williams (ref.8) also investigated condensing characteristics under low 'g' conditions during parabolic aircraft flights. The experiment used Refrigerant-12 flowing in transparent, uniform diameter test sections to visualize the flow. Stable operating conditions were obtained under all flow conditions examined. Ground test data were also used to verify a pressure drop predictive method based on the Martinelli (ref.9) technique.

Separation processes under earth gravity conditions normally use drains, sumps, etc,. Other forces such as surface tension, centrifugal or viscous forces must be utilized in space operation systems. Both ground tests

and low gravity aircraft tests have been conducted in order to examined space-design separator systems, (ref.10). These systems demonstrated excellent separation efficiencies in ground tests (>95%) but performed poorly under low gravity conditions. Further low gravity testing will be necessary to develop operational liquid/vapour separators.

A very limited number of low gravity boiling experiments have been performed, and most of these were based on drop tower facilities, with a limited low gravity times of less than 5 seconds. Siegel (ref.11) has summarised (up to 1967) pool boiling experiments under low gravity conditions and the main conclusions were that: the lower bound on pool boiling critical heat flux behaviour is proportional to $g^{1/4}$, nucleate pool boiling heat transfer appears to be unaffected by zero gravity conditions, since local bubble actions near the heated surface dominates the behaviour, transition boiling is unaffected by zero gravity conditions, and the maximum film boiling heat flux point is proportional to $g^{1/4}$.

More recent pool boiling experiments by Weinzier (ref.12) were performed during rocket flights, with low gravity times of over 300 seconds. These nucleate boiling experiments confirmed the earlier conclusions regarding nucleate boiling, and also confirmed that the onset of nucleate boiling occurs at both lower heat fluxes and temperatures than found under ground conditions.

To date very little information is available regarding forced convection low-gravity boiling behaviour. By examining both upflow and downflow experiments, Seigel (ref.13) suggested that a flow velocity exists above which gravitational effects are negligible. Cochran (ref.14) conducted drop tower tests examining bubble characteristics under forced convection conditions. He noted that the the bubbles tended to form a boundary layer surrounding the heated surface. Formation of a bubble layer could be expected to substantially reduce the surface heat transfer under low gravity conditions. Fluid velocities during these tests were up to 11.5 cm/s.

Otsuji and Kurosawa (ref.15) have recently examined the critical heat flux behaviour of Freon 113 under oscillating accelerations varying from one 'g' to -0.5 'g', their results indicated that the $g^{1/4}$ criteria gave a reasonable lower bound on the critical heat flux behaviour when flow oscillations were not present.

Successful prediction of the heat and mass transfer rates of two-phase thermal control systems hinges on the ability to identify the system flow regime. The flow regime is characterized by the two-phase fluid distribution within the flow tube. Figure 1.2 shows various two-phase flow regimes possible in a horizontal heated tube in a one 'g' field. The flow at the entrance to the tube is one of single-phase; as the fluid bulk temperature increases towards its saturation point, bubbles begin to form at nucleation sites on the tube wall which are carried into the main stream, this flow regime is typically termed 'bubbly flow'. As the vapour volume fraction increases, the individual bubbles begin to agglomerate and form plugs and slugs of vapour as shown in Fig. 1.2. The plugs of vapour are compressible volumes which produce flow oscillations within the tube even if the entering flow is steady. While both the bubbly and slug-flow regimes are interesting, it is noted that the vapour quality associated with these two regimes is low.
As the fluid flows further along in the tube and the vapour quality increases, the vapour plugs coalesce at the middle and upper portion of the tube with liquid and entrained bubbles in the other parts of the tube, referred to as 'wavy flow'.
With a further increase in quality most of the liquid layer is gathered around the periphery and bottom of the tube, 'annular flow regime' with vapour flowing through the center. In this flow regime the vapour is generated primarily by vapourization from the liquid-vapour interface inside the tube.
As the evaporation process continues at the liquid-vapour interface, a point is reached where a small dry spot forms suddenly at the wall and grows in all directions, as the adjacent liquid layer vaporizes due to conduction heat transfer through the liquid, this is referred to as 'local dryout' and characterised with a sharp drop in rate of heat transfer.

The interaction among various parameters namely total mass flow rate, vapour mass fraction (quality), liquid/vapour density and viscosity, tube diameter, tube acceleration field, fluid surface tension, tube inner wall roughness, and tube inclination all determine which regime is present.

Figure 1.2 Two-Phase flow regimes (1g) in a horizontal tube.

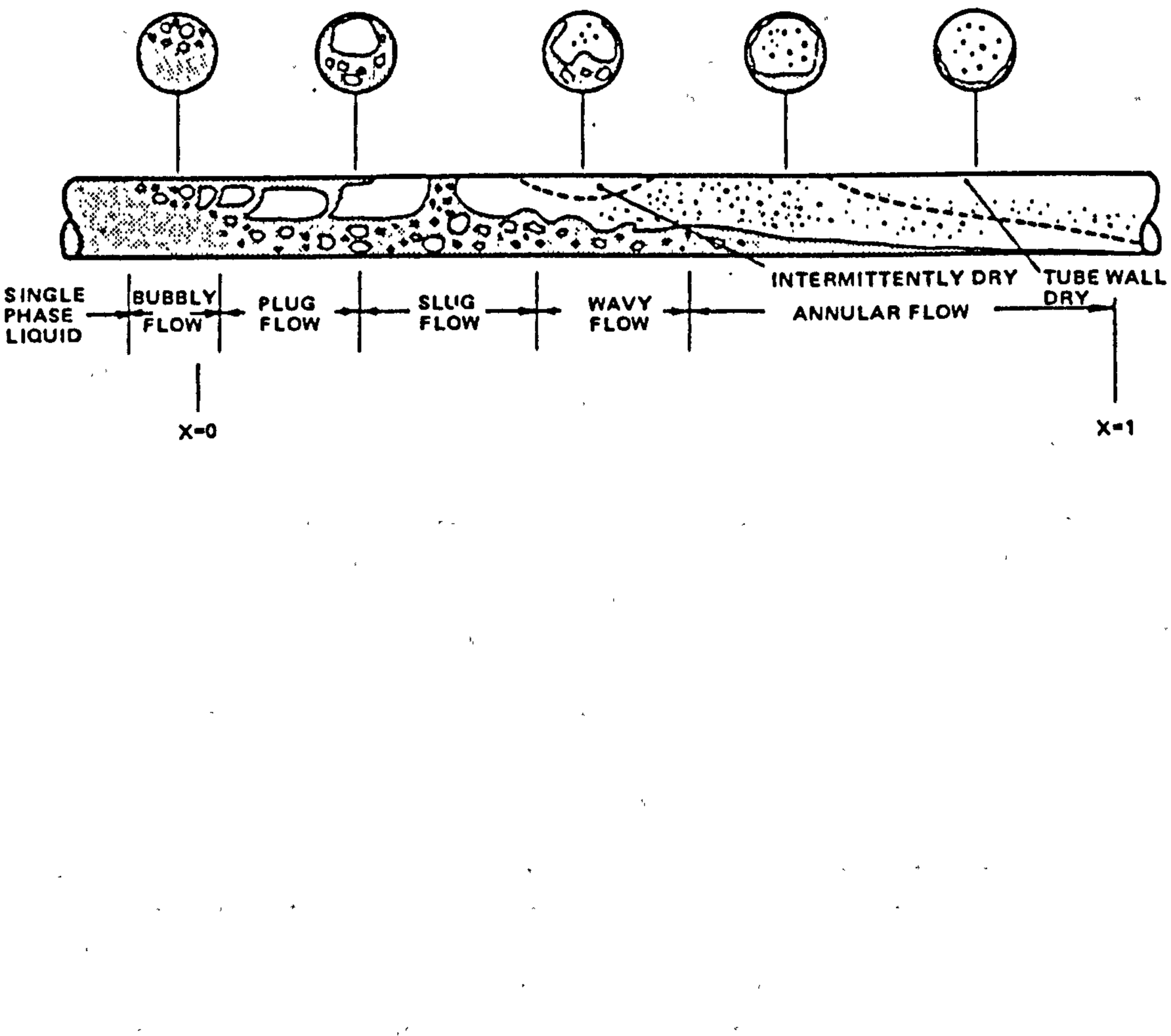

Although one 'g' test data are available there is a scarcity of micro-gravity test data. It is therefore desirable to promote in the design of two-phase systems and equipments a flow regime (such as annular flow) which would occur in both micro-gravity environment as on ground. This approach can provide an inherent degree of confidence in ground design analysis and performance predictions.

The overall pressure drop of space-based thermal control systems can be directly translated into required power input to the circulating pump. The pump power directly impacts the overall total system power requirements, which also needs to be launched, the pump power therefore is an important contributor to the launch mass of such systems. Although the pressure drops of the two-phase system will be a fraction of the equivalent single-phase loop, its prediction is important to evaluate its mass impact.

Dukler et al (ref.17) summarised the pressure drop that results from the flow of a two-phase fluid through a circular duct. They classified the methods of evaluation into three categories: empirical correlations, equations of motion and mathematical analysis of simplified physical models with equations that relate the variables.
Of these the most common are those utilizing empirical correlations which can be further categorized into two groups: those derived on the basis of horizontal flow (ref.18), and those resulting from vertical flow data (ref.19).
The reliability of these relationships has been proven when they are used within the range over which the data were collected. However when they are used beyond that range the reliability is poor. Levy (ref.20) has presented a solution using the equation of motion, but the most accurate solutions are those resulting from the mathematical analysis of a simplified physical model (ref.21). Knowledge of the pressure drop resulting from the phase interactions is based primarily on experimental evidence and is largely dependent upon the void fraction and hence flow regime. But again there are open questions regarding the actual flow regime that will occur in two-phase systems in zero gravity environment.
In one 'g' environment it has been shown that as the fluid flows through the cold plate / heat exchanger the mode of flow slowly changes from bubble flow to annular flow, to slug flow, and in cases of high heat loads to total vapour flow (ref.22).

In micro 'g' or zero 'g' environments however, the type of flow would not necessarily follow this pattern. In micro 'g' environment, the surface tension, a force which is largely neglected in one 'g' becomes one of the dominant forces and hence in the absence of launch acceleration loads, and on-orbit perturbations, provided the local dryout can be avoided, annular flow could be the dominant flow regime, and the pressure drop can be most accurately predicted using one of the annular flow models.

Flow similarity between micro-gravity and one 'g' conditions can be encouraged using small diameter helical flow passages. In a one 'g' environment, condensation tends to form a puddle in the bottom of a horizontal tube creating a stratified flow (gas flowing above a liquid layer). This puddling must be minimized to make the one 'g' evaporator or condenser similar in flow regime to that experienced in a micro-gravity field, ref.(23).

A two-phase flow through a helical coil can exhibit a variety of phase distributions. The flow patterns are a function of mass velocity and density ratio in normal gravity field. Annular flow exists for a liquid with a large liquid to vapour density ratio and a low mass velocity. In annular flow regime a secondary flow in the vapour core causes a circulation pattern in the liquid film. At moderate values of radial acceleration, the liquid will form a continuous layer around the tube wall (ref.24 and 31). A helical flow path, can therefore be used to create similar evaporator and condenser flow regimes in micro gravity environment as on ground environment.

Within the framework of a technology study, issued by the European Space Agency (ESA), on mechanically pumped two phase heat transport systems a two phase flow technology development model was conceived (ref.25). This allowed investigation of two-phase fluid loop critical components and in particular the design drivers for a two-phase evaporative heat exchanger for space-based systems.

In the context of exploring the technologies and the design of critical components for two-phase heat transport systems, a mechanically pumped two-phase heat transportation system for thermal control of a future European Space Station was selected for further investigation. A schematic of such a loop is given in Fig.1.3.

The main specifications for such a system are summarised below:

- To provide a heat collection, transport and rejection capability of 10-20kW
- Utilise Freon 114 as the working fluid
- To provide nearly isothermal sink temperature of 20°C at user interfaces
- Maximum vapour quality of 0.8
- Parallel arrangement of evaporators and condensers.

Figure 1.3 Reference Configuration of a two phase mechanically pumped heat transport system.

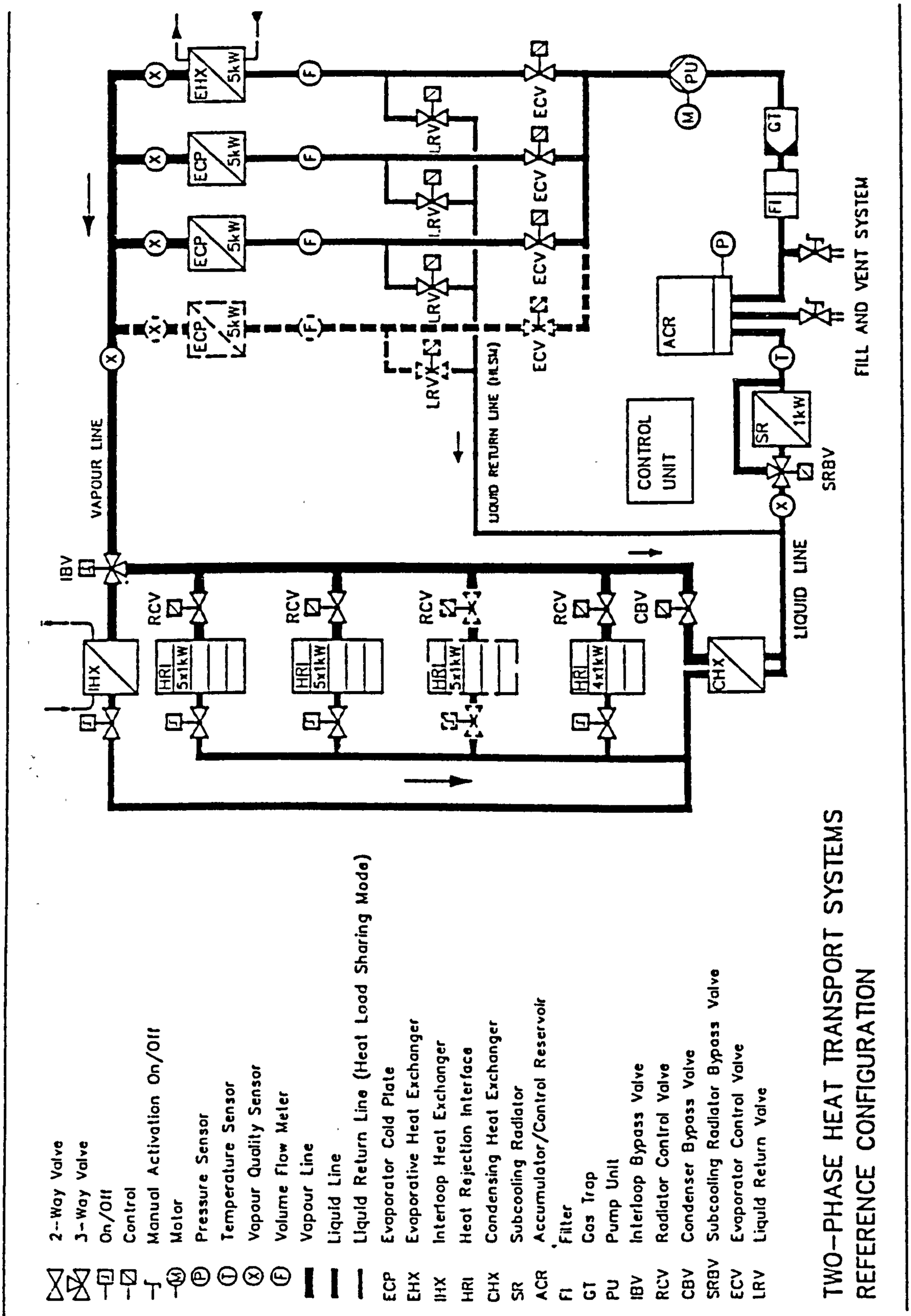

The above reference configuration included several critical components which were required to be specifically developed for zero 'g' operation. In these cases, either no clear design concepts existed or there were serious development risks associated with the components. These components are summarised below:

- Heat Collection Devices: Evaporative Cold Plates
- Heat Transfer Devices: Evaporative Heat Exchangers
- Sensors: Vapour quality Sensors
- Control devices: Fluid Accumulator/control Reservoir Control System
- Safety Devices: Gas Trap

Although the scope of this thesis is mainly the conceptual design and development of a two-phase evaporative heat exchanger, the chosen design concept of other critical components in the rest of the system, in order to have a functional loop, is briefly described below. A summary of the main technical characteristics of these components along with a schematic of the working principle is given in Appendix (D).

Heat Collection Device

The heat collection from the payload or electronic equipments is achieved by use of an evaporative cold plate on which the equipment is directly mounted.
The minimum thermal resistance is the contact conductance between the equipment and the cold plate, (ref.26). Heat is transferred into the working fluid Freon 114, evaporating it as it passes through the cold plate. A schematic of the working principle of an evaporative cold plate is shown in Appendix (D).

Heat Transfer Device

The evaporative heat exchanger as a heat transfer device, transfers heat from a single-phase pumped water loop system to an evaporating two-phase Freon loop. The design concept and internal structure of the evaporative heat exchanger is treated later on, in the main body of the thesis.

Vapour Quality Sensors

The purpose of a vapour quality sensor is linked to the flow regulation valves upstream of the cold plates to avoid the formation of superheated vapour and dryout of the capillary wick material inside the cold plate.
The vapour quality concept is based on an axial capacitor, which when properly calibrated (from measurement of the capacitance across the two-phase fluid), it is possible to derive the total void fraction and hence vapour quality of the fluid.
For proper performance, the concept relies on an annular flow regime inside the sensor. At high vapour qualities (greater than 0.4) this flow pattern dominates under micro-gravity conditions and in downward moving two-phase flow on earth. A schematic of a vapour quality sensor is shown in Appendix (D).

Heat Rejection Interfaces

The heat rejection interface/condenser is designed to be thermally coupled to a space radiator panel via heat pipes and each is able to reject 1kW.
A schematic of the heat rejection interface is shown in Appendix (D).

Accumulator/control Reservoir

The accumulator, which is placed upstream of the pump, is a variable volume reservoir flowed through by R114. Its function is twofold: one is to compensate for possible leakages from the overall system and the other is to control the system pressure and hence system temperature levels, and control the rejection temperature of the space radiators by back-flooding of the condensers when necessary.
The reservoir is made of a stainless steel vessel including a metal bellows; its volume can be varied mechanically by an electromotor drive. The drive unit consists of a brushed DC-motor, gears, a re-circulating roller, and other small mechanical devices.
A schematic of the accumulator/control reservoir is shown in Appendix (D).

Gas trap

Coupled with the safety and reliability aspects of the two phase systems, there is a need to include a gas trap

and filter in the system. Its function is to filter the working fluid and keep it continuously free from contamination which may cause failures of the system particularly at the pump level through cavitation. Special emphasis is directed to trapping of non-condensable gases and water particles which may cause decomposition of the Freon.
The design solution is based on use of adsorption by zeolites in trapping both water and gases with the characteristics given in Appendix D .

Technology Development Model

Based on the reference configuration (Fig.1.3), a technology development model (TDM) was subsequently conceived (ref.27). The TDM represents the reference configuration but in a reduced form amenable to be integrated in a test bed, with testing and monitoring capabilities. Each of the above critical items were incorporated in the TDM, with parallel arrangement of evaporators (one cold plate and one evaporative heat exchanger) and condensers (two 1kW units supplemented by a single large commercial condenser) (see Fig.1.4).

The main specifications of the technology development model were:

Maximum Heat Load:	10kW
Working Fluid:	Freon 114
Operating Temperature Range:	0-25°C
Vapour Quality range:	0.4-0.8
Liquid Line Diameter & Length:	15mm, 24m
Vapour Line Diameter & length:	21mm, 17m

Figure 1.4 Technology Development Model Schematic

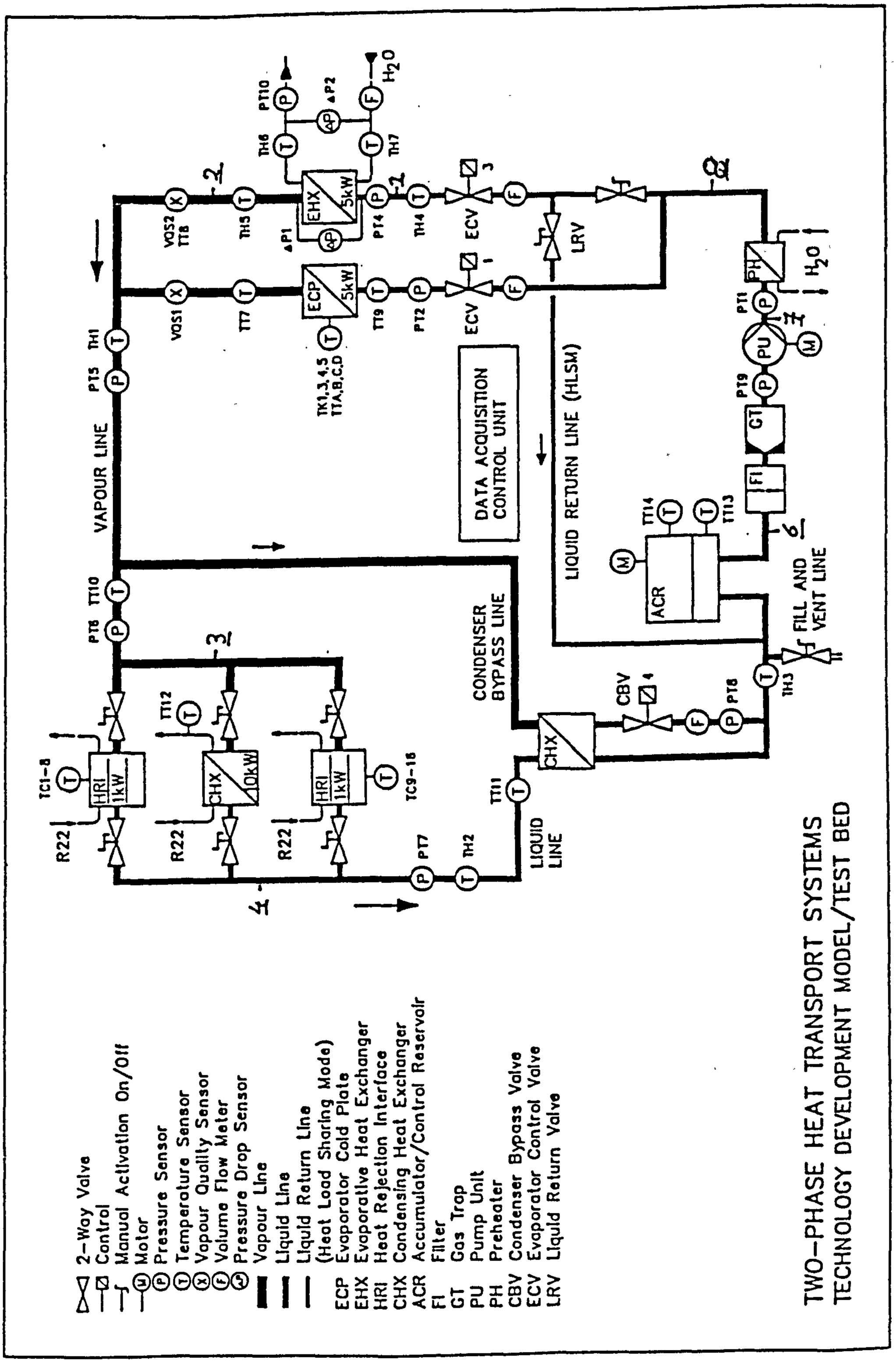

Description of the TDM LOOP

In order to investigate what the thermodynamic state of the Freon was in different zones of the TDM loop, the fluid condition was assessed with the aid of the pressure-enthalpy diagram for Freon 114 (see Fig.1.5).

The system considered was for the following case:

- Both the 5 kW cold plate and heat exchanger were active.

- Maximum vapour quality of 0.8 at cold plate and heat exchanger outlet.

- The heat rejection was accomplished by use of two 1kW heat rejection interface units, and an additional 13kW condensing heat exchanger in parallel, to provide the required subcooling.

- A maximum 10°C subcooling at the pump inlet.

- A variable speed control valve

- Control valves upstream of the evaporative heat exchanger and cold plates are used to control the flow of evaporant Freon 114 through them. This assures the outlet vapour quality set point to 0.6 ± 0.2 when a heat load is applied, either directly on the cold plate or transferred from the water loop across the Freon loop of the evaporative heat exchanger.

- When the dissipation is nill, the vapour quality sensor is still needed to detect this condition, and send measurement signals to the controller to initiate closure of the Freon 114 liquid feed lines.

Starting at a point (1) upstream of the heat exchanger, (Fig.1.4 & Fig.1.5), the fluid is 5°C subcooled at 210 kPa. With the aid of the flow control valve the heat exchanger outlet quality is controlled. The fluid enthalpy increases until the set outlet vapour quality is reached. Due to the pressure drop through the heat exchanger, there is an associated temperature drop at the exit of the exchanger; point 2 (Fig.1.5) is reached with a pressure of 200kPa and a temperature of 23°C. As the fluid flows through the vapour lines and subsequently the condenser, there is a decrease in enthalpy with associated pressure and temperature drops

(points 3 and 4 of Fig.1.5). Thereafter the fluid is subcooled further (point 5) prior to entering the accumulator which conditions the fluid prior to entering the pump. As the fluid enters the pump it is about 10°C subcooled at a pressure of 140kPa (point 6), it is then pumped up to 260kPa (point 7).
As it is necessary to raise the enthalpy of the fluid to have a 5°C subcooling at the inlet to the two-phase exchanger, a pre-heating single-phase heat exchanger was introduced upstream of the evaporator. The degree of heat input is then a function of the fluid temperature at the pump outlet, and the position of the flow control valve, hence the pressure drops, upstream of the heat exchanger, (points 8 and 1 of Fig.1.5).

A summary of the Freon 114 states can be found in Table 1-1.

Table 1-1 Freon 114 Thermodynamic properties corresponding to the points of Fig.1.5.

	Freon State Points							
	1	2	3	4	5	6	7	8
Pressure (kPa)	210	200	180	155	145	140	260	250
Temperature(°C)	20	23	20	16	5.5	5	5	20
Enthalpy (kJ/kg)	218	826	926	214	203	202	202	218
Vapour quality	--	0.8	0.82	--	--	--	--	--

Figure 1.5 Pressure Enthalpy Diagram (part) for Freon 114

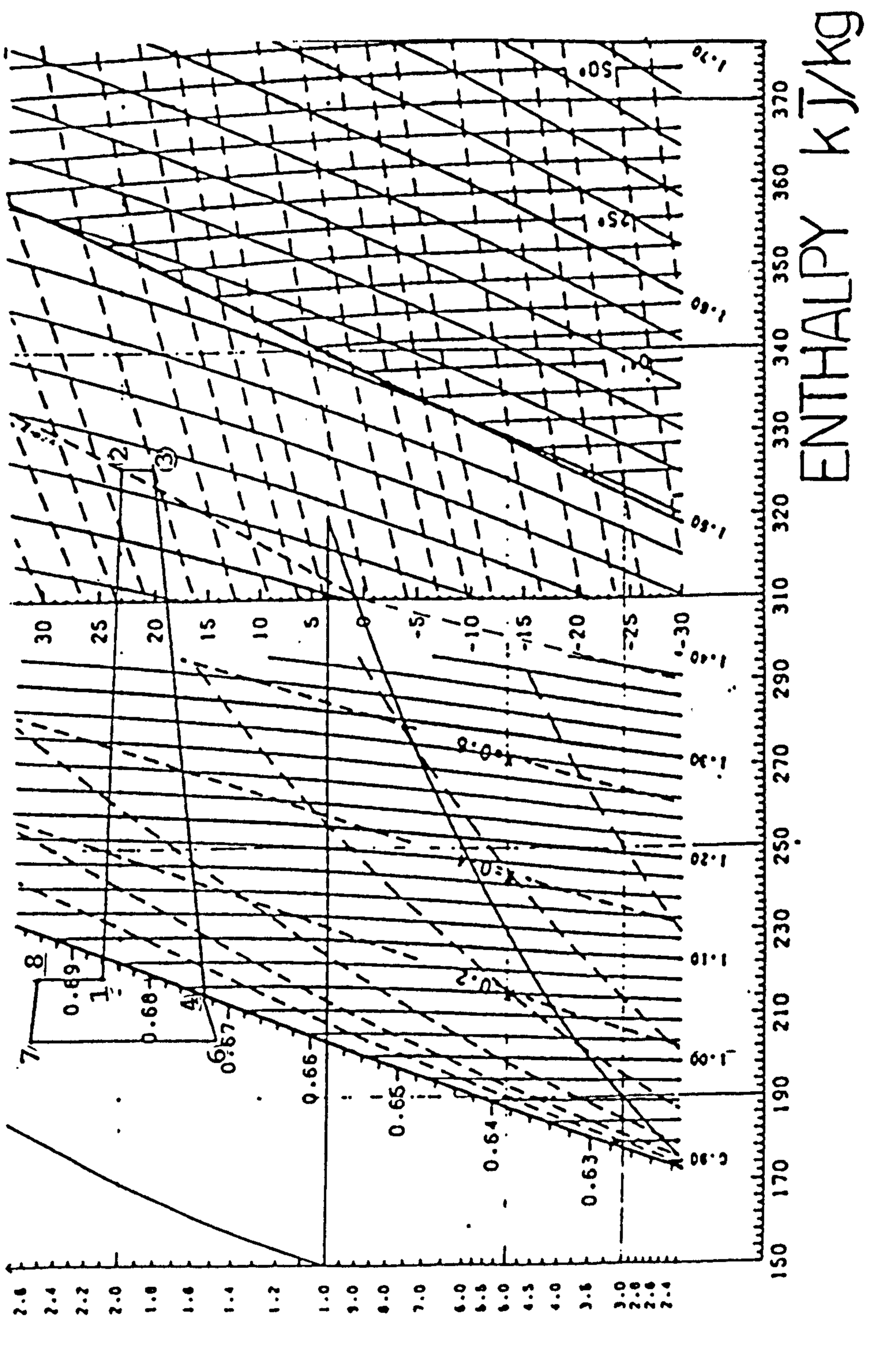

2.0 ANNULAR FLOW ENHANCED EVAPORATIVE HEAT EXCHANGE FOR MICRO-GRAVITY OPERATION.

The choice of an evaporative heat exchange design for zero or near zero 'g' operation was driven mainly by considerations concerning the boiling mechanism and the two-phase flow regimes in the absence of a gravity vector.

The different flow patterns (spatial distribution of the two-phase flow in a channel) were classified previously by Dukler et al (ref.28) into three different flow regimes; namely segregated (stratified, annular flow), intermittent (plug,slug flow) and distributed (drop and bubble-mist) flow regimes.

In most two-phase heat exchanger designs, the evaporant (at saturated or subcooled liquid conditions) enters a duct in which it is heated, progressively vapourizing it. Figure 2.1 shows a qualitative graph on which the heat transfer coefficient in the heated tube is plotted as a function of the local quality, for different flow regimes. The preference of operating in the annular flow regime is clear as it corresponds to the region with the highest heat transfer coefficients.

An experimental study on gas-liquid flow in micro-gravity conditions was performed by Heppner et al (ref.29) and the experiments with air and water in a straight tube of 2.54cm diameter with a length (L) to diameter (d) ratio of 20 were carried out on board a KC-125 aircraft flying parabolic trajectories. In these studies it was observed that annular flow regimes predominated. Other experimental work (ref.30) showed the presence of both annular flow as well as slug and bubble flow for a longer straight test section, having an L/d ratio of about 50. These works as well as others (referred to in the introduction) constitutes the sparse literature on this subject which deals with two-phase flow in the absence of a heat flux through the channel walls.

This condition is much different from that which occurs inside a two-phase heat exchanger in a zero 'g' environment.
On earth, boiling modifies the flow patterns that would exist in an unheated tube at the same local flow conditions, This is mainly due to additional forces generated by momentum transfer that is associated with mass transfer between the phases, and the departure from thermodynamic equilibrium. In micro-gravity conditions this is expected to be further modified. Vapour is

formed at the wall along a section of the evaporator duct, and the removal mechanism of the growing vapour bubbles from the surface is suppressed as there is no buoyancy force acting on them; the effects due to the inertia forces however remain. In the absence of experimental evidence, it might be postulated that the occurrence of dry-out at the wall, hence drop flow regime, could occur sooner in micro-gravity environment compared with one 'g' environment at the same flow conditions. The drop flow regime, characterized by liquid droplets in a vapour stream, results in a poor heat transfer due to the low heat transfer coefficient between the heated duct wall and the vapour.

Annular flow regime that allows higher heat transfer coefficients to be obtained at the wall, can be promoted in coiled duct geometries. The presence of the curvature induces a secondary flow in the fluid in the form of a double vortex which separates the phases (Fig.2.2).

In two-phase flows, the presence of secondary flow patterns in helically coiled tubes is now a well established phenomenon and has been confirmed by: experimental measurements of the heat transfer coefficients on the tube periphery, measurements of local velocities distributions inside the tube, as well as visual observations conducted by many investigators (see ref.24, 42 and 54).

Crain and Bell (ref.31) performed an experimental study on flow boiling (as opposed to pool boiling) of water in a helically coiled tube. The heat transfer coefficients, evaluated from temperature measurements at different circumferential positions at the exit of the tube (Fig. 2.2, 2.3 and 2.4), indicated the presence of a liquid film attached to the wall even at values of vapour quality beyond 0.8 (Fig.2.3).

The graphs of heat transfer coefficient against vapour quality (see Figs. 2.3 and 2.4), reflects the characteristic for a different fluid inlet condition.
Fig. 2.3 shows that, initially, the heat transfer coefficient at the 270° position is the highest, the 90° position is the lowest, with the 0° and 180° positions falling in between. Deteriorating heat transfer conditions exist for the full length of the tube with the steam quality increasing from 71% to about 86%. The heat transfer coefficients at the 270° position exhibit a more rapid decrease than the coefficients for the other three positions.
Fig.2.4 shows the heat transfer coefficients around the periphery of the tube with a flux density increase of a factor of 2.4 with respect to the tube conditions of

Fig. 2.3. The values of the coefficients are slightly higher due to the higher mass velocities. The graph shows that the heat transfer coefficients deteriorate with an increase in vapour quality up to 90%, at which point the coefficients at the 0° and 180° positions decreases rapidly, followed by the 270° heat transfer coefficient at a quality between 91% and 95%. The coefficient at the 90° position however exhibits an increase at the same point and continues up to the fully saturated vapour condition. This behaviour indicates the presence of water at the 90° position even at high vapour qualities. The data also indicates that dryout occurs first in the 0° and 180° positions and soon after at the 270° position.
The above experimental evidence is reinforced by visual flow observations (ref.24 and 31) where for high quality mixtures of air and water, the major portion of the liquid is concentrated in a relatively slow moving stream at the 90° position. Drops of liquid are entrained from this stream by the air and are deposited at the 270° position as fine droplets. The drops then spiral back to the 90° position as they move across the tube along the secondary flow paths.

As the centrifugal forces and the secondary flow paths are not present in straight tubes, there is no continuous wetting mechanism of the heated tube walls. This aspect has been experimentally established (ref.16) in which the dryout in heated straight tubes occurs much earlier than in coiled tubes.

A comparison of data for dryout in coiled and straight tubes is given in Fig.2.5, where there is a very large increase in the quality at dryout for a given heat flux level, in the case of the coil (compared to the straight tube). The temperature increase associated with dryout occurs first on the outer surface (position 270°) of the coil. A confirmation of the higher liquid film flows on the inside of the bend (position 90°) has also been obtained from tube peripheral flow rate measurements see Fig. 2.6, [ref.16].

Figure 2.1. Characteristics of forced-convection vaporization: heat transfer coefficient versus quality and type of flow regime.

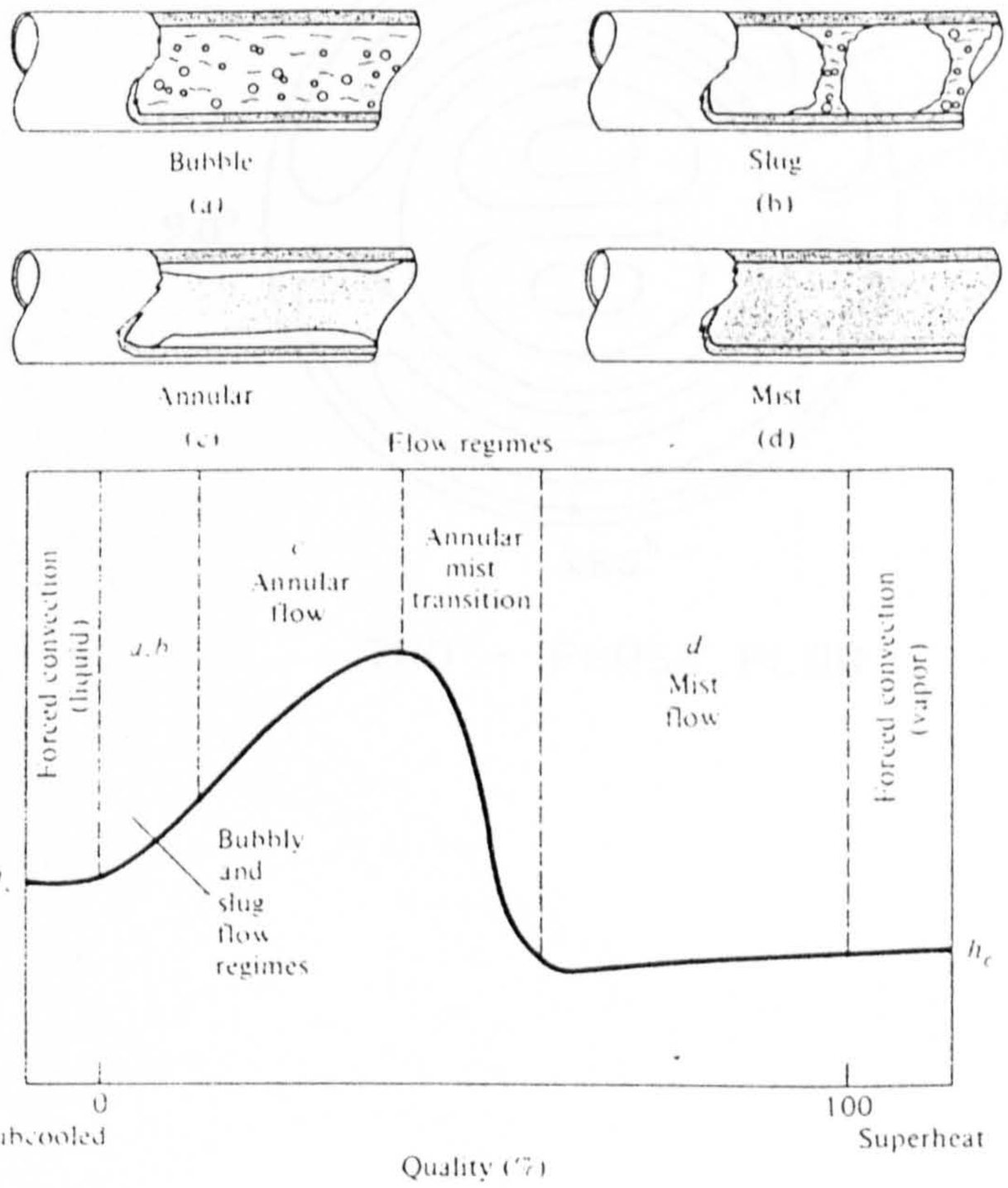

Figure 2.2. Secondary flow and measurement points, [ref.31].

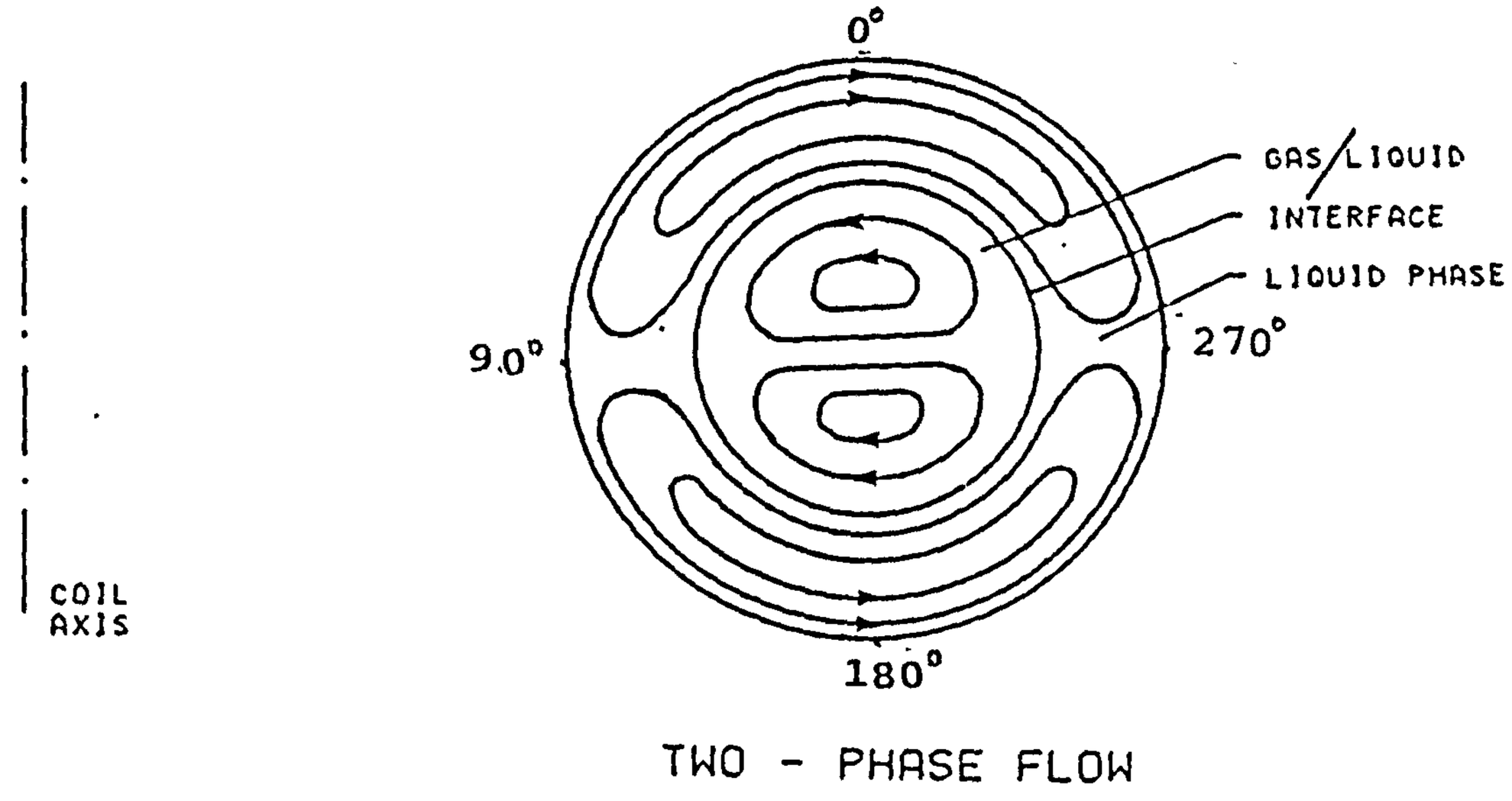

Figure 2.3. Circumferential heat transfer coefficients at tube exit. (up to 87% vapour quality) [ref.31].

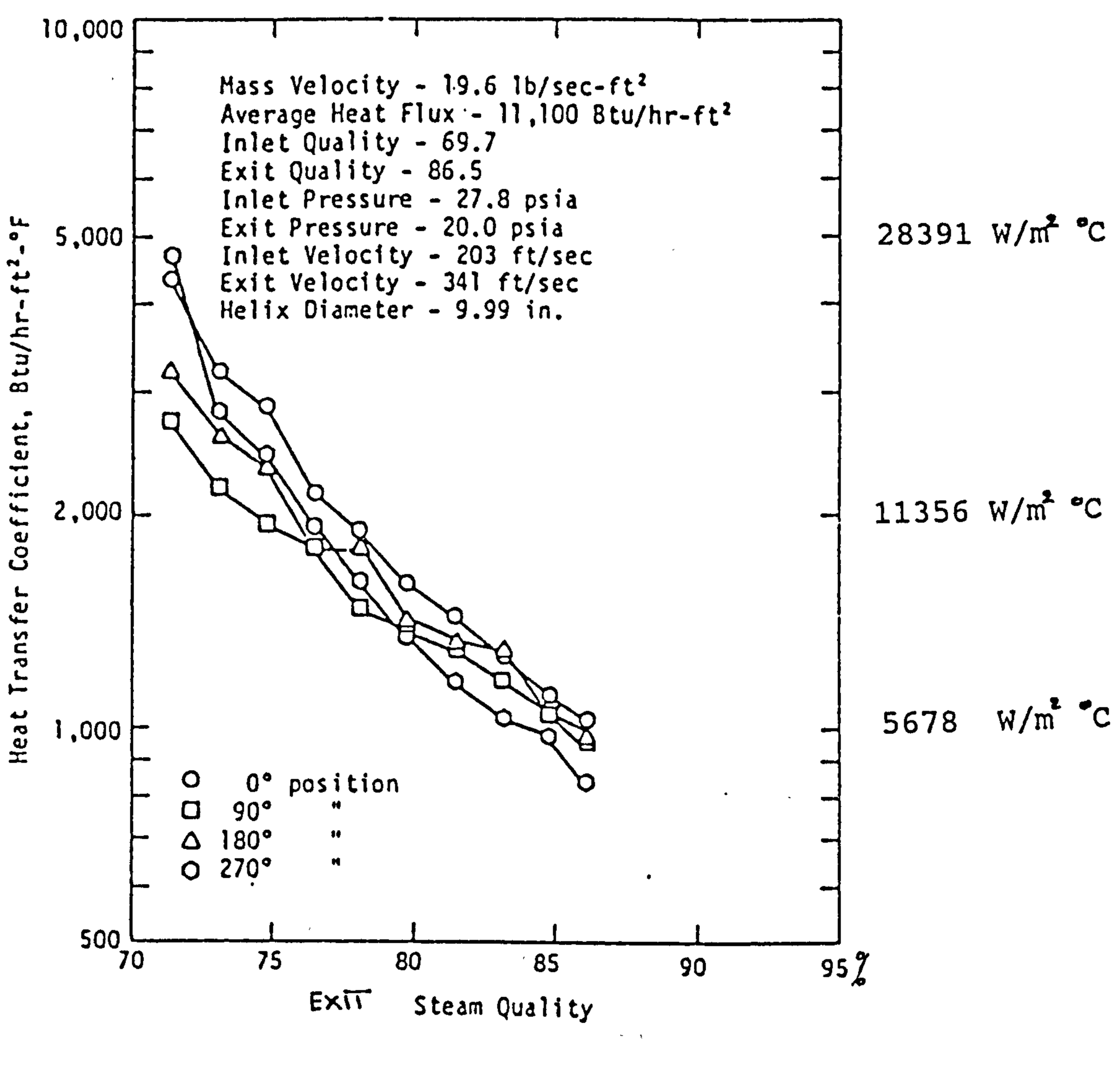

Figure 2.4. Circumferential heat transfer coefficients. at tube exit. (87% vapour quality to superheated) [ref.31].

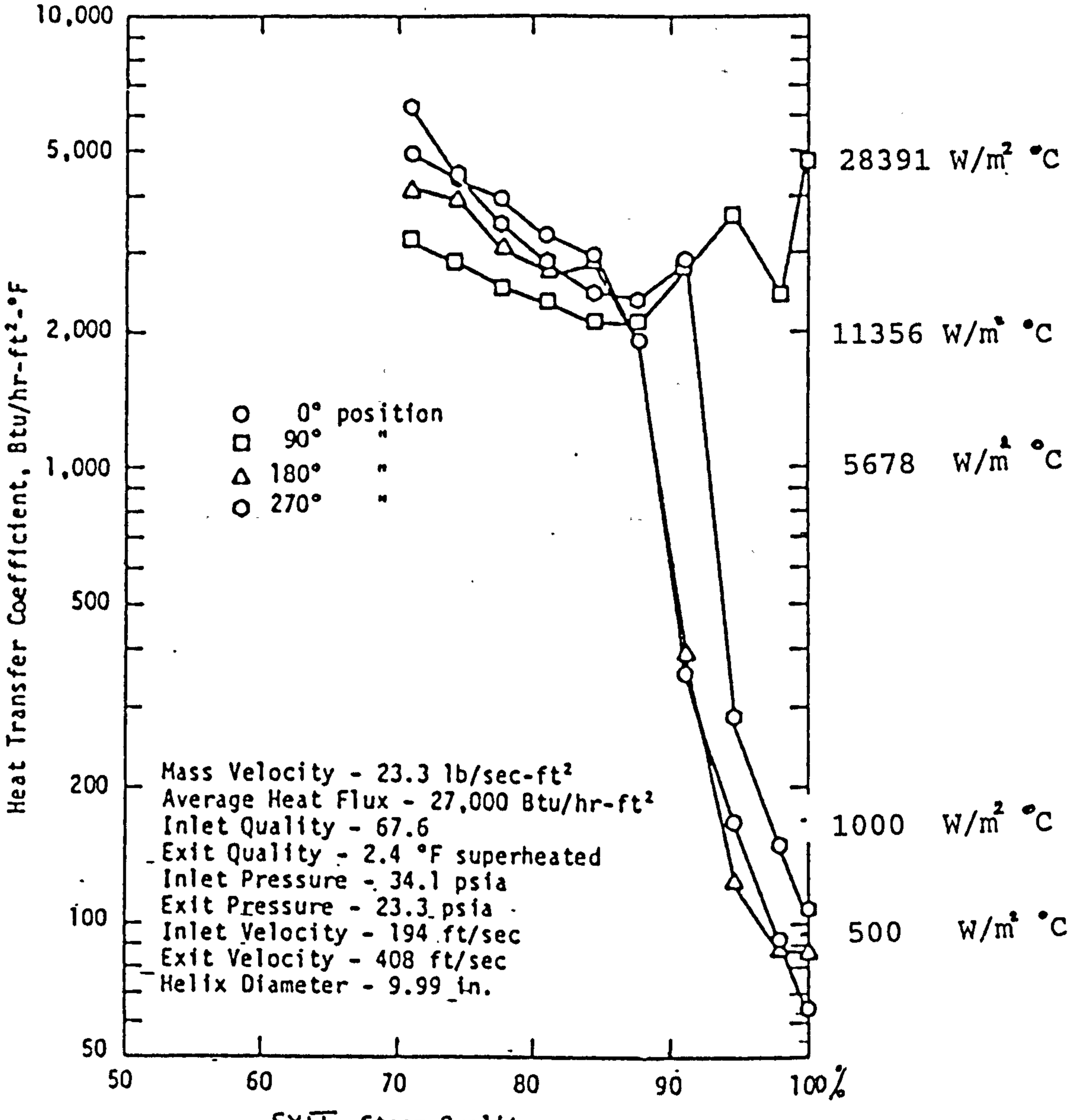

Figure 2.5. Dryout data for high pressure steam-water flow in a straight and coiled tube. [ref.16]

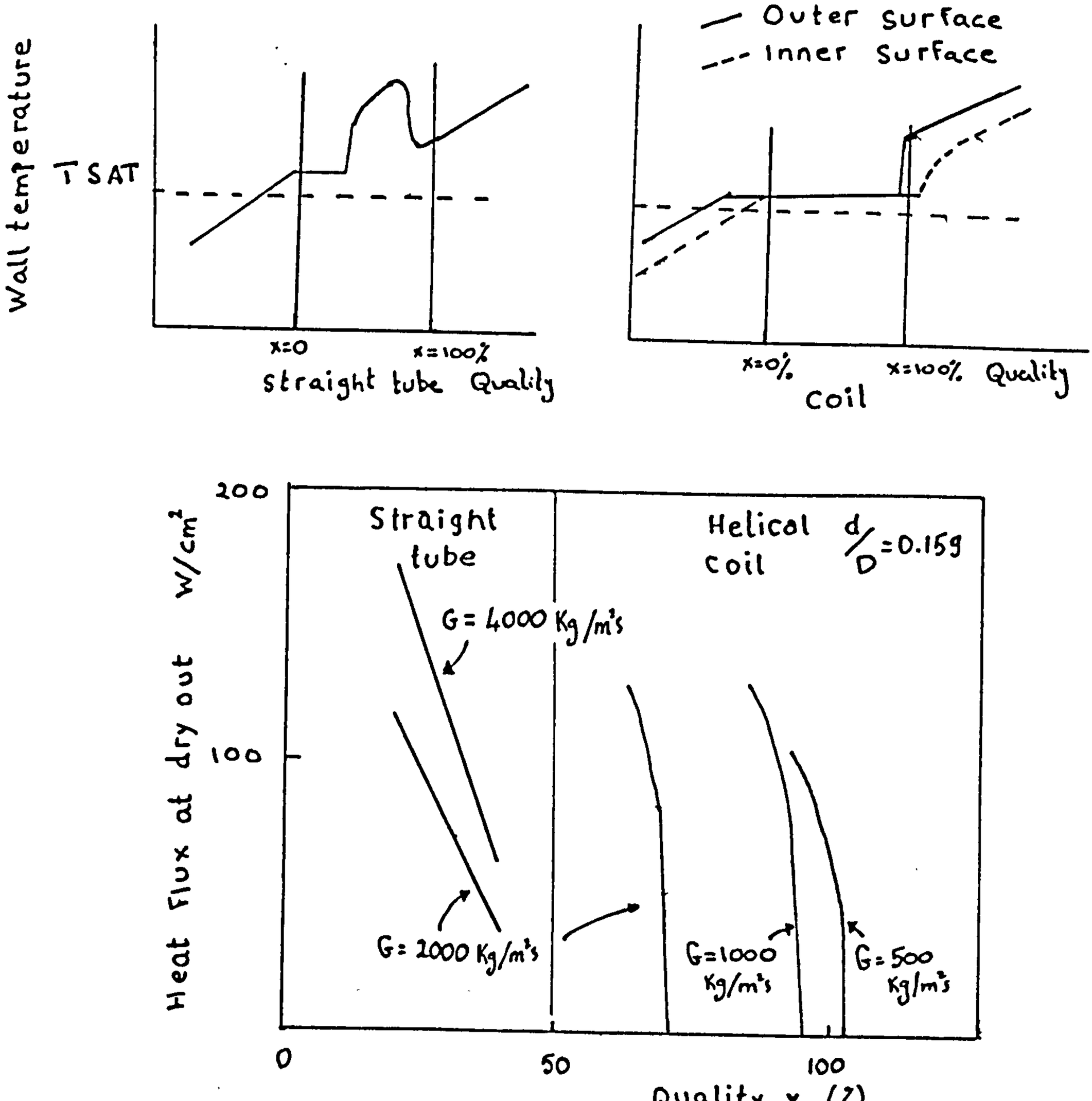

Figure 2.6. Liquid film flow rate distribution as function of peripheral position in a coiled tube. [ref.16]

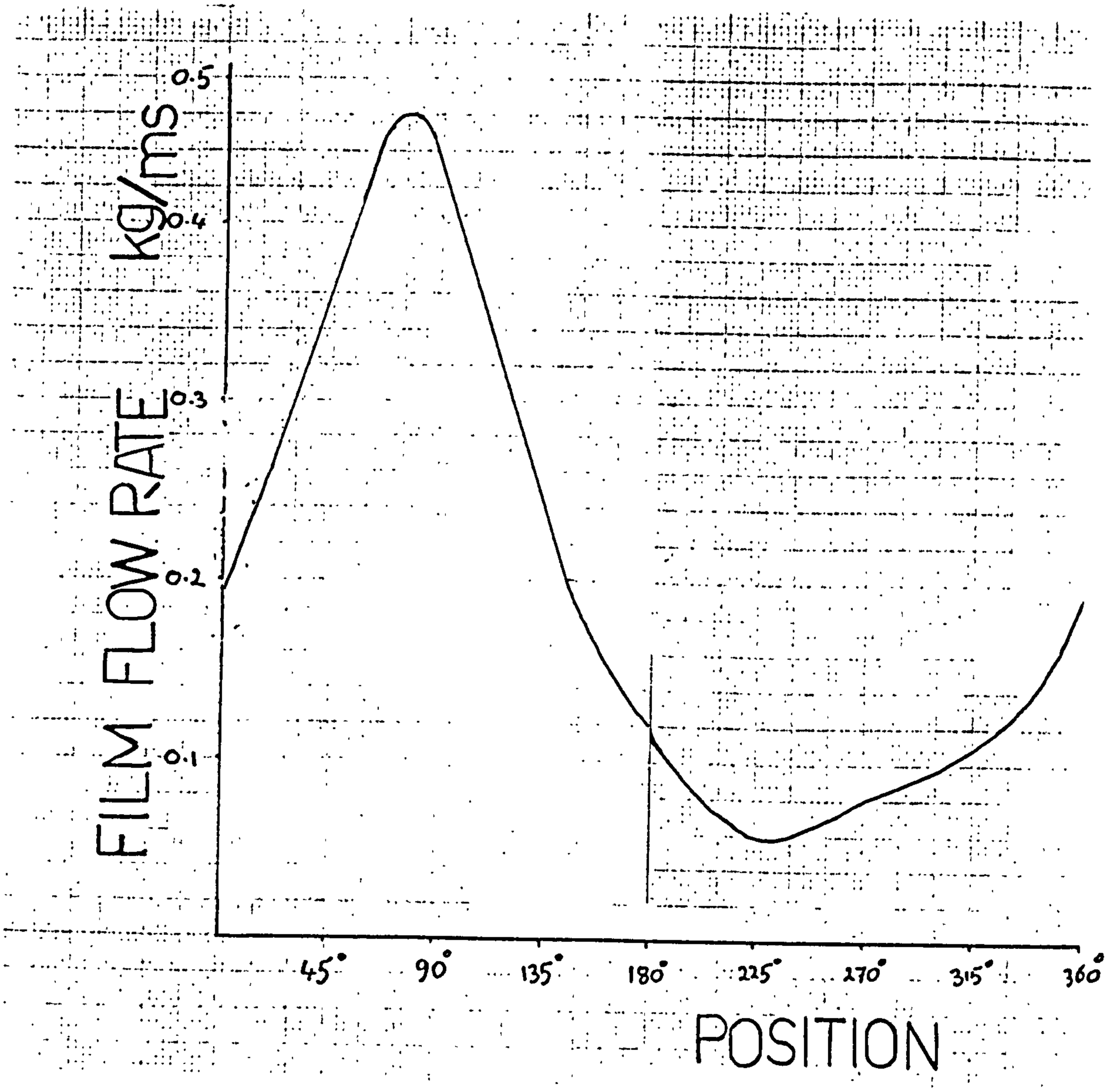

On the basis of such considerations, it is a plausible idea to investigate ways of promoting, this desired flow characteristic (annular flow) in the flow inside a heat exchanger. The heat exchanger primary side supplies the heat source by circulating hot water, and the cold side removes heat through the progressive evaporation of Freon 114. By forcing such flow regime, the heat transfer characteristics also in zero 'g ' conditions can be reasonably predicted, and as a consequence if the exchanger is sized and designed correctly it could operate in space environment.

Therefore a helically coiled heat exchanger geometry was selected so as to create a similar and predictable flow regime (annular flow) which could be comparable both in micro 'g' and in one 'g' environment.

3.0 FUNDAMENTAL THEORY OF EVAPORATIVE HEAT-EXCHANGER CONCEPT FOR SPACE-BASED SYSTEMS

One 'g' boiling inside helically coiled tubes under forced circulation has been studied by many investigators (ref.32). The aim of the present work is to gain a general understanding of the boiling inside helically coiled tubes and how to practically use the one 'g' behaviour to design a zero 'g' heat exchanger.

The practical incentive for exploring this configuration is the possibility to maintain, up to high vapour qualities, a continuous de-entrainment of the large droplets from the vapour. This would thus ensure a stable liquid film on the duct wall to higher vapour qualities than in straight conduits and therefore delays the onset of departure from nucleate boiling. The departure from nucleate boiling has been experimentally observed to be proportional to $g^{1/4}$ and therefore would be reached sooner in micro 'g' environment compared with ground conditions.

A visual flow study using air-water mixtures in a coiled transparent plastic tube was made by Banerjee et al (ref.33). For most of their runs, they observed that the liquid film was displaced towards the 90° position (Fig.2.2), whereas one intuitively expects the liquid to be centrifuged to the outer wall. They termed this phenomenon " film inversion" and explained the effect by a force balance at the gas-liquid interface, assuming a large slip velocity between the phases and neglecting secondary flow effects.

Other studies by Owhadi et al (ref.24 and 34), on axial mixing in two-phase flow in helical coils have visually confirmed that the major portion of the liquid was concentrated in a relatively slow-moving stream on the inside of the tube surface at the 90° (Fig.2.2 and 2.4) position. The surface of this stream was strongly rippled and liquid was entrained into the vapour. This liquid was deposited at the 270° position as fine droplets which spiraled back to the 90° position in paths that appeared to be symmetrical about the plane through the 90-270° points. These spiral paths were considered to be formed as a result of a longitudinal drag force on the drops by the primary gas flow and peripheral drag force due to the twin vortices of the secondary flow. The fluid from the center of the tube has the highest velocity and is most strongly acted up on by the centrifugal force. This force drives the fluid from the center to the outer wall of the tube. This in turn induces a motion from the outer wall around the

tube and back to the center. The net result is a pair of symmetrical re-circulation patterns superimposed on the main flows, which results in a liquid film layer all around the periphery up to high vapour velocities.

A theoretical analysis of the heat transfer in a two-phase flow is difficult, due to the complex flow pattern, slip between vapour and liquid, and the unknown conditions at the vapour liquid interface with the formation of bubbles. Rohsenow (ref. 35) has suggested that forced convection heat transfer in subcooled or saturated boiling may be considered to be composed of nucleate boiling component and a convective component. According to Lockhart and Martinelli (ref.36), the effects of these can be additive.
Heat transfer to a two-phase flow in a straight tube has been correlated as a function of the Lockhart and Martinelli parameters by nearly all the authors in this field (see ref.37 for a summary of existing correlations).

The experimentally observed variation of heat transfer coefficient around the coiled tube wall (ref.32), as a function of different vapour qualities is shown in Fig.2.3 and Fig.2.4 for a maximum 87% vapour quality and superheated conditions at the exit of the duct.
Radial acceleration were computed using the local mean vapour velocity assuming that the vapour fills the entire cross section of the tube. Since the area fraction occupied by the liquid is small, the calculated vapour velocity should be very close to the actual one.
Moreover from the inlet, the heat transfer coefficient often went through a minimum. This was especially true at the 90° position. This behaviour was thought to be as a result of the suppressing effect of turbulence on nucleation, causing a drop in the nucleate boiling component while not enhancing the convective component to a comparable extent. The total heat transfer is assumed to consist of a nucleate boiling component superimposed (not necessarily in a linear way) on the forced convective heat transfer. As vapourisation proceeds, the vapour volume increases and the remaining liquid is concentrated as a thin film on the wall; nucleate boiling is suppressed and the heat transfer mechanism becomes predominantly convective.

Watterdorf (ref.38) has shown that in a single-phase flow in a curved channel of rectangular cross section, the shear stress on the concave wall (as seen by the fluid) was higher than on the convex wall. By analogy to momentum transfer, the resistance to heat transfer is expected to be less at the concave wall compared to the convex wall.

The heat transfer coefficient for all four points (see Figs.2.1, 2.2 and 2.3) decreased as vapourisation takes place until in the very high quality range 90-95% the coefficient for the 90° and 270° positions are still quite high, while for the other two positions they diminish and approach the values of a gas coefficient. This is attributed to a liquid deficiency at the 0° and 180° positions, and as the vapour quality approaches 100%, the liquid deficiency, (i.e dry out) also develops at the 270° locations and the heat transfer coefficients drop rapidly. At the 90°position the heat transfer remains high until the last remaining liquid layer at the wall is completely vapourized.

Unlike the experimental conditions where the flow tubes were directly heated, in the case of the two-phase heat exchanger, as the Freon flows through the heat exchanger, it is progressively vaporised by the heat supplied from the water loop giving rise to a two-phase flow along the helical duct. Different flow patterns can then take place depending on the vapour mass fraction and the mass flow rate.

For a straight vertical tube regions of nucleate and convective boiling are shown in Fig.3.1.

Figure 3.1 Flow patterns & heat transfer regions within a vertical tube [ref.16]

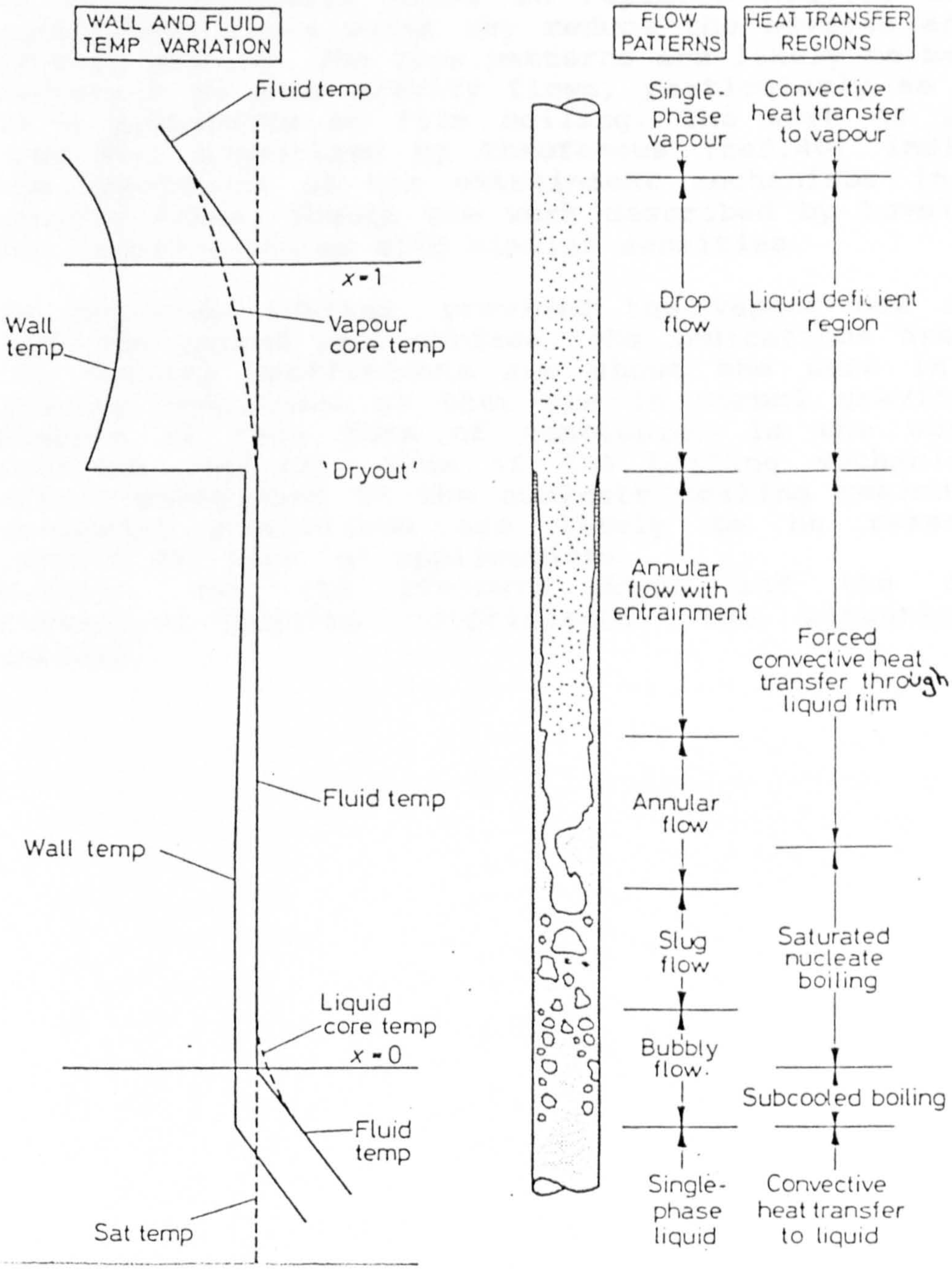

Micro-Gravity Conditions

Design for zero gravity conditions poses special problems and there are no straightforward solutions even for straight tubes. The use of a coiled tube is likely to be advantageous since it replaces gravity with a centrifugal force which may reduce the adverse effects of zero gravity. The flow patterns are likely to be very different in zero gravity flows, particularly as there is a propensity to film boiling. The work of Lovell (ref.39), summarized by Theofanous (ref.40) indicates the importance of the entrainment mechanisms in zero gravity flows, though the work described by Lovell was for liquid mixtures with similar densities.

In two-phase systems, provided the vapour can escape from the heated wall surface, the indications are that the boiling coefficients are about the same in zero gravity conditions as they are in normal gravity. An example of this form of conclusion is the work of Cochrane (ref.41). Thus if the boiling mechanism is mainly restricted to the nucleate boiling region, the on-ground predictions are likely to be reasonably correct for zero 'g' applications.
However, for the pressure drops and the forced convective boiling coefficients, the situation is unclear.

HEAT EXCHANGER DESIGN REQUIREMENTS

The evaporative heat exchanger design requirements (ref.25) are summarized below:

Operating Fluid: The heat exchanger needed to operate with water as the hot fluid and Freon 114 as the cold evaporating fluid.

Water inlet temperature: 38°C.

Water mass flow rate: 320 kg/h

Freon operating temperature: 20°C.

Heat Transfer rate: 5 kW.

Vapour Quality: The vapour quality at the exit of the evaporative heat exchanger of < 0.8.

Pressure drops: The pressure drop across the heat exchanger of < 20 kPa for the both water and Freon ducts.

Environments: The heat exchanger design concept needed to be compatible with on-orbit micro-gravity operations.

Mass: The mass of the exchanger needed to be < 20kg for space-based systems.

4.0 THERMO-HYDRAULIC ANALYSIS OF AN EVAPORATIVE HEAT EXCHANGER

Based on considerations of the single and two-phase flow dynamics, a mathematical model of a heat exchanger using helically coiled primary and secondary flow paths was developed and implemented in Fortran code (see Appendix C), to allow the optimization of the heat exchanger geometry. The main results of the optimization process are summarized in Table 4.1.

Table 4.1 Heat Exchanger Optimized Internal Data

- water duct hydraulic diameter	:	9 mm
- freon ducts hydraulic diameter	:	13 mm
- mean coil diameter	:	250 mm
- fin thickness	:	1.5 mm
- height of the EHX finned part	:	230 mm
- number of Freon ducts	:	2
- number of water ducts	:	2

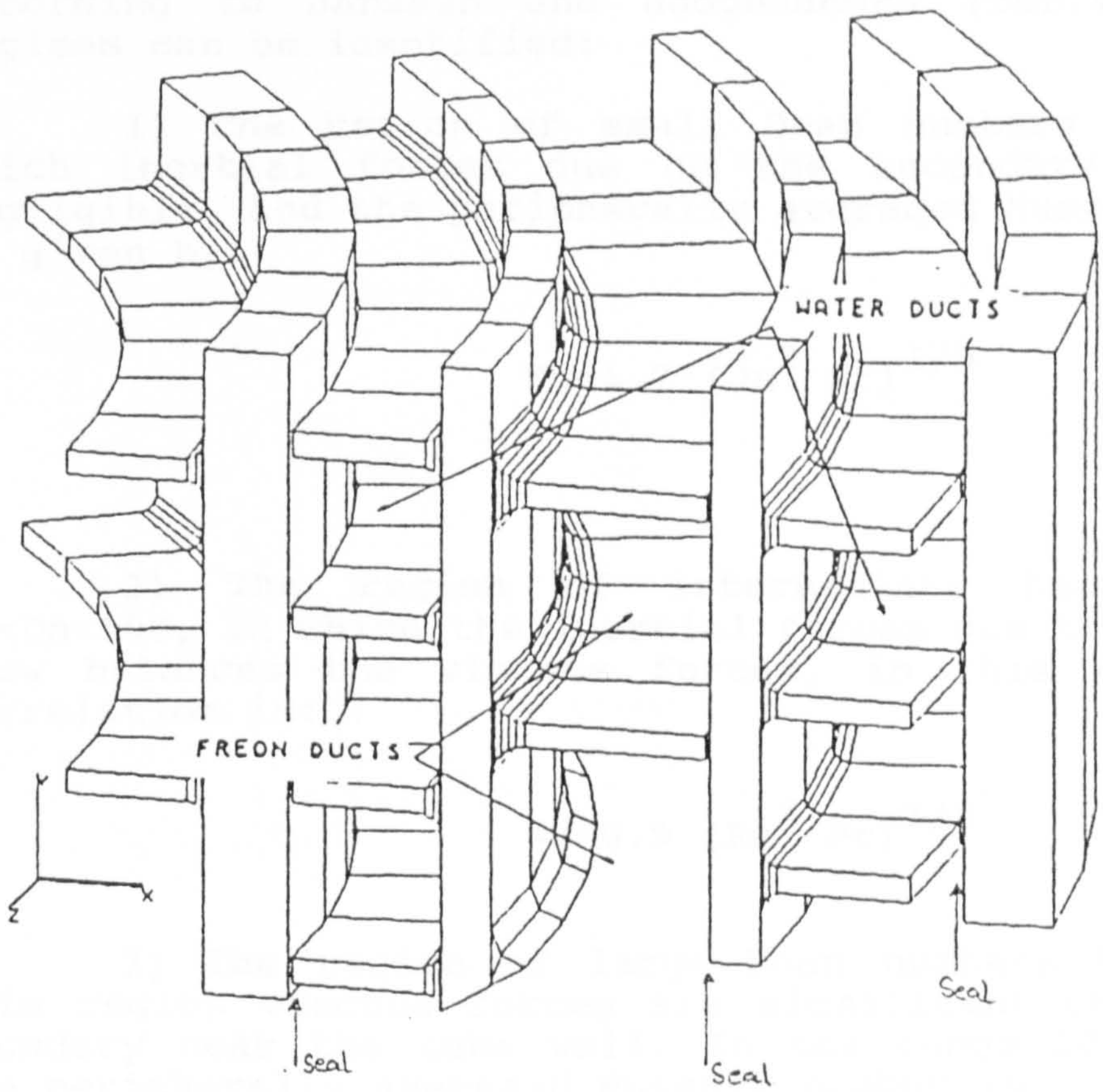

Flow Considerations in coiled ducts :

In coiled ducts there exist the flow velocity along the coil axis, the centrifugal fluid velocity along with a secondary flow velocity associated with the two vortices perpendicular to the circumferential flow direction. The heat transport will occur not only by diffusion in the radial direction, but also by convection. The contribution of this secondary convective transport mechanism dominates the overall process, and enhances the rate of heat transfer per unit length of tube compared to a straight tube of equal length, (for theoretical considerations see Appendix B).

The flow characterization and the associated convective heat transfer coefficient in coiled tubes is governed by the fluid Prandtl number, the flow Reynolds number (based on duct hydraulic diameter as the characteristic length), and the ratio of tube diameter to coil diameter.
According to Janssen and Hoogendoorn (ref.42), three regimes can be identified:

1) The region of small Dean numbers Dn<20, in which inertial forces due to the secondary flow are negligible, and the peripherally averaged Nussult number is given by:

$$Nu=1.7\ (Dn^2\ Pr)^{1/5}$$

2) The region of intermediate Dean numbers 20<Dn<100, in which the inertial forces due to secondary flow balances the viscous forces, in this region the correlation is:

$$Nu=0.9\ (Re^2\ Pr)^{1/6}$$

3) The region of large Dean numbers Dn>100. In this region viscous forces are significant only in the boundary near the tube wall. In the range 100<Dn<1000, the peripherally averaged Nussult number is:

$$Nu=0.7\ Re^{0.43}\ Pr^{1/5}\ \left[\frac{dc}{D}\right]^{0.07}$$

SINGLE PHASE FLOWS

Single-phase pressure Drops:

The friction factor for flow in coiled tubes is greater than in straight tubes, due to the energy losses in the vortices of the secondary flow. Studies by Wattendorf (ref.38) of pressure drops in a coiled duct have shown that the friction factor is slightly greater than the friction factors in an uncoiled channel of the same cross section.

Generally the pressure drop in a duct section of a length dz, is given by the sum of three components (ref.32):

$$dp = dp_{Fr} + dp_a + dp_z$$

For a single-phase flow the three terms can be evaluated as follows:

$$dp_{Fr} = \frac{f}{2d} v G^2 dz$$

where f is computed according to the method summarized in Table 4.2.

$$dp_a = G^2 dv$$

$$\text{and } dp_z = \rho g \sin \vartheta dz$$

The single-phase flow friction factors were evaluated using White correlation (ref.43) for laminar flow, and Srinavasan correlation (ref.44) for turbulent flow. These correlations are summarized in Table 4.2.

Table 4.2 Summary of basic equations & correlations used for single-phase flows in helical coils

(ref.43)

LAMINAR FLOW: $D_n = Re(\frac{d}{D})^{\frac{1}{2}}$ $Re \leq 2100 \left[1 + 12(\frac{d}{D})^{0.5} \right]$

- $f_s = \frac{64}{Re}$
- $\frac{f}{f_s} = 1$ for $D_n < 11.6$
- $\frac{f}{f_s} = \left\{ 1 - \left[1 - (\frac{11.6}{D_n})^{0.45} \right]^{2.22} \right\}^{-1}$ for $11.6 \leq D_n \leq 2000$
- $\frac{f}{f_s} = 0.1064\ D_n^{0.5}$ for $D_n > 2000$
- $Nu = 0.836\ D_n^{0.5}\ Pr^{0.1}$

(ref.44)

TURBULENT FLOW: $Re > 2100 \left[1 + 12(\frac{d}{D})^{0.5} \right]$; $Re(\frac{d}{D})^2 > 6$

- $f = 0.336 \left[Re\ (\frac{d}{D})^2 \right]^{-0.2} (\frac{d}{D})^{0.5}$
- $Nu = 0.023\ Re^{0.8}\ Pr^{0.4} \left[Re(\frac{d}{D})^2 \right]^{1/20}$

Coefficient Of Heat Transfer for Single-Phase flow

As the heat transfer coefficient in laminar flow is sensitive to boundary conditions, for a constant wall temperature the Kalb and Seader equation (ref.45) was used. Nusselt numbers obtained applying this equation are about three times larger than those obtained using the equation of Seban and McLaughlin (ref.46) for laminar flows. The latter relationship does tend to underpredict the Nusselt number which has also been observed by Owhadi (ref.34) who attributed the difference to the high values of the Prandtl number of the liquids used in their experiments. For turbulent flow, the Seban and McLaughlin (ref.46) was employed, further work by Rogers and Mayhew (ref.47) extended the range of significant parameters.

The correlations used for the laminar and turbulent flow regimes for the friction factor and heat transfer coefficients are summarized in Table 4.2.

TWO-PHASE FLOWS

Two-Phase Flow Void Fraction

Experimental work reported by Premoli (ref.46). shows that the void fraction correlations for straight tubes fits the data for coils reasonably well. This correlation can be written in terms of the slip ratio (ratio of actual gas and liquid velocities) as follows:

$$SR = 1 + E_1 \left\{ \frac{y}{1+yE_2} - yE_2 \right\}^{\frac{1}{2}}$$

Where $y = \frac{\beta}{1-\beta}$

The other parameters in the correlation are defined as follows:

$$E_1 = 1.578\ R_e^{-0.19} \left[\frac{\rho_f}{\rho_g} \right]^{0.22}$$

$$E_2 = 0.0273\ W_e^{-0.51}\ R_e^{-0.08} \left[\frac{\rho_f}{\rho_g} \right]$$

The void fraction can be calculated from the slip ratio by the expression:

$$\alpha = \frac{x}{x + SR(1-x)\frac{\rho_g}{\rho_f}}$$

The void fraction calculations can be made at several positions along the flow channels.

Two-Phase Pressure Drops

Two main approaches can be followed to predict the pressure drops through the two-phase duct; namely the homogeneous and separated flow models (ref.32).

The acceleration pressure drop has the following expression (ref.32):

$$\Delta p_a = G^2 \left[\frac{x^2 v_g}{\alpha} + \frac{(1-x)^2 v_f}{1-\alpha} - v_f \right]$$

The gravitational pressure drop is given by the following expression:

$$dp_z = g \sin\vartheta \{ \rho_g \alpha + \rho_f (1-\alpha) \} dz$$

Most of the available correlations for determining the frictional pressure drop in straight ducts are based on the computation of the single-phase pressure drop for a liquid flowing in the channel. Amplification factors which are functions of the two-phase parameters are subsequently applied to the results of the single-phase model (ref.32).

Generalization of this method to helical coils can be done by evaluating the single-phase pressure gradient, taking into account the increase of the friction factor due to coiling (ref.32). The two-phase multiplier, valid for straight pipe flow, was applied, and Friedel's correlation was used to evaluate the two-phase multiplier (ref.32). The basic correlations applied are summarized in Table 4.3.

Table 4.3 The adopted two-phase flow friction pressure drop correlations for helical coils. [ref.32]

- $E = (1-x)^2 + x^2 \frac{\varrho_f f_g}{\varrho_g f_L}$
- $F = x^{0.78} (1-x)^{0.24}$
- $H_i = (\frac{\varrho_f}{\varrho_g})^{0.91} (\frac{\mu_g}{\mu_f})^{0.19} (1 - \frac{\mu_g}{\mu_f})^{0.7}$
- $\phi_f^2 = E + \frac{3.24\ F\ H}{Fr^{0.045}\ We^{0.035}}$
- $\left(\frac{dp_{Fr}}{dz}\right)_f = \frac{1}{2d} f\ G^2\ v_f$
- $\frac{dp_{Fr}}{dz} = \phi_f^2 \left(\frac{dp_{Fr}}{dz}\right)_f$

Two-Phase Coefficient Of Heat Transfer

The Lockhart-Martinelli parameters X, based on an analysis and empirical correlation of isothermal two-phase pressure drop data in a straight horizontal tube, is defined as:

$$X = \frac{\left[\frac{dp}{dL}\right]_{liq}}{\left[\frac{dp}{dL}\right]_{g}}$$

If both phases are turbulent, this parameter becomes:

$$X_t = \left[\frac{(1-x)}{x}\right]^{0.9} \left[\frac{\rho_g}{\rho_{liq}}\right]^{0.5} \left[\frac{\mu_l}{\mu g}\right]^{0.1}$$

A generally accepted correlation for evaluating the coefficient of heat transfer was proposed by Chen (ref. 48). Such correlation covers both the saturated nucleate boiling region and the two-phase forced convective region.

It was assumed that nucleation and convective mechanism occur to some extent over the entire range of the correlation and that the contributions of the two mechanisms are additive, the two-phase heat transfer coefficient (h_{Tp}) becomes:

$$h_{Tp} = h_{ncB} + h_c$$

where h_{ncB} is the contribution from nucleate boiling and h_c the contribution from convection through the liquid film. The analytical expressions for h_{ncB} and h_c are summarized in Table 4.4. It is noted that the film coefficient associated with nucleate boiling becomes smaller as the temperature difference between the Freon and the wall decreases and the convective mechanism becomes dominant.

A comparison between the predictions of Chen (ref.48) and available experimental results on Freon 114 has been

presented by Herd et al. (ref.49). In their work it was shown that the convective components of the film coefficients are in fairly good agreement while the nucleate boiling component is underpredicted by Chen correlation.

Therefore the application of Chen's correlation results in a conservative (that is lower) estimate of the film coefficient for Freon 114.

The two-phase pressure drop was derived from the Friedel correlation (ref.37). For the two-phase heat transfer it was assumed that the nucleation and convective heat transfer mechanisms are additive, and that the Chen correlation covering both the saturated nucleate boiling region and the two-phase forced convective region was used.

Table 4.4 Two-phase flow coefficient of heat transfer correlations for helical ducts.[ref.48]

- Compute Nu_f considering the liquid phase flowing alone in the duct.
- $X^2 = \left(\frac{dp_{Fr}}{dz}\right)_f \; / \; \left(\frac{dp_{Fr}}{dz}\right)_g$
- $F = 2.35 \left(\frac{1}{X} + 0.213\right)^{0.736}$
- $h_C = \frac{k}{d} Nu_f F$
- $S = \left(1 + 2.53 \times 10^{-6} \; Re_f^{1.17}\right)^{-1}$
- $h_{NcB} = 0.00122 \left[\frac{k_f^{0.79} \; c_f^{0.45} \; \varrho_f^{0.49}}{\sigma^{0.5} \; \mu_f^{0.29} \; \lambda^{0.24} \; \varrho_g^{0.24}}\right] \Delta T_{SAT}^{0.24} \; \Delta P_{SAT}^{0.75} \; S$
- $h_{TP} = h_C + h_{NcB}$

Critical Heat Flux

Several studies have shown that the dryout flux is higher in a helical coil than in horizontal channel of of the same diameter and, in some cases, even higher than that in a vertical channel. The onset of dryout is complex and no general relationships have been derived. For the present purposes, a conservative estimate of the dryout flux can be obtained using the Merilo (ref.50). In the normal application of the evaporative heat exchangers (for space-based systems) with the enhanced annular flow regime, as there is continuous wetting of the walls, the heat fluxes at which dryout occurs are quite high and not encountered provided the maximum vapour quality at the heat exchanger exit remains below 0.8.

4.1 ASSUMPTIONS OF THE MATHEMATICAL MODEL OF THE HEAT EXCHANGER

The methodology adopted for the thermo-hydraulic analysis is based on the following assumptions:

- the saturation temperature of the Freon is directly linked to the inlet pressure.

- the pressure drop of the Freon does not affect the thermodynamic equilibrium of the two-phase flow,

- heat transfer coefficient on the water side remains constant,

The thermo-hydraulic analysis of the heat exchanger was made by means of a numerical solution through discretisation along the flow duct length; the solution is computed for increasing the axial co-ordinate (z). Considering a channel element of length Δz, the extreme points have as their abscissa and, such that:

$$z_{i+1} = z_i + \Delta z$$

Assuming that there is no net exchange of energy with the environment, the following first order equation could be applied:

$$\frac{d\overline{T_w}(z)}{dz} + \frac{1}{RQ_w c_w}\overline{T_w}(z) = \frac{\overline{T_F}}{RQ_w c_w}$$

If a linear variation of R over the element Δz is considered, solution of the above equation yields (ref.51):

$$T_w(z_{i+1}) = \left[\overline{T_w}(z_i) - \overline{T_F}\right]\left(\frac{R_i}{R_{i+1}}\right)^{\frac{\Delta z}{(R_{i+1} - R_i) Q_w c_w}} + \overline{T_F}$$

where R_i and R_{i+1} represent the thermal resistance at z_i and z_{i+1} respectively. If $R_i = R_{i+1} = R$ the above

equation can be replaced by the following expression:

$$\overline{T_w}(z_{i+1}) = \left[\overline{T_w}(z_i) - \overline{T_F}\right] e^{-\frac{\Delta z}{R Q_w c_w}} + \overline{T_F}$$

The rate of heat transferred to the Freon (considered at constant pressure and temperature) can be expressed as:

$$\Delta q_F = \lambda Q_F \Delta x$$

Δx is the increment of vapour mass quality of the Freon.

The heat flow rate released from the water can be expressed as:

$$\Delta q_w = c_w Q_w \left[\overline{T_w}(z_i) - \overline{T_w}(z_{i+1})\right]$$

If the thermal resistance used in the above equation was correct then Δq_F and Δq_w would be equal. In general as these two values are not equal and all the above equations are solved iteratively every integration time step until Δq_F and Δq_w become equal.

The flow chart of the iterative process is shown in Fig. 4.2.

Figure 4.2 Flow chart of the iterative mathematical model

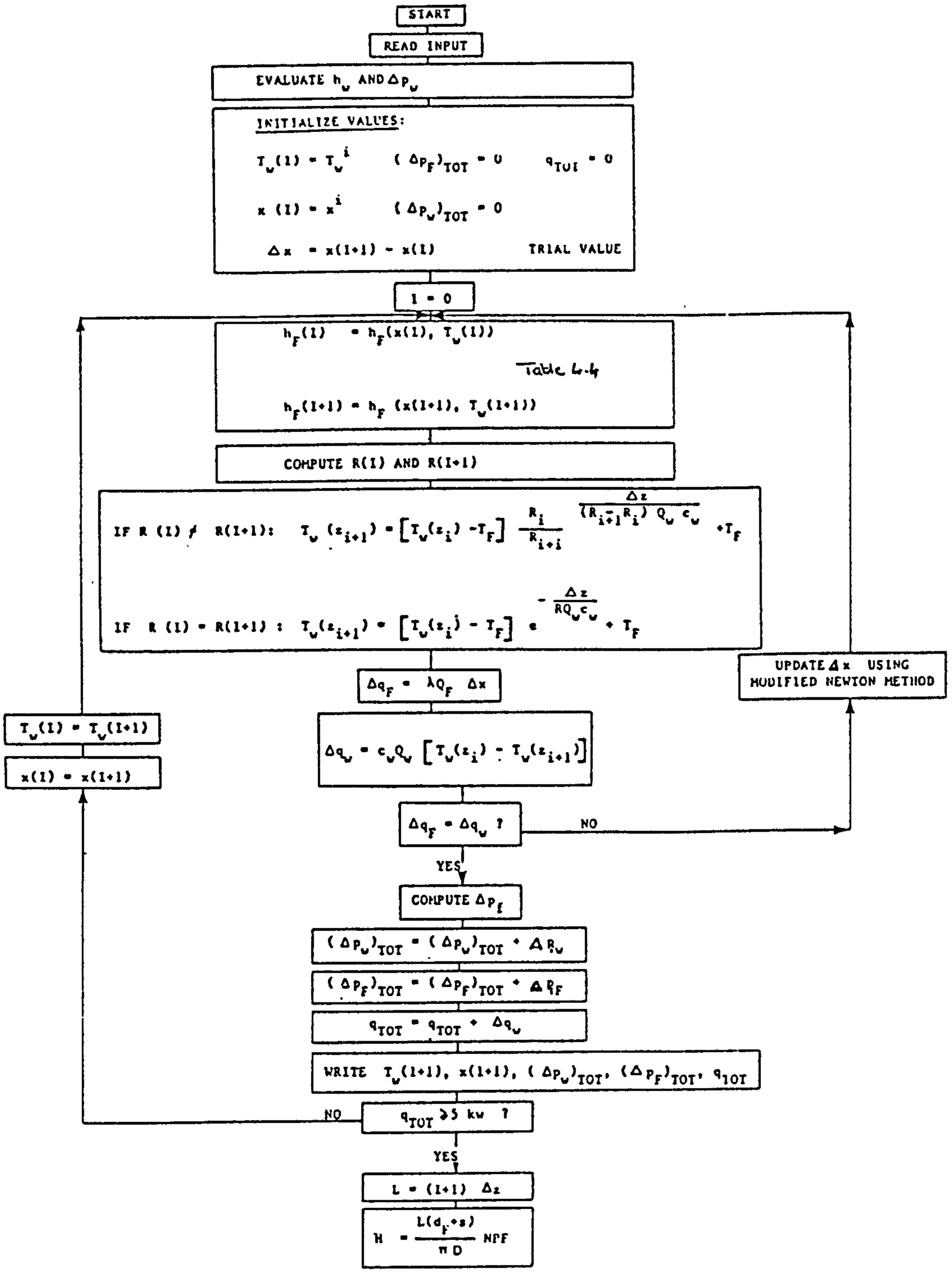

HEAT EXCHANGER GEOMETRICAL OPTIMIZATION

The selection of the internal configuration of the heat exchanger was carried out on the basis of a parametric study, varying the duct cross sectional areas and heat exchanger duct lengths to evaluate heat transferred and pressure drops using the computer program.
Both the thermo-hydraulic performance and the manufacturing aspects also needed to be assessed. The manufacturing considerations included material compatibility, the ease in which the exchanger can be machined and the manner in which the heat transfer paths and internal fins are manufactured by turning or milling or other methods such as extrusion.
In addition in the manufacturing of the exchanger the inlet and outlet manifolds need careful design and machining to avoid maldistribution within the ducts.
Other factors to consider include galvanic corrosion between the heat exchanger parts, weldability, sealing, mass and cost.

A schematic of the internal configuration of the helical duct geometry evaporative heat exchanger is shown on Fig.4.3.

Figure 4.3 Evaporative heat exchanger internal configuration

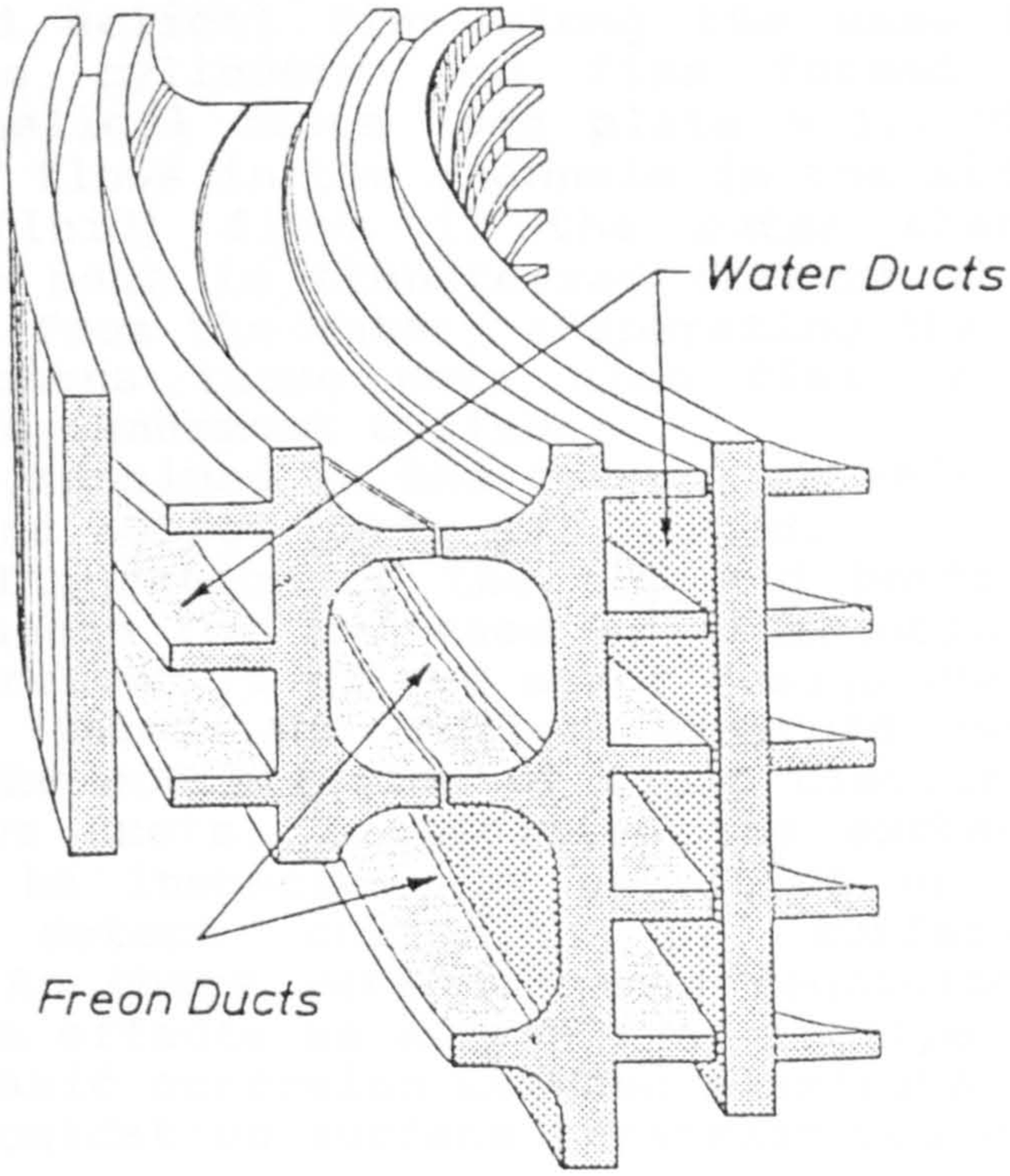

5.0 MANUFACTURING OF BREADBOARD MODEL OF HEAT EXCHANGER

The 5kW evaporative heat exchanger consists of a bolted assembly of two aluminium covers and four aluminium cylinders with helical fins. The fins are machined on the cylinder walls, following a single and double helix profiles.
The helical duct geometry for the heat exchanger core was obtained by integrating four aluminium cylinders with machined helical fins along the same axis. Once assembled the cylinders and fins formed a set of independent helical ducts (see plate 5.1). The coolant fluid (Freon) flows in two channels in the middle, while water (hot fluid) flows in the outer channels (see Fig.5.1). The heat is transferred through the cylinder wall and fins from the water, evaporating the Freon. For stiffness reasons there were also fins on the outer surface of the innermost cylinder.
Manifolds are machined in the covers, to which stainless steel inlet and outlet ports are bolted.
A bolted configuration of the top and bottom manifold covers was chosen for the ease of dismounting the heat exchanger. Moreover it allows minor design changes to be made to the inlet and outlet manifold covers, and facilitates the optimization of fluid distribution into the respective ducts. In addition the exchanger inner surfaces can be inspected (by unbolting of the header covers) to detect corrosion or surface coating degradation. As there were concerns regarding the long term corrosion effects as a result of incompatibility in terms of galvanic corrosion between aluminium and water, a protective oxidation surface treatment was applied.

In future flight models the detachable cover can be replaced by a more permanent welded manifold.

Plate 5.1 Evaporative heat exchanger aluminium cylinders during integration.

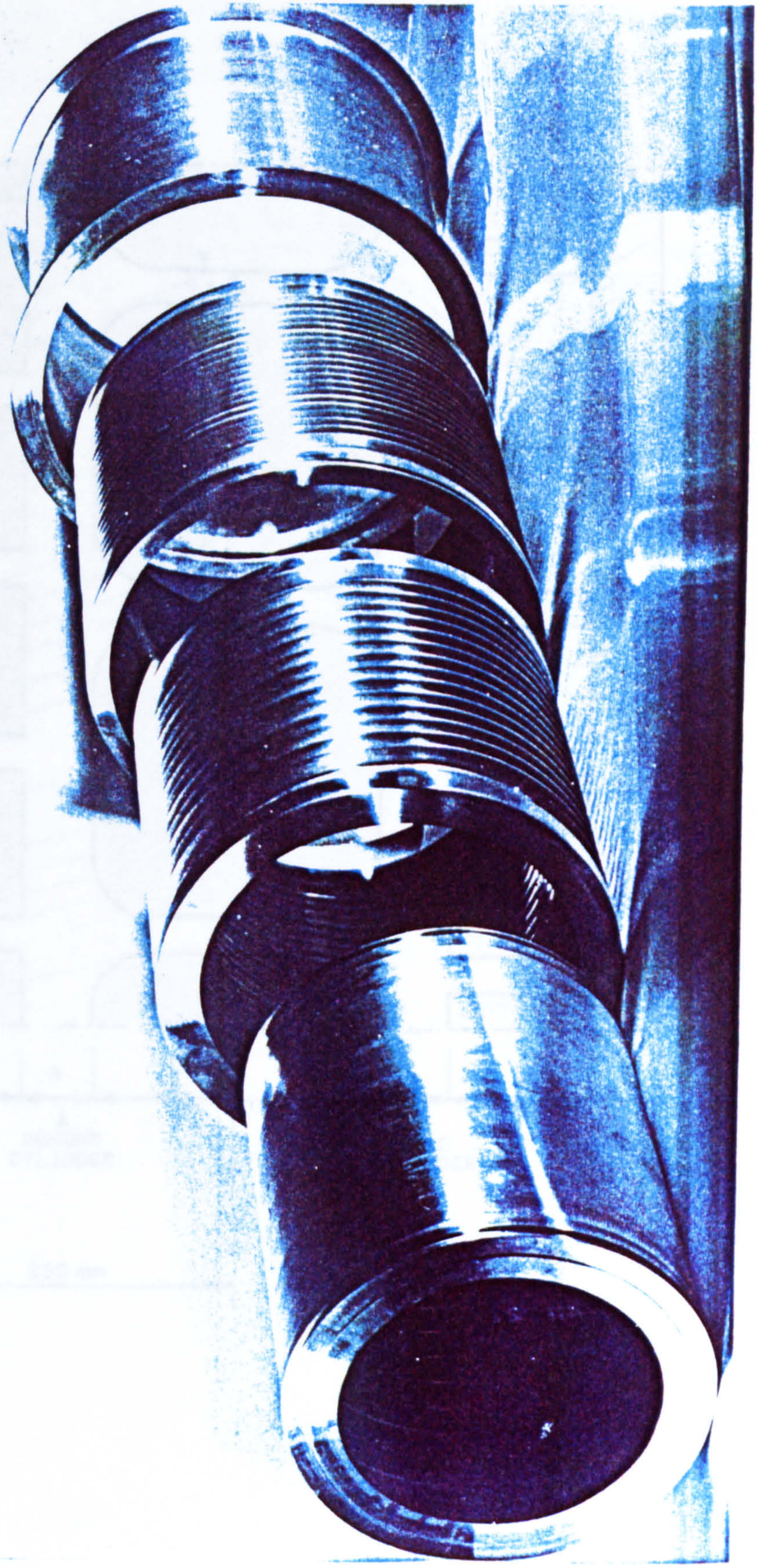

Figure 5.1 Manufactured evaporative heat exchanger internal configuration (dimensions in mm)

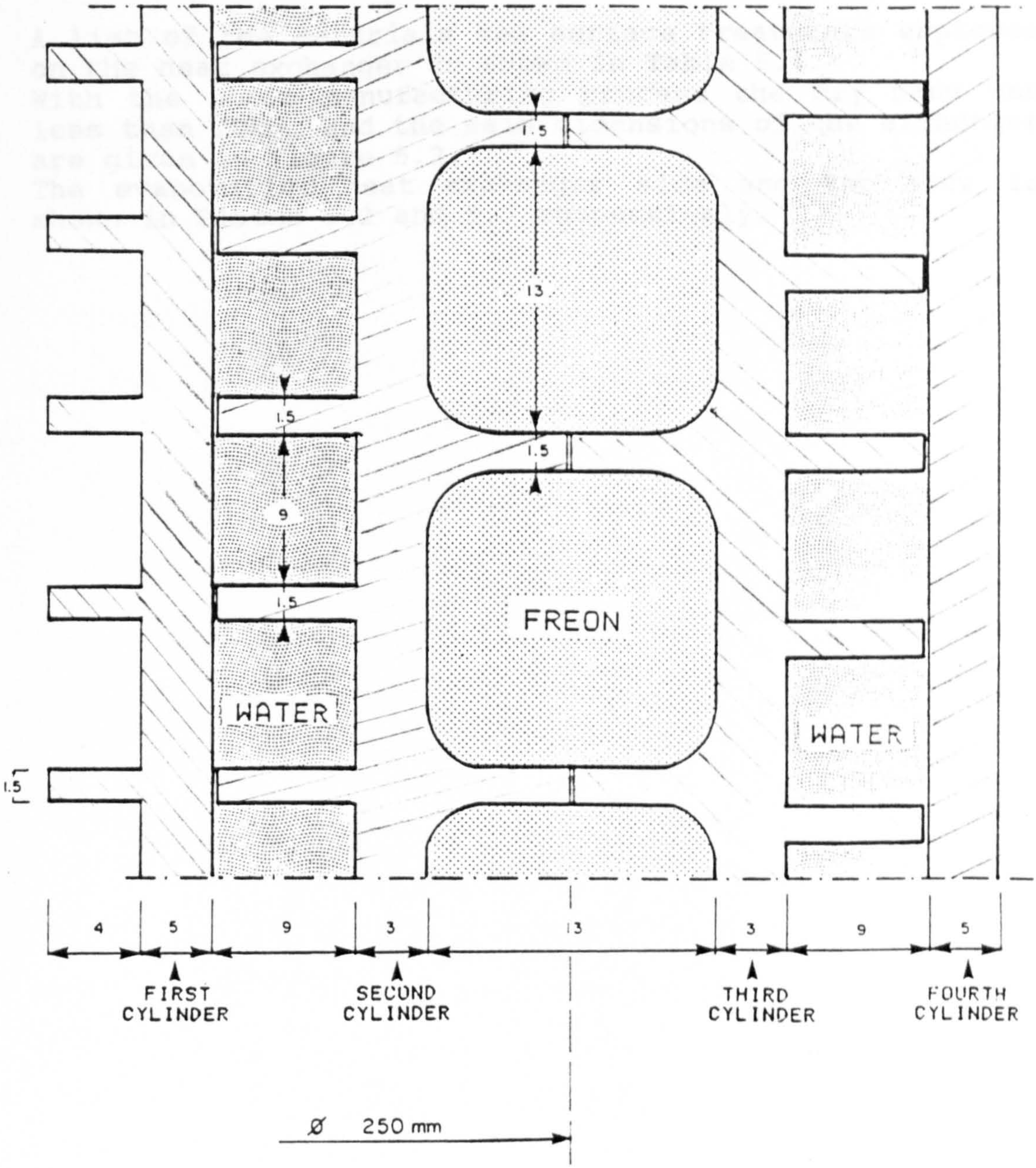

The Neoprene O-rings, housed between the cylinders provided the primary seal between the flow channels, and a Neoprene flat gasket (see Table 5.1) under the top and bottom header covers provided the secondary seal between the header and the heat exchanger core. It must be noted that at the inlet and outlet of the Freon and water header section, the only seal is provided by a flat gasket.

A list of the materials and surface treatments employed on the heat exchanger is shown in Table 5.1.
With the above manufacturing process the dry mass was less than 20kg, and the main dimensions of the exchanger are given in Figure 5.2.
The evaporative heat exchanger side and top view is shown in Plates 5.2 and 5.3 respectively.

Table 5.1 Heat exchanger materials and surface treatments

HEAT EXCHANGER PARTS	MATERIAL	SURFACE TREATMENT
CYLINDER	ALUMINIUM AL 6061	CHROMIC ANODIC OXIDATION
HEADER COVERS	ALUMINIUM	CHROMIC ANODIC OXIDATION
FITTINGS	STAINLESS STEEL AISI 321	----
O-RINGS	NEOPRENE C557-70	----
FLAT GASKET	NEOPRENE C557-70 (PARKER)	----

Figure 5.2 Geometrical characteristics of manufactured heat exchanger

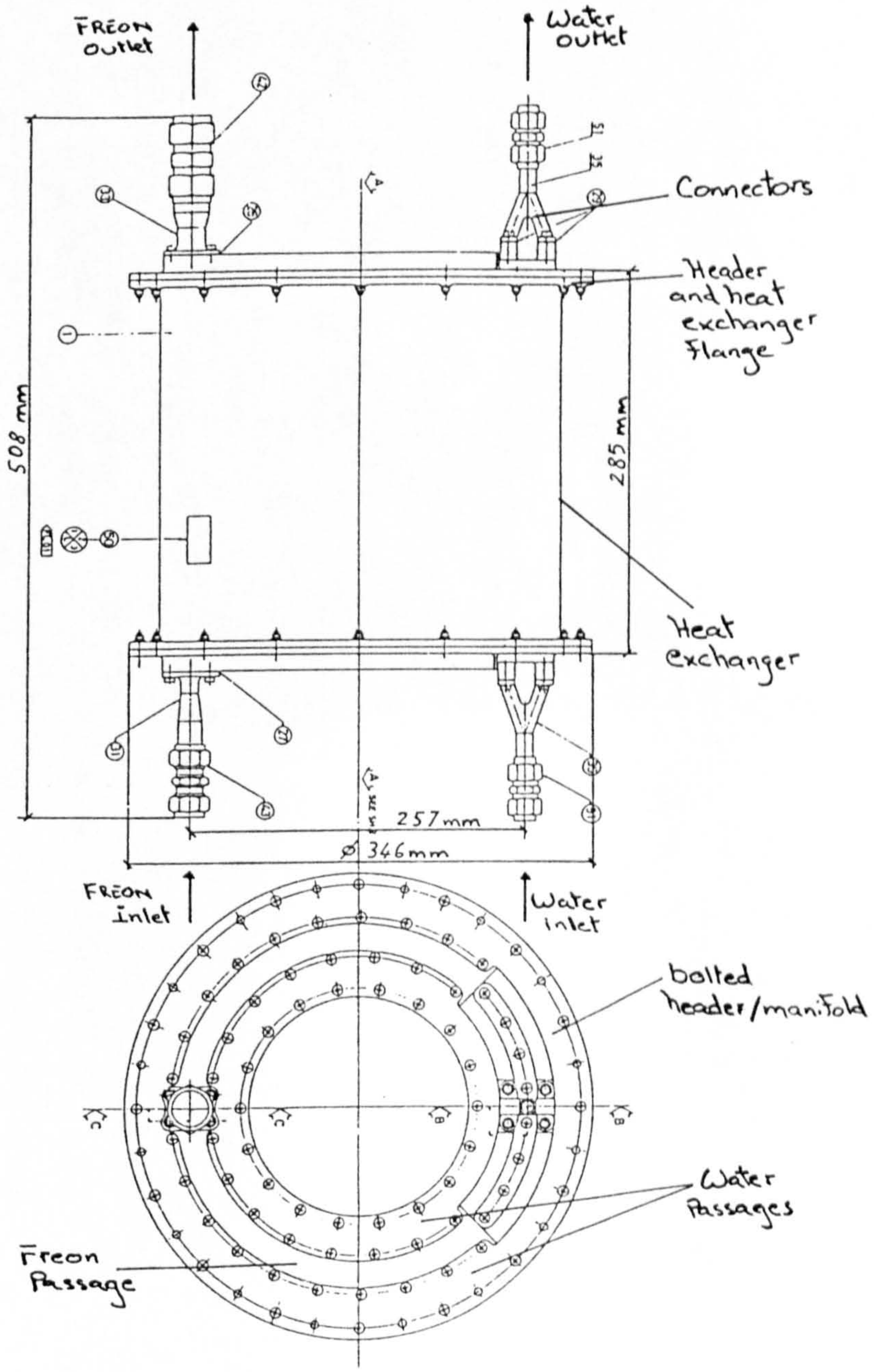

Plate 5.2 Evaporative heat exchanger (side view)

Plate 5.3 Evaporative heat exchanger (top view)

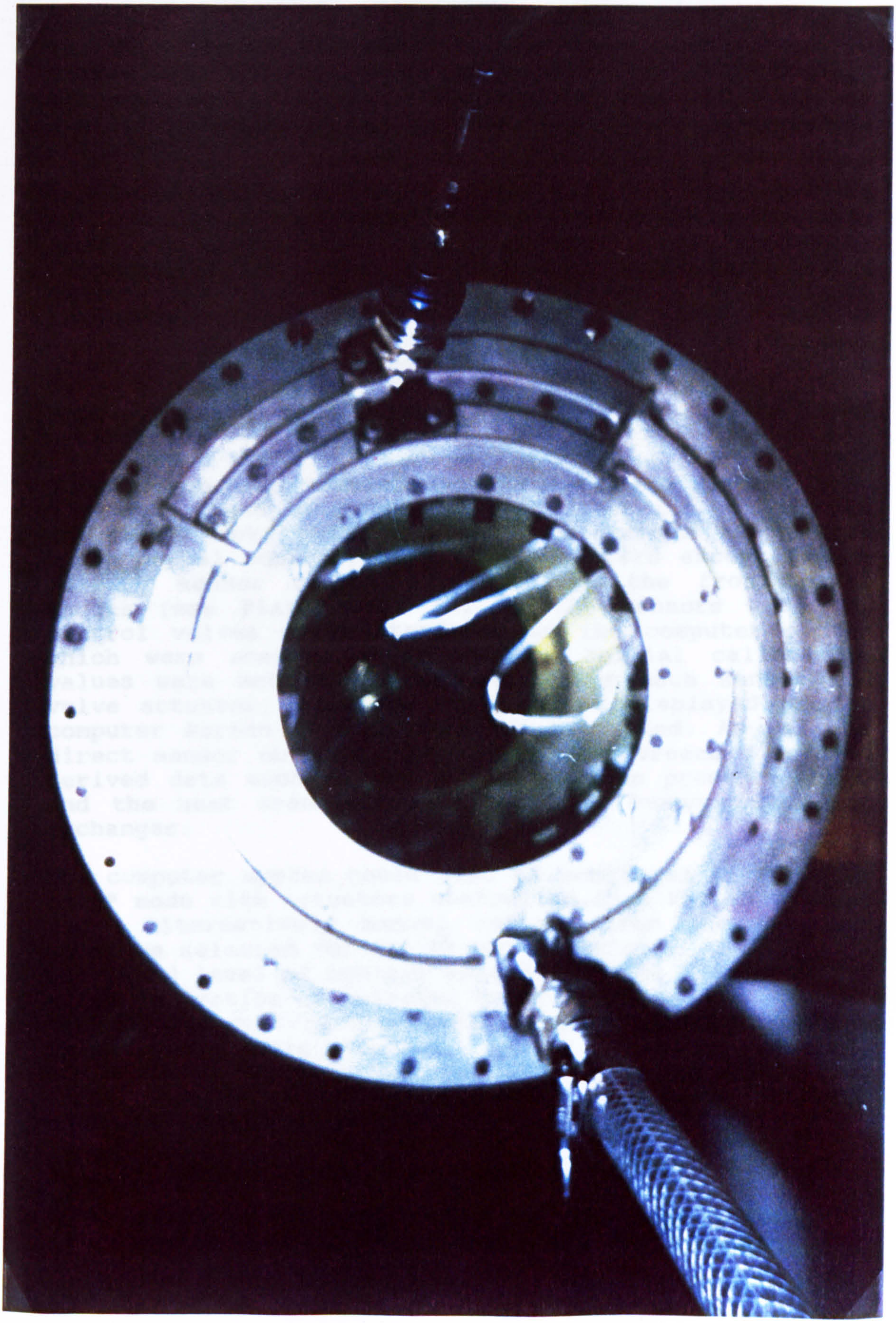

6.0 TDM STEPWISE START UP PROCEDURE

Prior to start of the evaporative heat exchanger tests, the Technology Development system test bench (shown in Plates 6.1, 6.2 and 6.3 and Figs. 6.1, and 6.2) which is the test bench for the Technology Development Model of Fig.1.4 was powered up and the following system checks performed:

The Technology development model test bed was equipped with extensive instrumentation, 49 thermocouples were used to measure fluid, pipework and component temperatures to examine temperature distributions along evaporating and condensing equipments. 10 pressure transducers were spaced around the loop, and 2 differential pressure transducers measured the pressure drops through the evaporative heat exchanger in the water and Freon loops.
Both evaporator supply lines and condenser by-pass lines were fitted with flow meters.

Three separated levels of monitoring and control were provided. These included the instrumentation and control interface rack, which was used to operate the system under manual control, with all parameters except vapour quality sensor output displayed on the front panel gauges (see Plate 6.3). All of the sensors and flow control valves were interfaced to the computer system which were scanned every second. Initial calibration values were set in the software, for each sensor and valve actuator, such that the values displayed on the computer screen were calibration corrected. As well as direct sensor outputs, the monitoring screens displayed derived data such as the overall system pressure drop, and the heat transferred through the evaporative heat exchanger.

The computer system could also be monitored in "monitor only" mode with actuators controlled from the instrument rack. Alternatively manual control from the keyboard could be selected for any or all actuators.
The third level of control allowed control algorithms to allow activation of selected control valves.
Each of the control algorithms (vapour quality control, inlet temperature control, vapour pressure control) could use a Proportional and Integral and Derivative (PID) loop based on sensor output and valve actuator position to determine the new commanded position.

6.1 Water Heating System Checkout

- Check of the header tank for the water heating system to be approximately half full.

- Check of status of all hand valves on water heating system (see Figure 6.1) to be as follows:

V26 Open Position
V27 Closed Position
V28 Open Position
V29 Open Position
V30 Closed Position

- Check of all pressure and temperature transducers (Figs 1.4, 6.1, and 6.2) to be providing sensible readouts on the control panel (see plate 6.3) as follows:

- Delta Pressure Sensor (P2) about 0 bar.
  Pressure Sensor (PT10) about 0.2 bar
  Temperature Sensor TH6 to be between 18°C to 25°C
  Temperature Sensor TH7 to be between 18°C to 25°C

- After turn "ON" of water pump PP2 check of the flowmeter to be giving sensible readout.

- Adjustment of valves V28 provide 80% of flow on meter of front control panel.

- Activation of wall isolator for the evaporative heat exchanger.

- Turning on of the water heater by setting meter No.3 (HX1) to 3kW, 50% mark on control panel.

- The rise in temperature as indicated by thermocouples TH6, TH7 to be detected along with a positive differential pressure on delta pressure sensor (P2) to a value of about 0.15 ± 0.05 bar

- Turning off of heater H4 and PR4 and pump PP2 and observing of temperature and pressure decay.

<u>Secondary Refrigeration System Checkout:</u>

- Check of the vent stack to be in dry condition.
- Check, through sight glass, that oil level in compressor crankcase is adequate.

- Check that crankcase heater is operational and warm to touch.
- Check, through sight glass, that refrigerant level in condenser is adequate.

- Check that cooling water tank is full and the water supply valve is open and ballcock functions correctly.

- Check that the following refrigeration system

valves are open and that pressure gauges read sensibly.

- Check status of secondary valves to be the following (Fig.6.1):

V4 Closed Position
V5 Closed Position
V6 Open Position
V7 Open Position
V8 Closed Position
V9 Closed Position
V10 Closed Position
V11 Closed Position
V12 Closed Position
V13 Open Position
V14 Closed Position
V15 Closed Position

- Set the saturation pressure of secondary R22 refrigeration system (Fig.1.4) to be in the 7 to 10 bar range.

- Check out of the high pressure compressor cut out to be set at 18bar.

- Check out of the low pressure compressor cut out to be set at 4 bar.

- Check that cooling water pump by-pass valve is in open position before switching the water pump on. Check that drains are not flooding.

- Turn on compressor and observe pressure rise in Condenser.

- Observe compressor inlet (vapour return) pressure decay.

- Turn off of compressor.

- Turn off of water pump.

<u>Primary System Checkout:</u>

- Turn control panel mains switch on

- Ensure all panel indicators are functioning

- Turn on pump/valve controller isolator

- Ensure all pressure transducers have sensible

values (between 1.6 to 2.0 bar)
- Ensure all thermocouples read 15°C to 25°C

- Check that liquid fluid line sight glass is full

- Set the accumulator in the 0% (system full) position.

- Close electronically operated valves CV1, CV3, CV4 (Fig.1.4)

- Perform preliminary leak checks using a Freon leak detector

Plate 6.1 shows the heat exchanger located in the test bed; the Freon outlet is the vertical tube leaving the top of the exchanger.

Plate 6.2 is another view of the heat exchanger located in the test bed; the flow control valves upstream of the heat exchanger and the evaporative cold plate (see Appendix D) is also visible.

Plate 6.1 Evaporative heat exchanger in test bed

Plate 6.2 Evaporative heat exchanger in test bed

Plate 6.3 Test bed instrumentation

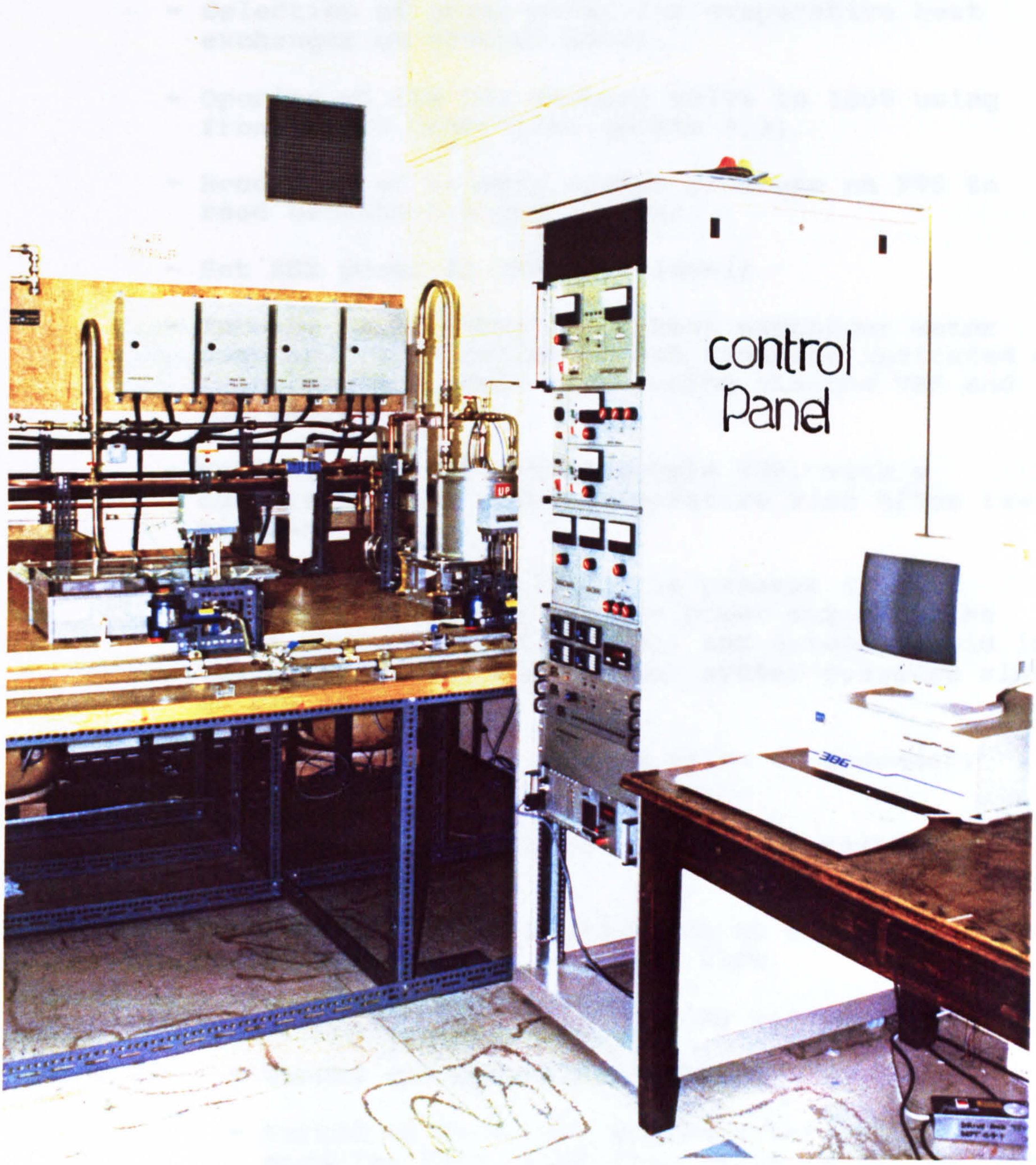

6.2 SYSTEM START UP

After all above checkouts have been performed, the following start up procedure was followed (see Figs. 1.4, 6.1 and 6.2):

- Assure all isolators are on the "ON" position with a null power setting on front control panel.

- Selection of power meter for evaporative heat exchanger on control panel.

- Opening of the CV3 control valve to 100% using front panel controller (plate 6.3).

- Recording of Primary System pressure on PT5 to read between 0.6 and 1.0 bar.

- Set EHX power to 3kW (50% level)

- Turning on of Evaporative heat exchanger water pump and verification of 80% flowrate indicated on front control panel fine tuning via the V28 and V31 valves.

- Monitoring of the thermocouple TH6, with a confirmation of water temperature rise after few minutes.

- Ensuring initially liquid is present in heat exchanger by giving a short power surge to the Freon pump (5 to 10 seconds) and detect liquid in the sight glass, and monitor system pressure rise on PT5 (Fig.1.4).

- Opening of hot gas by-pass valve on secondary cooling system.

- Ensuring secondary water pump spill return is fully open.

- When system pressure had risen by 0.3bar, turn on of Freon Pump to 20% full flow.

After about two minutes the following was performed:

- turned off crankcase heater

- turned on secondary system water pump, ensuring that water flow valve is set to "ON" position along with that of the spill return.

- monitoring of drain for any overflow.
- starting of compressor and concurrent opening of liquid valve V4 (Fig. 6.2).

- check that liquid sight glass is full.

- monitoring of vapour return pressure and preparation to crack open valve V10 (Fig.6.2).

- When the vapour return pressure dropped below 2 bar gauge, valve V10 was opened to give a steady pressure reading between 1 and 2 bar gauge.

- The drain was monitored at all times during this exercise to avoid flooding.

- The primary system pump speed was subsequently increased to maintain 30% of full flow through the evaporative heat exchanger.

- The Freon/Water temperature was monitored to ensure system was working correctly. thermocouple TH3 (Fig.1.4) to read a value of about -5°C after 10 minutes.

- When the TH3 thermocouple values dropped below 0°C, the preheater pump was activated to prevent icing.

- Once steady state conditions had been achieved the test cases where then initiated.

- Occasional checks of the secondary systems where then performed to assure a continuous correct running of the system test loop.

The following steps were taken regarding regulation of the water flow rate in the evaporative heat exchanger:

- the evaporative heat exchanger water flow rate was regulated by maintaining the valves V28 AND V29 in the open position.

- during the evaporative heat exchanger tests occasional checks were made to ensure that the pump PP2 (Fig.6.1) was operative.
- To decrease water flow through the heat exchanger, valve V28 is rotated clockwise, and anticlokwise to increase flow.

- During flow trimming operation,the valve V27 remains open, whilst V28 is adjusted, further

control was possible by adjusting valve V31 but ensuring that it was never in the closed position as it would reduce flow in the pump and cause overheating.

- The flow rate was measured by reading meter M4.

The following steps were taken regarding regulation of the heater power for the evaporative heat exchanger test set up:

- adjustment of controls in the front control console to increase current to element heaters respectively.

- Monitoring of heating effect by observing the temperature of TH6 (Fig.6.1).

SYSTEM SAFETY ASPECTS

Great care was taken to ensure that the two-phase experimentation is carried out in a safe environment. This included incorporating safeguards to ensure that accidents, errors or failures do not result in damage to other parts of the test bed and equipment or pose a risk to personnel.

The working fluid Freon 114 was selected for the reference configuration because of its working temperature range and suitable vapour pressure (182 kPa at 20°C) and its favourably low toxicity category 6 (exposures to concentrations of up to at least 20% by volume for two hours duration does not produce injury, (ref.51 & ref.52).
This is also the selected working fluid of the European manned COLUMBUS space station.
Both pressure relief and temperature cutout systems were installed, and heater controls were inter-locked to the pump controller.

Figure 6.1 Schematic of secondary test loop

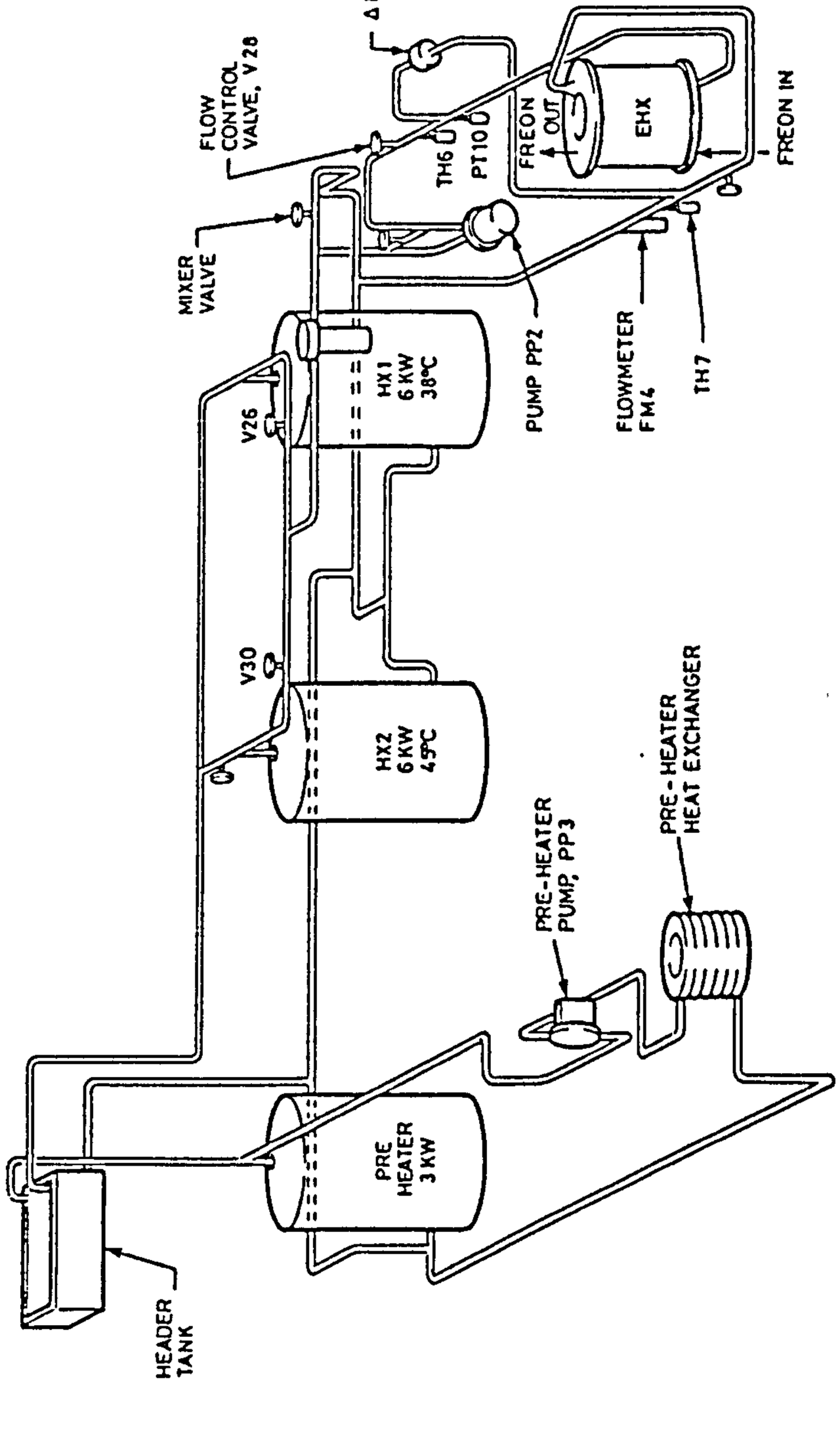

Figure 6.2 Schematic of test bed valves

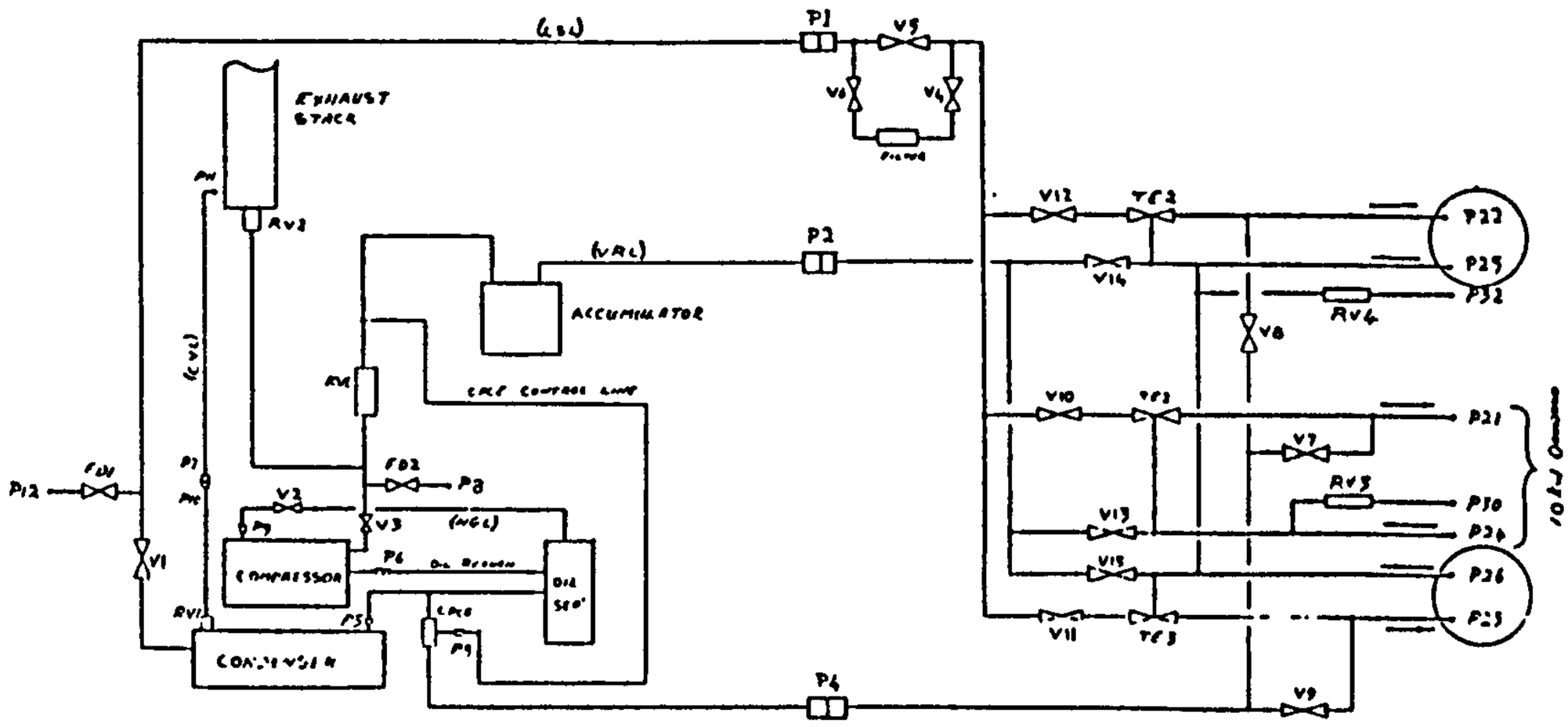

(LSL) LIQUID SUPPLY LINE
(VRL) VAPOUR RETURN LINE
(HGL) HOT GAS LINE
(FD) FILL / DRAIN (VALVE)

7.0 BREADBOARD HEAT EXCHANGER TEST SET-UP

Prior to carrying out the thermo-hydraulic performance tests of the evaporative heat exchanger, a leakage and pressure test was performed.

Leak Test Configuration

The tests comprised both helium and water leakage tests. The leakage tests were performed to detect the internal leakage rate (between the Freon side and the water side) and external leakage rates (from both sides to the outside).

The water leakage tests were performed by pressurising the water side of the heat exchanger with water up to a pressure difference of 2 bar between the two sides. The water leakage from the water side to the Freon side was detected by means of a moisture meter. The water leak test set-up (Fig.7.1) consisted of the following equipments:

- water feed line
- nitrogen feed lines
- valves and hydraulic couplings
- differential pressure transducer
- moisture meter (SHAW SADP-TR)
- gas flowmeter (0-5l/min range)
- digital voltmeter
- power supply

Figure 7.1 Water leakage test set-up.

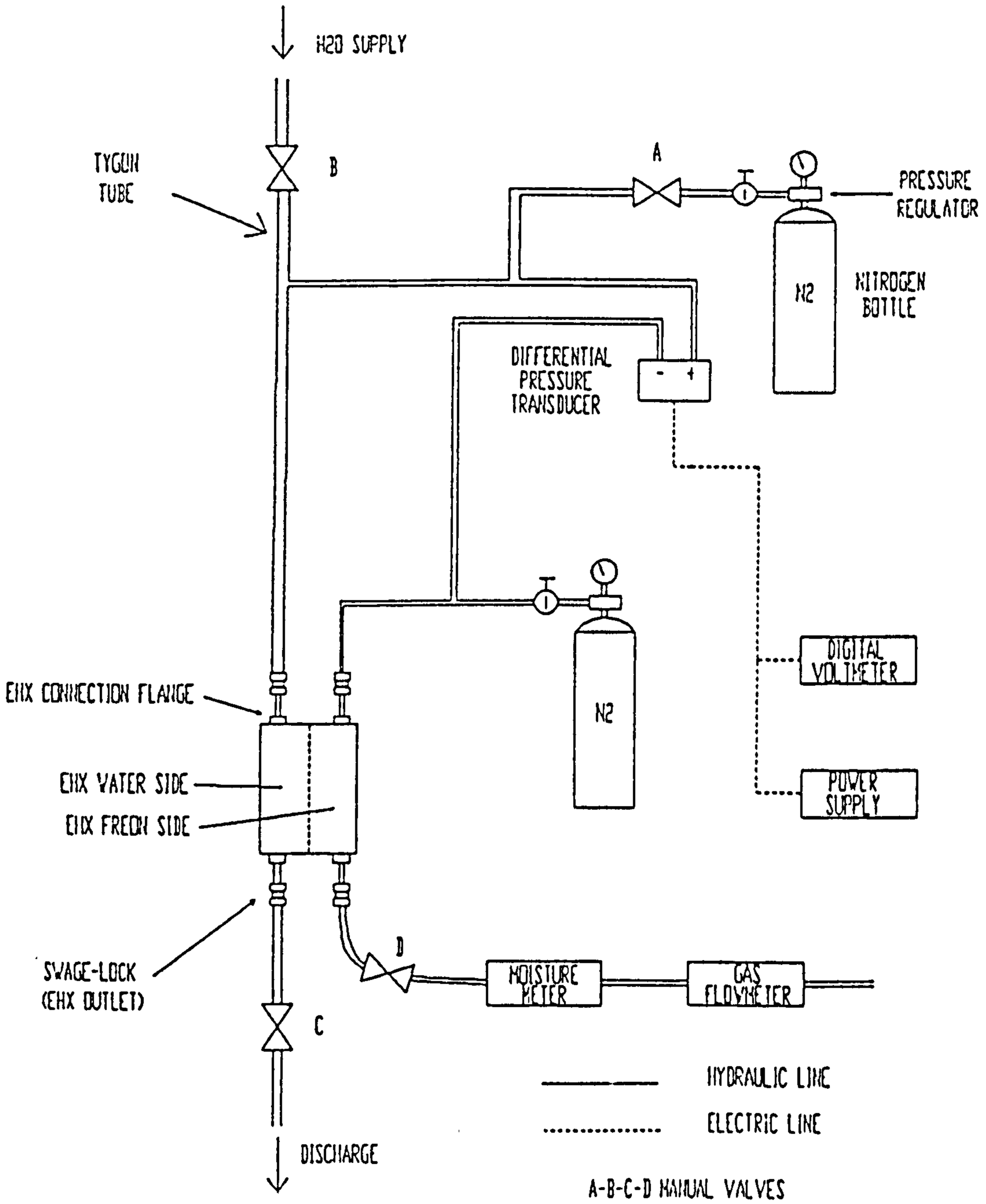

Initially the water and Freon channels were pressure tested to a maximum differential pressure (with respect to ambient) of 12 bar and 5 bar respectively.
Subsequently leakage checks were performed by pressurizing the water side with helium at a relative pressure up to 3bar.

First checks of leakage from inside to outside showed large leak rates in areas of the heat exchanger cover manifold, indicated in Fig.7.2. Moreover an internal leakage check from one side to the other was performed with a pressure difference of 3bar revealed large helium leakages from the water side to the Freon side.
An assessment of the main problem areas and the description of the recovery measures are briefly treated below and more extensively in Appendix D:

With the type of gasket material used (NEOPRENE), a leakage of the order of 10^{-2} cc/h was obtained. This value was above the target leakage value of below < 10^{-3} cc/h.

Figure 7.2 Critical leakage areas in heat exchanger header covers

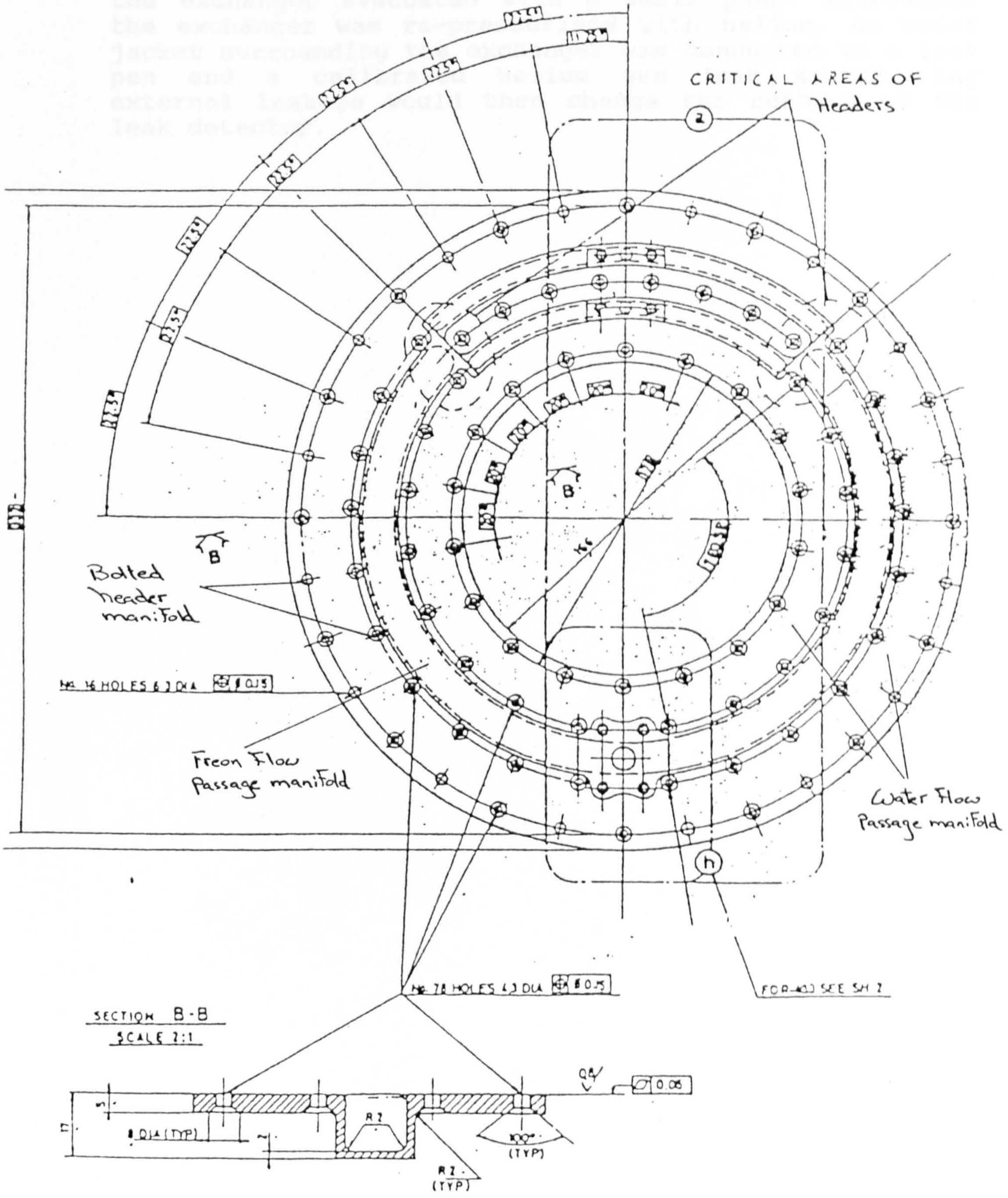

Initially the external leak test was conducted, based on the test set-up Figure 7.3 in which the heat exchanger water side was initially purged with gaseous nitrogen, and subsequently all the outlet ports were sealed and the exchanger evacuated with a small pump. Afterwards the exchanger was re-pressurised with helium. An outer jacket surrounding the exchanger was connected to a leak pen and a calibrated helium gas leak source. Any external leakage would then change the reading on the leak detector.

Figure 7.3 Helium external leakage test set-up

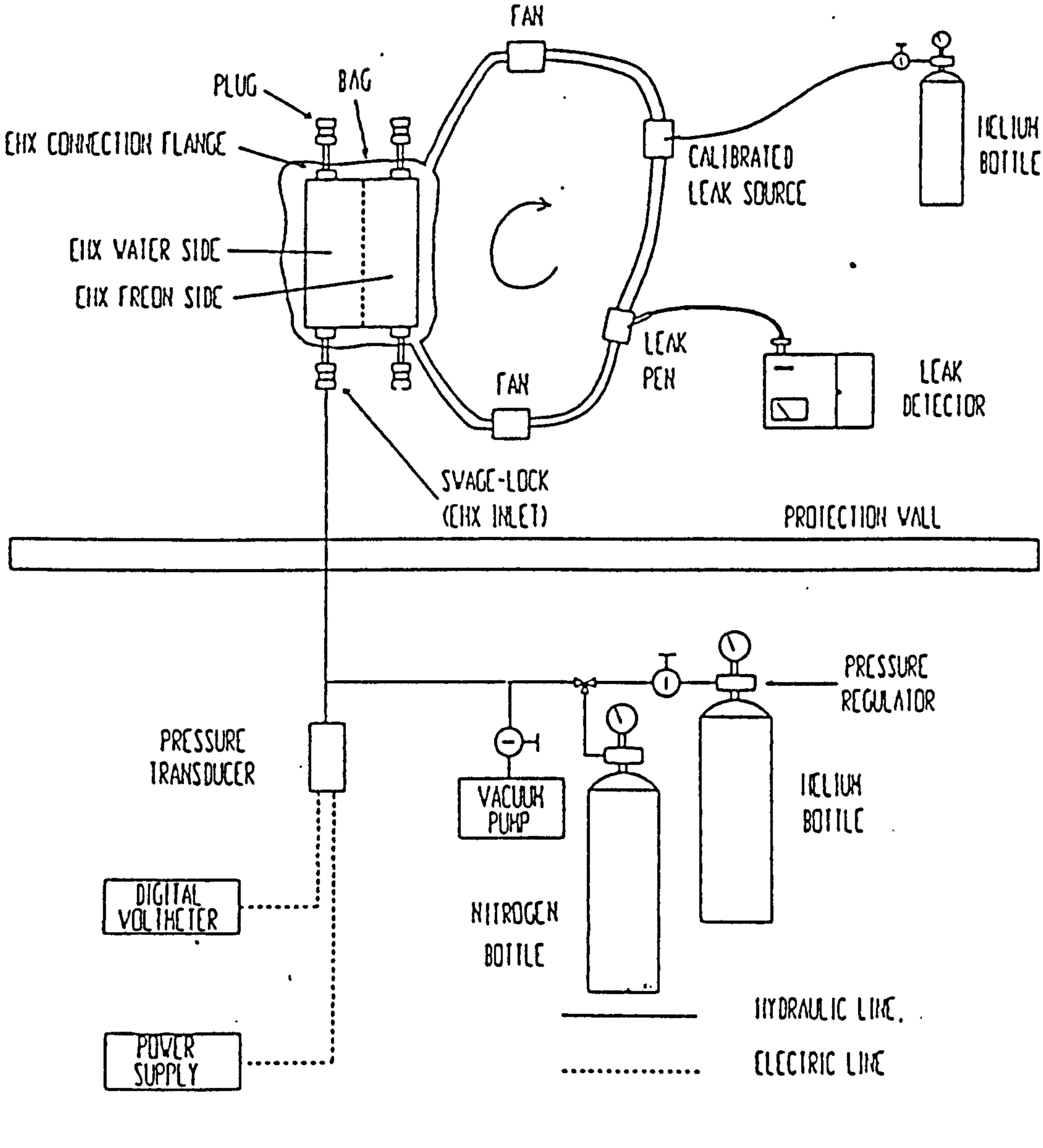

The internal leakage tests however are more important, as they can also influence the performance of other components in the two-phase loop. The test approach was similar to the above with the exception of having to place the leak pen and calibrated leak source on the Freon side of the heat exchanger with the jacket removed, Fig.7.4.

Figure 7.4 Helium internal leakage test set-up

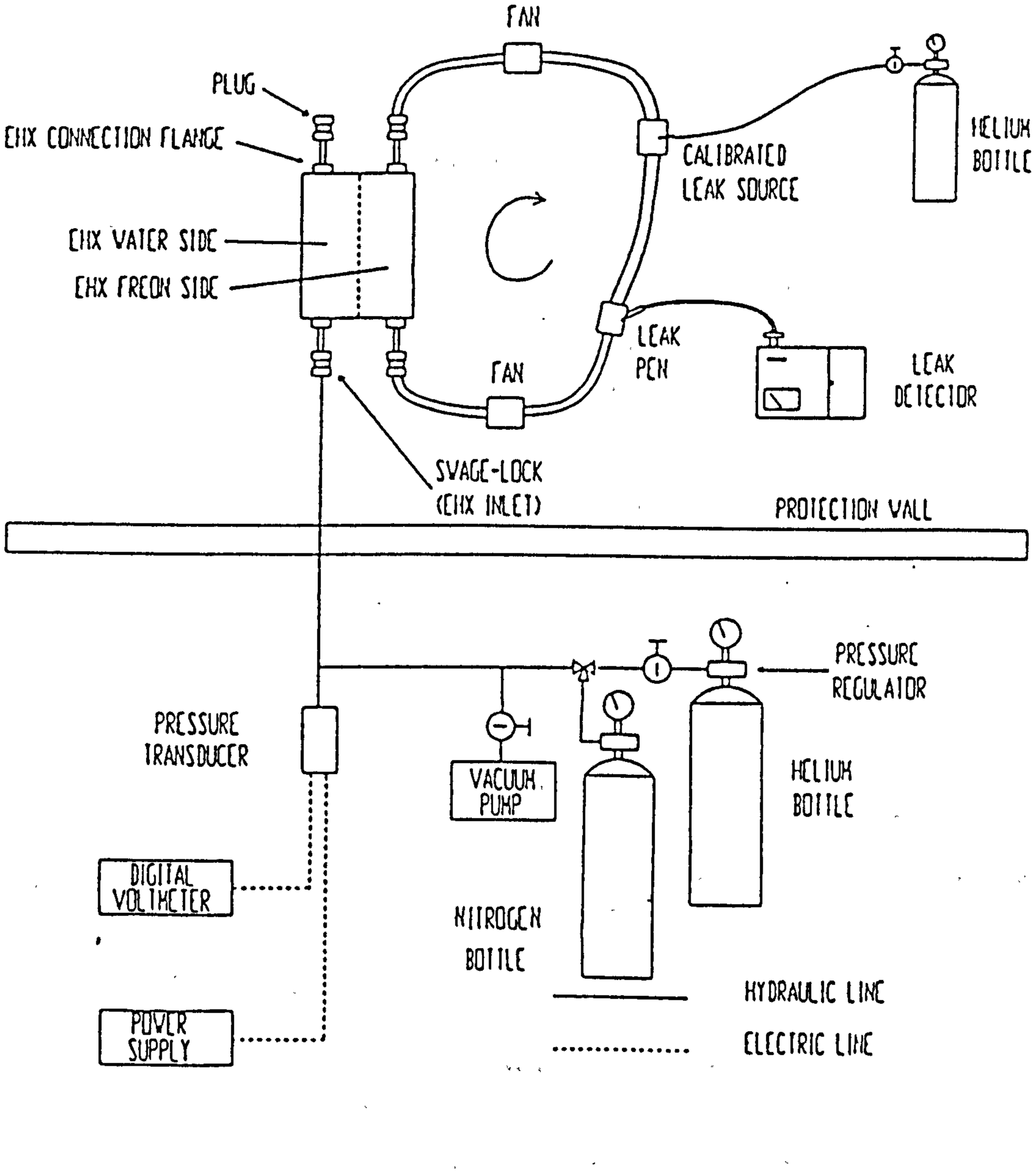

After a series of recovery measures (see Appendix C) the measured water leakage rate recorded was $< 2.4 \times 10^{-4}$ cc/h, hence the water leakage requirement was met.
The water leakage rate was $< 2.4 \times 10^{-4}$ cc/h, this value was the maximum value accounting for the instrument measurement accuracy. The above measured value was less than the required target of $< 10^{-3}$ cc/h and considered to be acceptable.

Thermo-Hydraulic Test Configuration

The heat exchanger was installed in a parallel flow arrangement (Freon and water in parallel flow) in the technology development model of a two phase heat transport loop, Fig 1.4. A helium leak check of the heat exchanger was done. It was then charged with sufficient Freon 114 and left for 48 hours, to allow the complete soaking of the NEOPRENE seal gaskets, inside of the exchanger manifolds.
A schematic of the test loop is shown in Fig.7.5 for primary loop and, Fig.7.6 for the secondary loop. The data acquisition system (plate 6.3) of the TDM was used to measure, display, and store temperature, pressure and flow rate data. Temperature measurements were taken with thermocouples placed inside the pipe inlet and outlet ports on both sides of the evaporative heat exchanger. Water and Freon differential pressures between inlet and outlet ports were measured using differential pressure transducers. Turbine flow meters were used to measure the Freon and water volume flow rates. In addition temperature measurements were taken using thermocouples attached to the external wall of the heat exchanger, in order to investigate possible flow maldistributions between the two outer water channels.

Instrumentation Accuracy levels:

The accuracy of the measuring instruments mentioned above were as follows:

Flow Meters: Freon Flow (FM3): ± 3.5 l/hr
Water Flow (FM4): ± 5 l/hr

Temperature Sensors: For the 'K' and 'T' type thermocouples, although the manufacturers quoted a general measurement accuracy of ± 1°C, each measurement channel was checked at the start and found to be within ± 0.5°C.

Pressure Transducers:

Freon Inlet (PT4) Pressure Sensor: ± 15mbar
Freon Outlet(PT5) Pressure Sensor: ± 50mbar
Water Inlet (PT10) Pressure Sensor: ± 50mbar

Differential Pressure Transducers:

measurement inaccuracies: ± 10mbar

Additional inaccuracies in measurement of the pressure difference due to the additional pressure head contributions of the tubes connected to the sensor were accounted for. In addition in order to ensure a correct reading it was necessary to assure that all the air was removed from the water system by opening of the bleed valves at the start of the testing. For the Freon tubes, and in order to remove hydrostatic error all liquid in the line was evaporated by externally applying warm air on the tube.
The two pressure measurement ports on the water were separated from the evaporative heat exchanger ports by flexible hoses. Before the commencement of the test, the pressure drop in these hoses were measured and correction factors obtained to allow correct pressure drop measurements of the heat exchanger to be made.

Calculations were made by the system software and by hand to evaluate the mass flow rate, water inlet-outlet enthalpy variations, and the Freon exit vapour quality.

Figure 7.5 Heat Exchanger Test Set-Up (Primary Side)

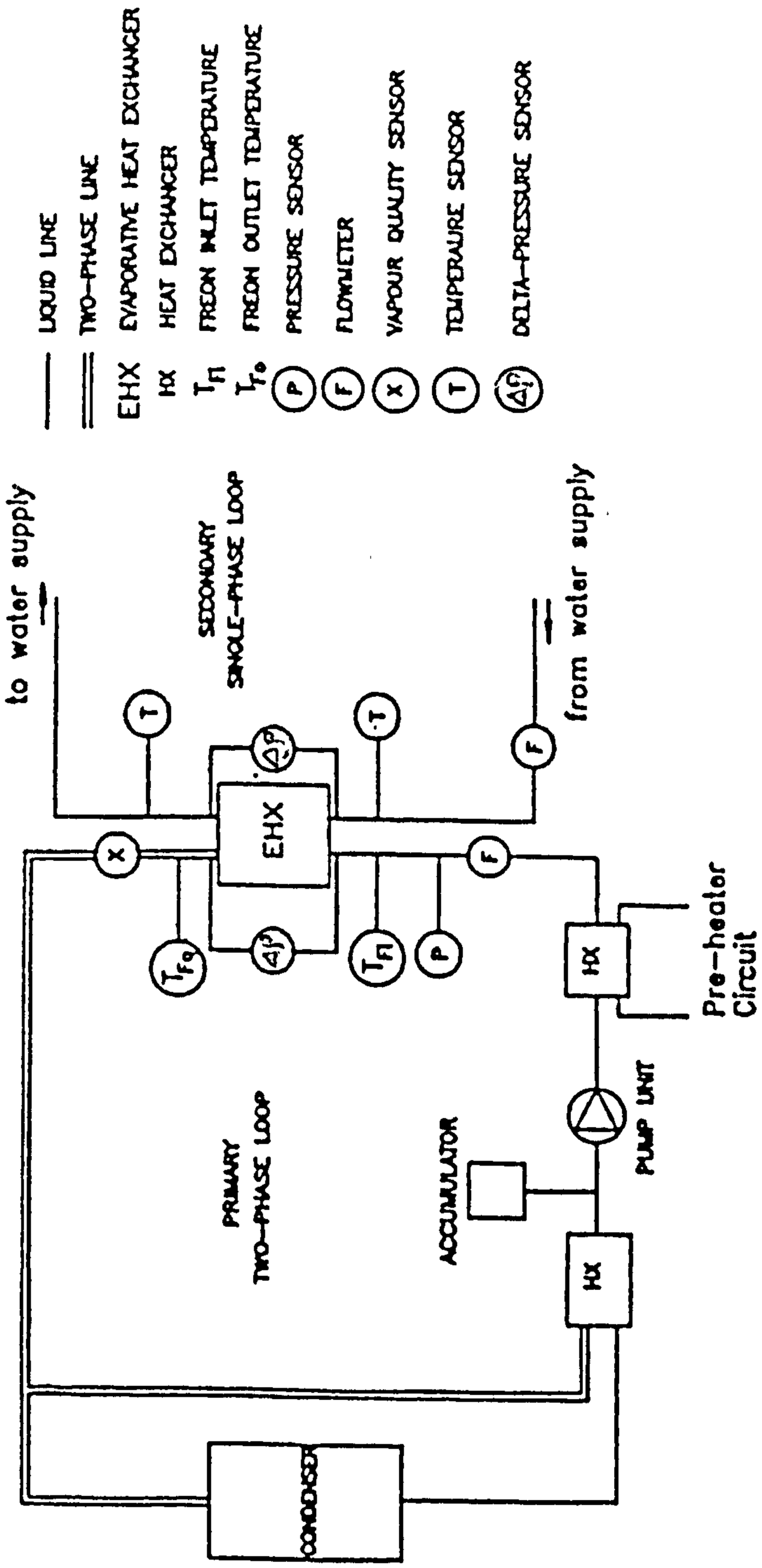

Figure 7.6 Heat Exchanger Test Set-Up
(Secondary side)

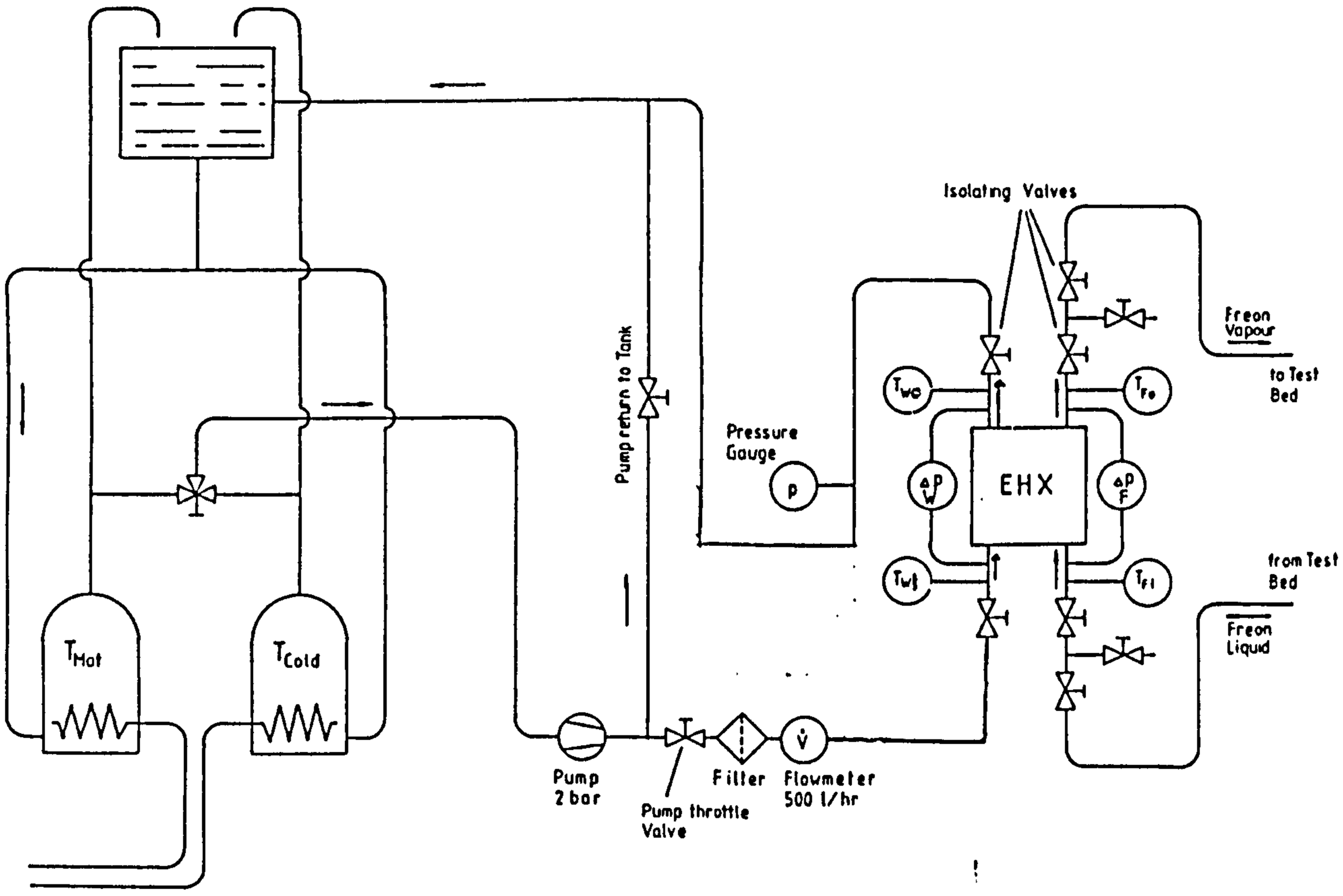

8.0 EXPERIMENTAL TEST CASES

A test plan was developed to derive the heat exchanger performance map under one 'g' environmental condition, and to examine if the heat exchanger will meet the requirements for the nominal operating case, shown in Table 8.1. In the test phase the heat exchanger was positioned along the vertical axis. Tests comprised of steady state and transient conditions. The steady state runs were performed for the Freon inlet temperatures between 0°C (subcooled condition) and 20°C (saturated conditions). Freon mass flow rates were varied between 200 kg/h and 350 kg/h.
The transient effects due to variations in water inlet temperatures (38°C and 45°C) at a water mass flow rate of 320 kg/h were also assessed.

List of the test runs and test parameters (nominal/actual) value for the test are given in Table 8.2.

Table 8.1 Nominal operating case

Water Mass flow rate	320 kg/h
Water inlet temperature	38°C
Freon mass flow rate	280 kg/h
Freon inlet condition	Saturated liquid at 20°C
Freon outlet vapour quality	0.4-0.8
Freon side pressure drop	< 0.2bar
Water side pressure drop	< 0.2bar
Heat transfer	5kW

Table 8.2 Steady-State and Transient Test Cases (analysed conditions/test conditions)

Test Run	Type	Freon Inlet Temperature [°C]	Freon Inlet Pressure [bar]	Freon Mass Flow Rate [kg/h]	Water Mass Flow Rate [kg/h]	Water Inlet Temperature [°C]
1	s. s.	0/0.4	1.8/1.84	280/277.	320/321.	38/37.7
2	s. s.	15/15.4	1.8/1.86	220/220.	320/321.	38/37.8
3	s. s.	20/19.6	1.8/1.88	200/202.	320/321.	38/37.8
4	s. s.	20/19.7	1.8/1.88	240/241.	320/324.	38/37.7
5	s. s.	20/19.2	1.8/1.86	280/277.	320/324.	38/37.9
6	s. s.	20/19.6	1.8/1.91	320/324.	320/324.	38/37.8
7	s. s.	20/19.2	1.8/1.94	350/353.	320/324.	38/37.9
8	s. s.	20/20.0	1.8/1.92	280/277.	320/321.	45/44.5
9(start)	tran.	20/19.9	1.8/1.80	280/277.	320/321.	38/38.8
9(end)	tran.	20/19.6	1.8/1.92	280/277.	320/321.	45/44.8
10(start)	tran.	20/20.1	1.8/1.89	280/277.	320/328.	38/37.8
10(end)	tran.	20/19.7	1.8/1.91	280/277.	350/349.	38/37.8
11(start)	tran.	20/19.7	1.8/1.92	280/277.	320/321.	38/38.2
11(end)	tran.	20/20.2	1.8/1.94	310/320.	320/321.	38/38.3

S.S. : Steady-state
tran.: transient

Table 8.3 Predicted Freon side pressure drops for the nominal test cases.

Test Case	Freon mass mass flow rate (kg/h)	Exchanger Freon side Pressure drop (pa) core	header	total
3	200	9933	3018	12951
4	240	11600	3612	15212
5	280	13030	4225	17255
6	320	14090	4695	18785
7	350	16550	4973	21523

9.0 EXPERIMENTAL TEST RESULTS

The results of the thermal tests of the heat exchanger in both steady-state and transient conditions are given in Table 9.1 and Table 9.2 (for steady-state tests) and Table 9.3 for transient test results. The transient temperature plots are shown in Figures 9.1 to 9.7.

Table 9.1 Steady-state results (inlet and outlet temperatures and mass flow rates)

TEST No.	SYSTEM PARAMETERS: WATER INLET TEMP °C	WATER OUTLET TEMP °C	FREON INLET TEMP °C	FREON OUTLET TEMP °C	FREON MASS FLOW kg/s	WATER VAPOUR MASS FLOW kg/s	OUTLET QUALITY .
1	37.7	25.3	0.4	17.6	0.077	0.089	0.320
2	37.8	25.4	15.4	17.3	0.061	0.089	0.558
3	37.8	25.6	19.6	17.9	0.056	0.089	0.627
4	37.7	25.5	19.7	17.3	0.067	0.090	0.527
5	37.9	25.4	19.2	16.7	0.077	0.090	0.472
6	37.8	26.0	19.6	17.2	0.090	0.090	0.370
7	37.9	26.4	19.2	17.7	0.098	0.090	0.330
8	44.5	28.3	20.0	18.1	0.077	0.089	0.612

Table 9.2 Steady-state results (heat transferred and pressure drops)

Test Run	T_{wo} [°C]	$\dot{q}$ [kW]	Δp_F [bar]	Δp_w [bar]
1	25.3	4.61	0.07	0.13
2	25.4	4.61	0.08	0.13
3	25.6	4.54	0.08	0.13
4	25.5	4.59	0.10	0.13
5	25.4	4.70	0.14	0.12
6	26.0	4.44	0.19	0.12
7	26.4	4.33	0.20	0.12
8	28.3	6.07	0.14	0.17

Table 9.3 Transient results of heat exchanger subjected to step input change

TEST CASE	9	10	11
PARAMETERS CHANGED	WATER INLET TEMPERATURE °C	WATER FLOW RATE Kg/s	FREON FLOW RATE Kg/s
INITIAL VALUE	39.7	0.091	0.077
FINAL VALUE	45.4	0.097	0.089
63% RISE	43.3	0.095	0.085
START TIME	411 sec	170 sec	262 sec
TIME TO 63% RISE TIME	433 sec 32 sec	172 sec 2 sec	264 sec 2 sec
OUTPUT PARAMETERS	WATER OUTLET TEMP. °C	WATER OUTLET TEMP. °C	WATER OUTLET TEMP. °C
INITIAL VALUE	25.8	25.8	NO CHANGE
FINAL VALUE	28.3	26.3	NO CHANGE
63% VALUE	27.4	26.1	----
TIME AT WHICH 63% VALUE ACHIEVED	521 sec	209 sec	----
Stability reached	YES	YES	YES

Figure 9.1 Heat exchanger transient result step change in water inlet temperature, (water outlet temperature plot).

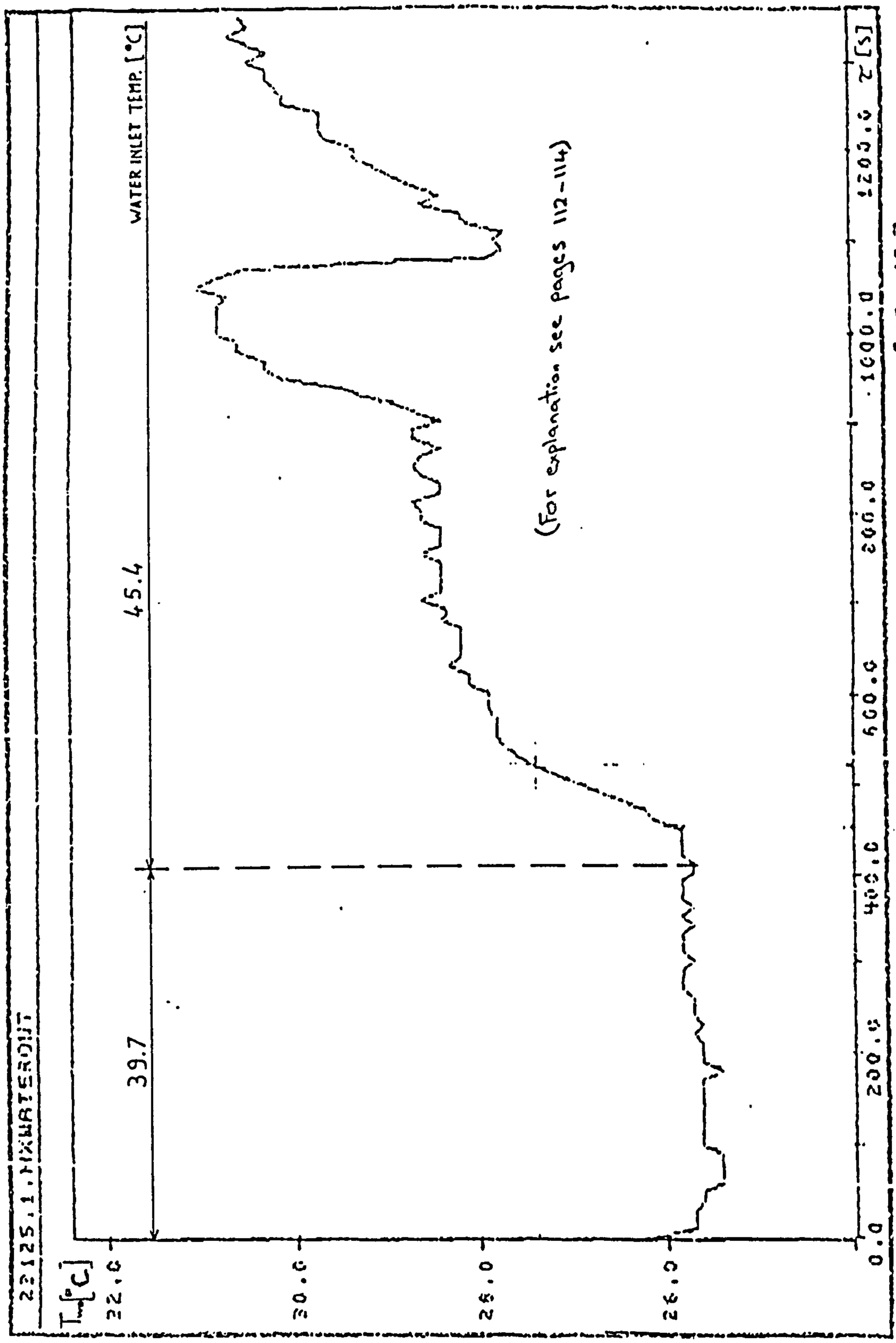

(For explanation see pages 112-114)

Figure 9.2 Heat exchanger transient result step change in water inlet temperature, (Freon outlet quality plot).

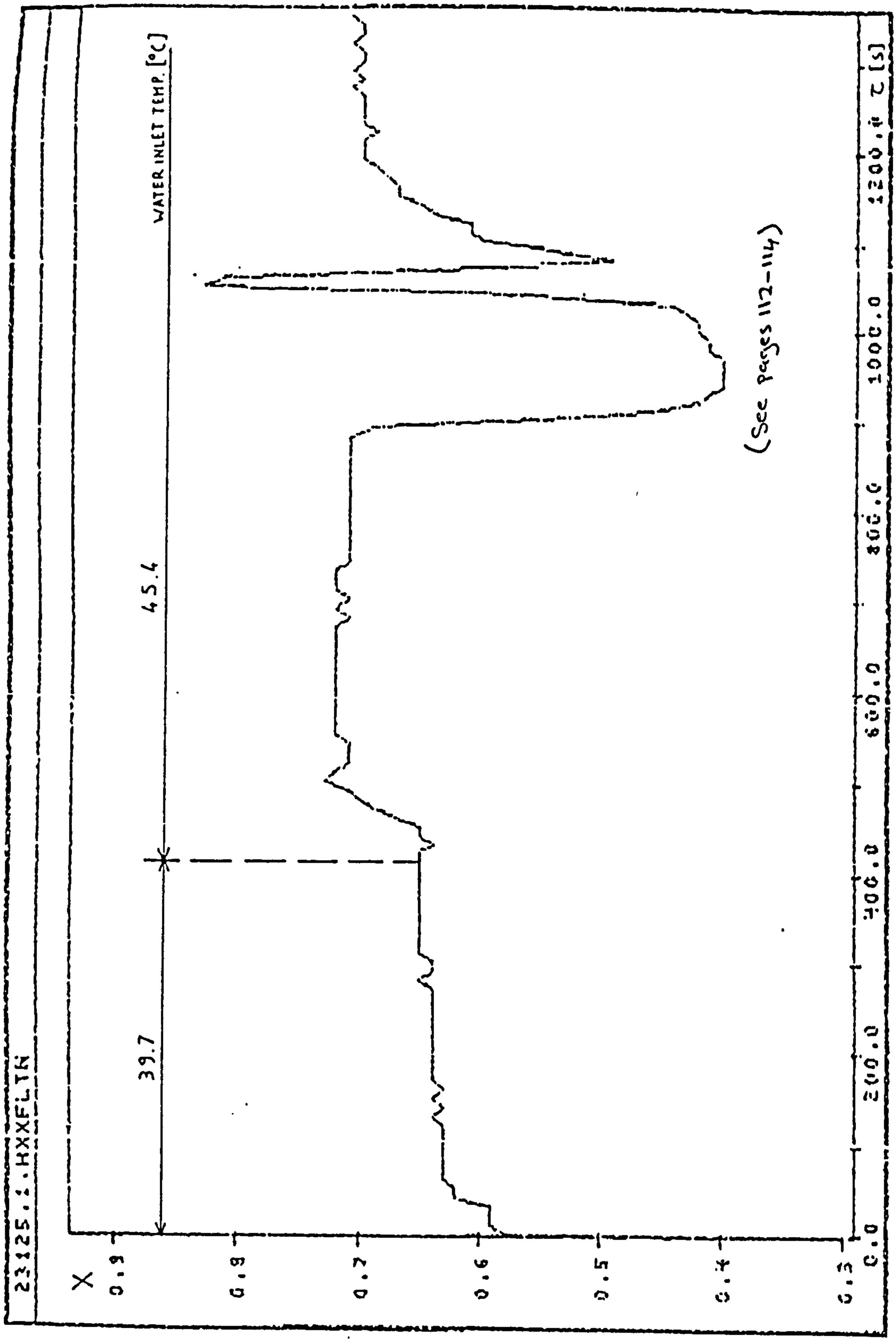

Figure 9.3 Heat exchanger transient result step change in water inlet temperature, (Freon inlet and outlet temperatures).

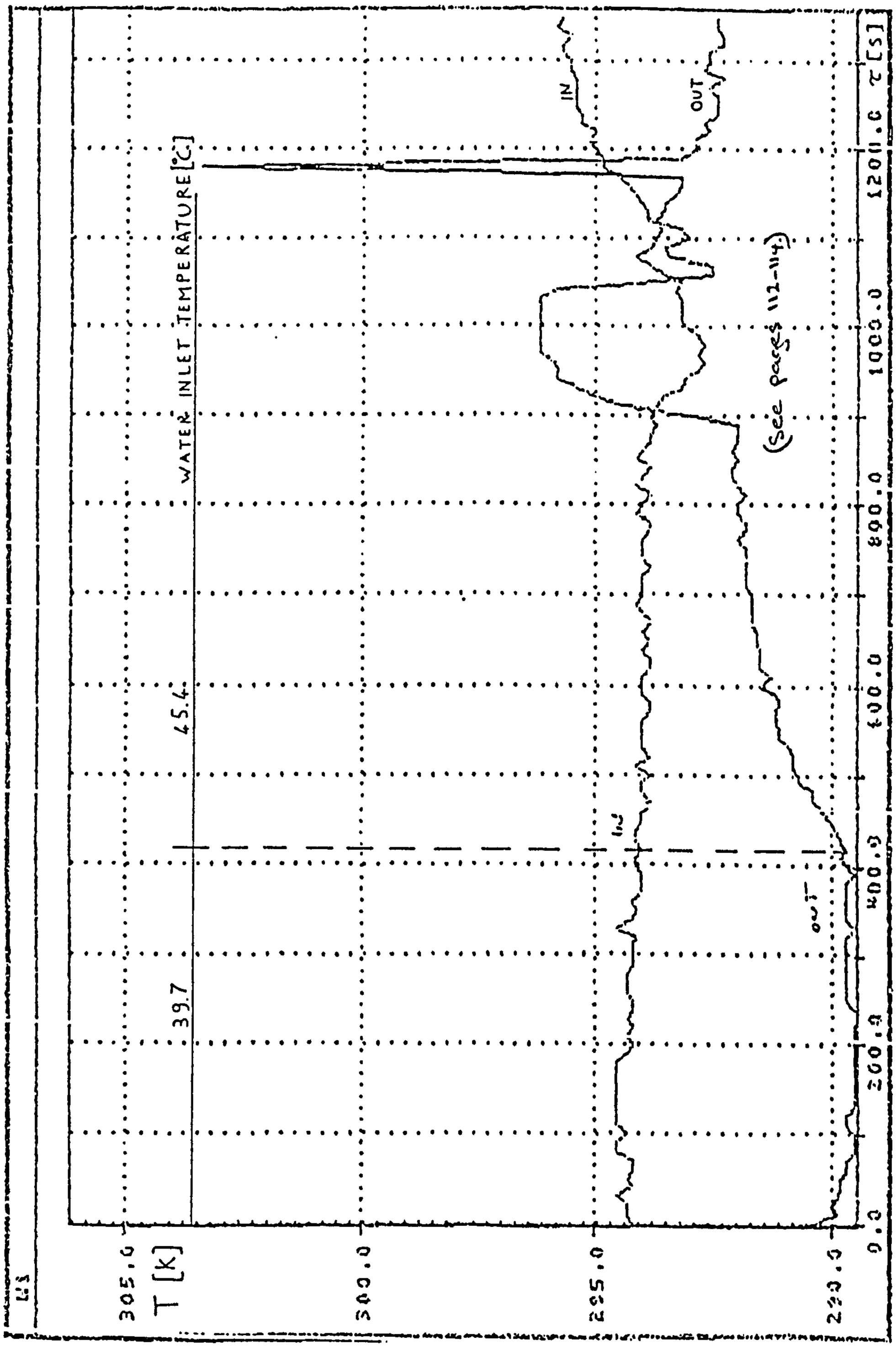

Figure 9.4 Heat exchanger transient result step change in water mass flow rate, (water outlet temperature plot).

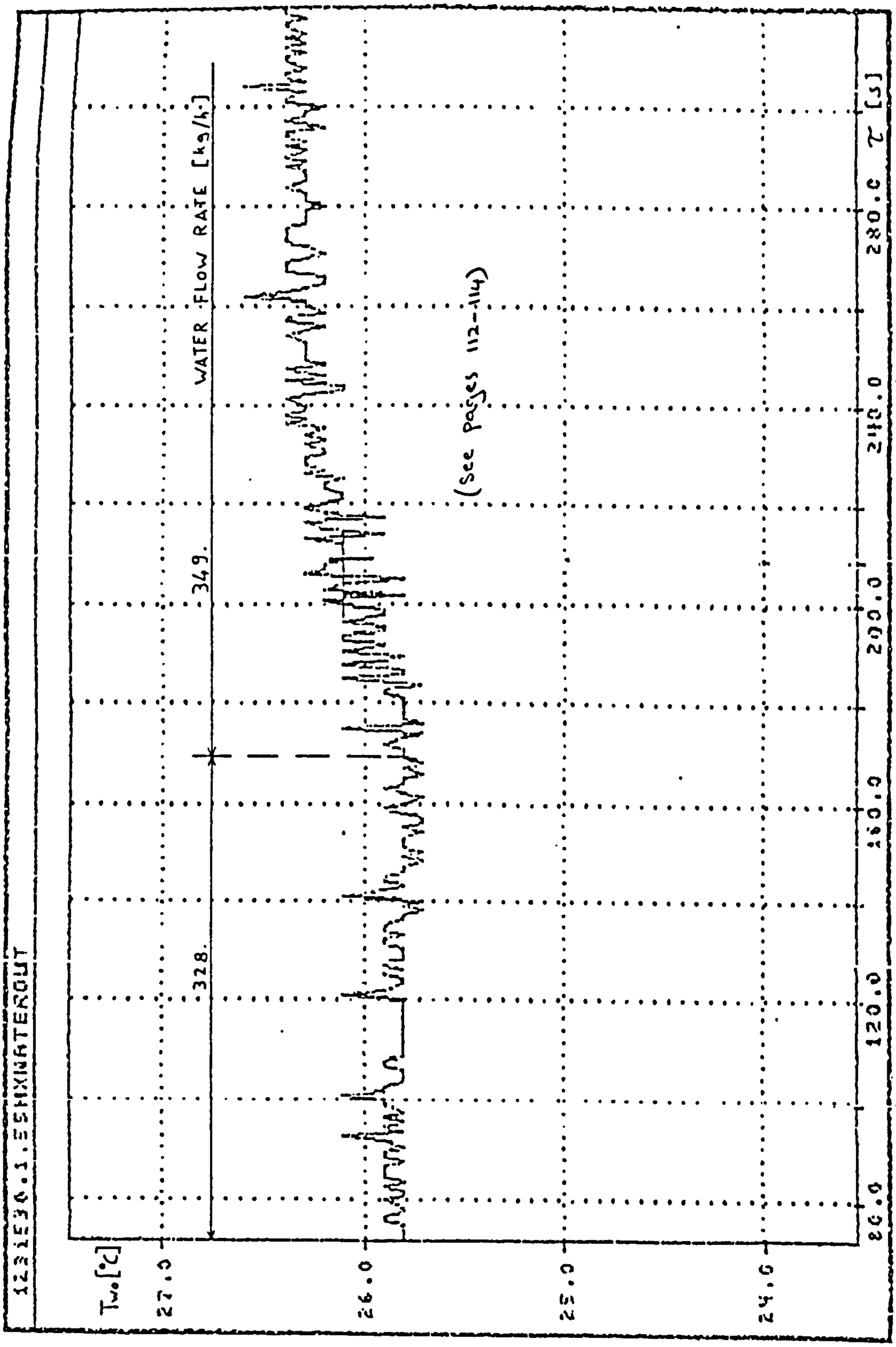

Figure 9.5 Heat exchanger transient result step change in water mass flow rate, (Freon outlet quality plot).

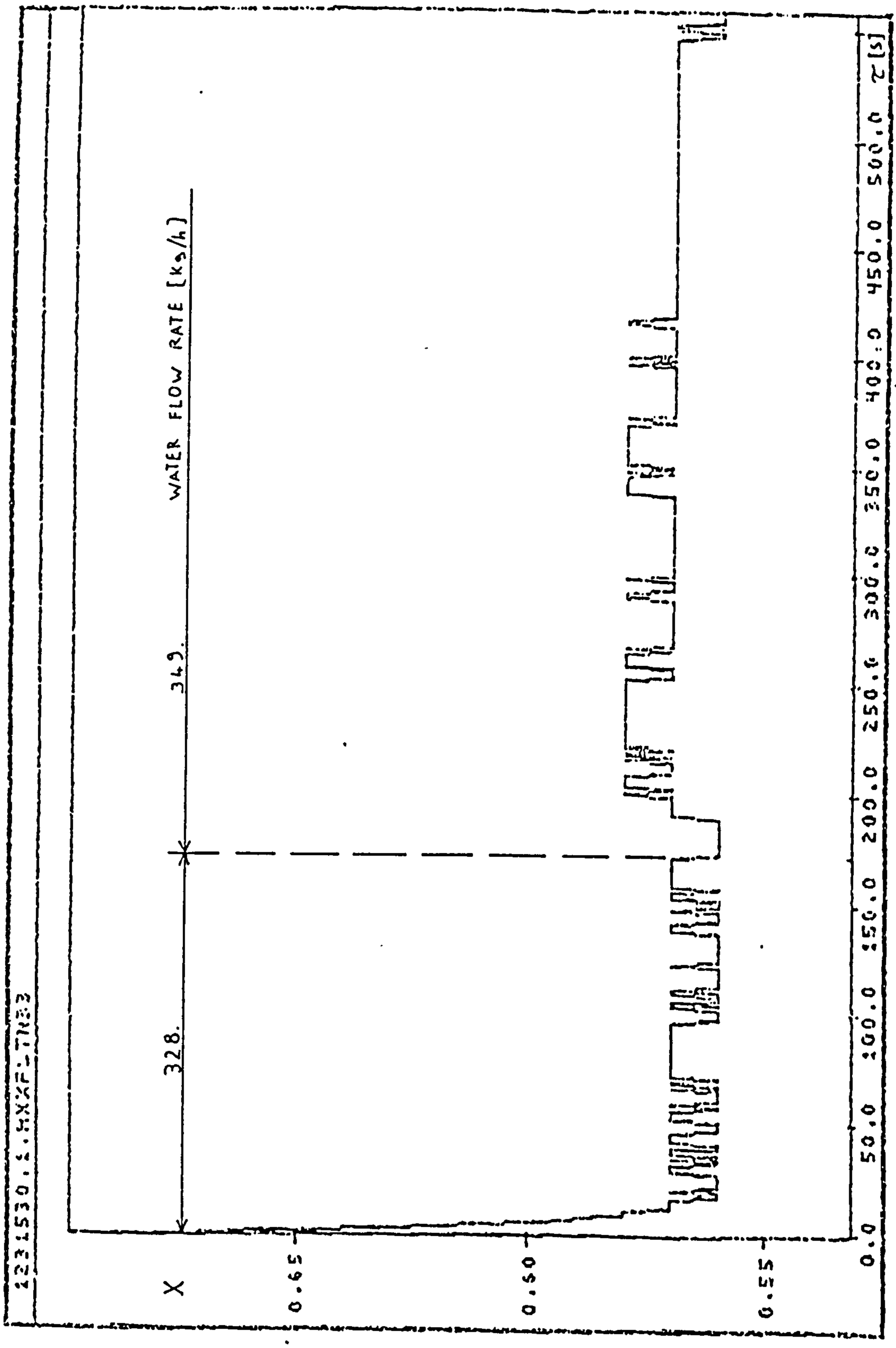

Figure 9.6 Heat exchanger transient result step change in Freon mass flow rate (water outlet temperature plot)

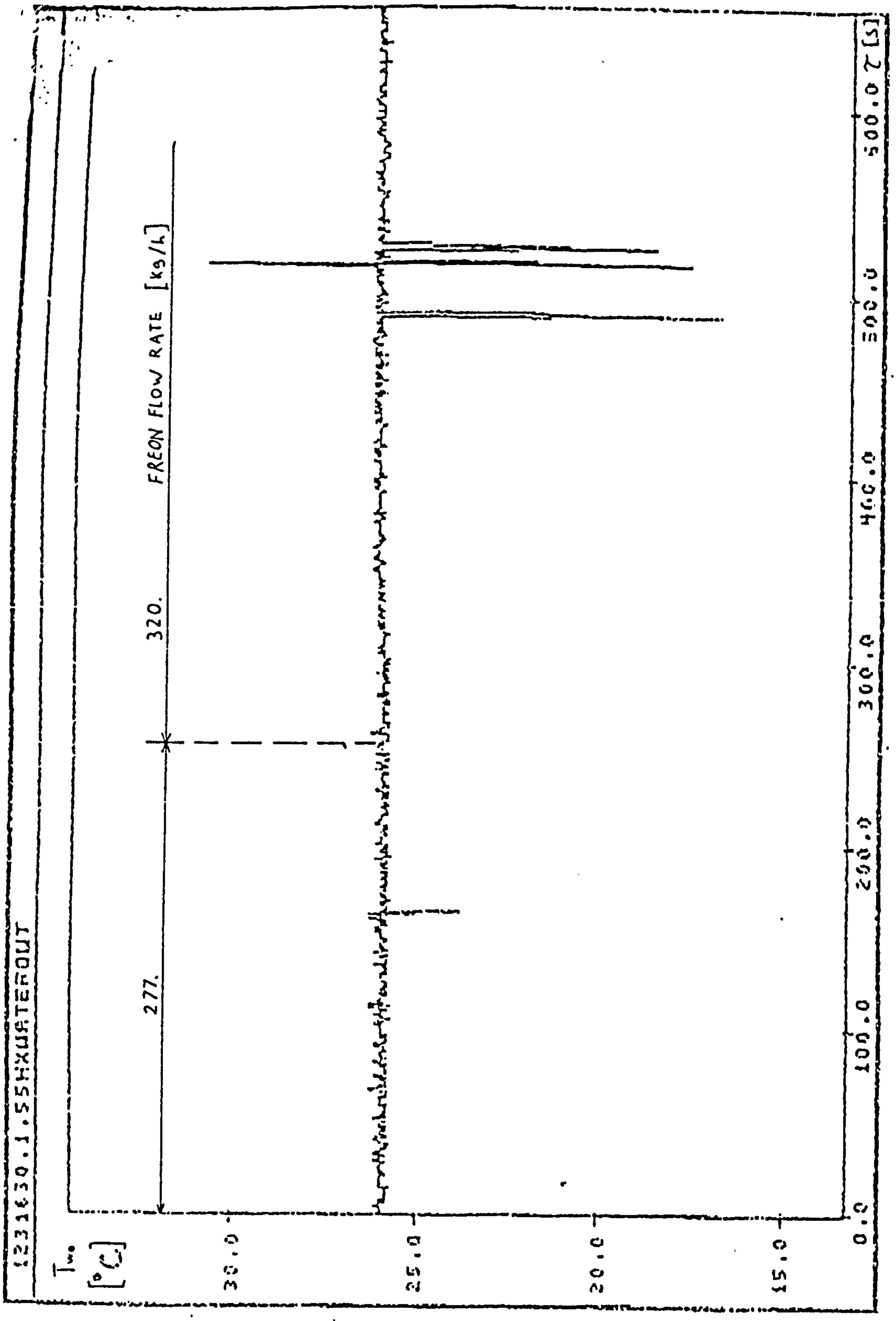

Figure 9.7 Heat exchanger transient result step change in Freon mass flow rate (Freon outlet quality response)

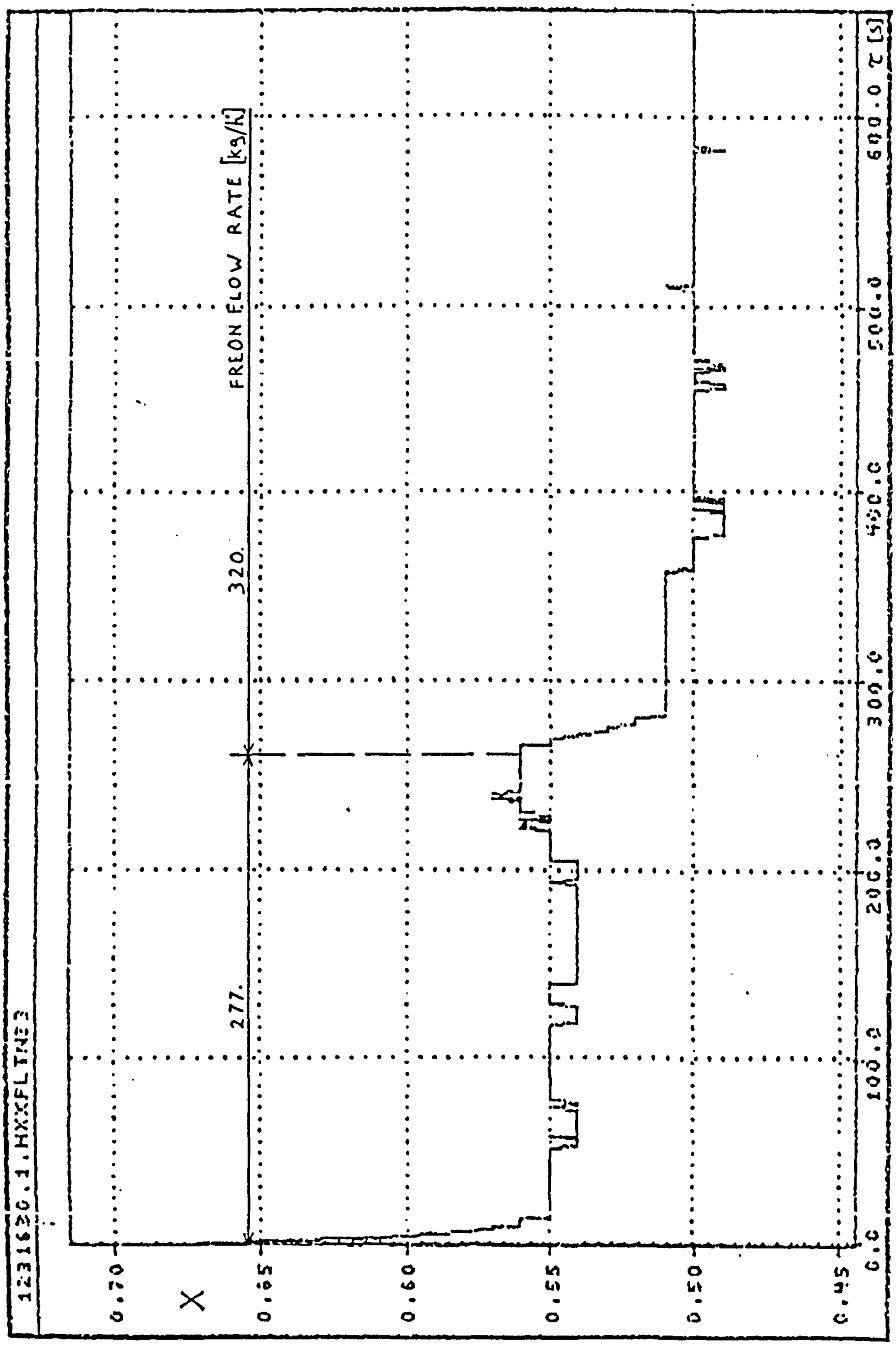

10.0 COMPARISONS OF RESULTS WITH CORRELATED TEST PREDICTIONS AND ASSUMPTIONS

The values of the heat transfer rate are based on single-phase enthalpy balance, using the following relationship:

$$q = G_w c_w (T_{wi} - T_{we})$$

The Freon outlet quality was evaluated accounting for the latent heat of evaporation of R114 at 20°C and assuming fully saturated Freon at the inlet at thermo-dynamic equilibrium.

$$x = \frac{q}{G_F \lambda_F}$$

In test cases where the inlet conditions to the heat exchanger was subcooled (5°C, 20°C subcooling) the sensible heat was accounted for by reducing the q by the sensible heat from the following relationship.

$$\text{sensible heat} = Q_F c_F (T_{sat} - T_{sub.cool})$$

The measured heat transfer rates for the heat exchanger based on single phase enthalpy balance, and those derived by analysis is shown in Table 9.1 at the heat exchanger design point. Generally there was a close agreement between test predictions and experimental results.

The variation of heat transfer, pressure drop and quality with different saturated Freon mass flow rate incorporating the error bars associated with the measurement points are shown in Figs.10.1, 10.2 and 10.3, respectively.

The measurements at the design point gave pressure drop of 14 kPa and 11 kPa for Freon and water respectively.

Summary of Nominal case Results

The test results for nominal case (case 5 in Table 8.2), summarised in Table 10.1, in terms of water outlet temperature, heat transferred q, Freon outlet vapour quality x, and Freon and water pressure drops (Δp_F, and Δp_W respectively.

The detected heat exchanger pressure drops across the water and Freon ports were close to those predicted and well within the requirements.

The heat transferred was slightly lower than the predicted. The discrepancy can be accounted for as a result of slightly different operating conditions at the inlet to the heat exchanger during the actual test. During the test the established saturation pressure was slightly higher than the operating condition, as seen in Table 8.2.

Table 10.1 Nominal case results

Parameter	Analysis	Test	Requirement
$T_{w,o}$ [°C]	24.0	25.4	-
q_t [kW]	5.1	4.7	5
x	0.53	0.49	0.4-0.8
Δp_F [bar]	0.16	0.14	<0.2
Δp_w [bar]	0.14	0.12	<0.2

Sources of Errors for The Test Results

The sources of error inherent in the test measurements were composed of random and systematic error.

The random errors were associated with the inaccuracies of the test measurements, such as the temperature sensor measurements, pressure transducer and mass flow rate measurements.

Based on calibration tests for the sensors used in the test bed, the following random errors due to the inaccuracies of the sensor are given below:

- Pressure transducers, PT2, PT4, PT10 all had an accuracy level of ± 1.5 %

- Freon flow meters had an accuracy level of ± 2.2 % at 400 l/h or ±8.8 l/h

- Water flow meters had an accuracy level of ± 2.0 % at 200 l/h or ±4.0 l/h

- Temperature sensors, computer display and recording instrumentation had an accuracy of ± 1°C

- Thermocouple temperature accuracy where ± 0.5°C

Systematic errors can be linked to the layout and geometry of the heat exchanger in its test bed.
Other uncertainties are associated with the heat loss from the heat exchanger to the environment.

There exists many statistical approaches to treat the combined effects of these error sources, however for space-based equipment design and applications a technique [ref.53], which uses the square root of the sum of the squares of all the random error sources is applied to obtain the total random error.

To the random error, the systematic error and other uncertainties are then algebraically added.

An estimate of the magnitude of the heat loss to the environment was derived based on the following assessment:

The heat transfer between the heat exchanger outer surface and the laboratory air is assumed to be by natural convection.
The ambient laboratory air during the test was

measured at 15°C and the average surface temperature of the heat exchanger was at 30°C. The natural heat transfer coefficient was calculated using the following correlation applicable for a vertical cylinder (ref.55):

$$h_C = 1.37 \left(\frac{(T_w - T_\infty)}{H} \right)^{0.25}$$

An estimate of the heat loss to the environment based on the heat exchanger external surface area (A_w) is:

$$q = A_w h_C (T_w - T_\infty)$$

As the heat exchanger was also finned externally, on the innermost cylinder (see Tab. 6.1), the overall external surface area of the heat exchanger was 1.2 m².

The natural heat transfer coefficient is therefore 3.7 W/m²K, leading to a heat loss of about 66 W.

Figure 10.1 Variation of heat transferred with Freon mass flow rate (error bars indicated)

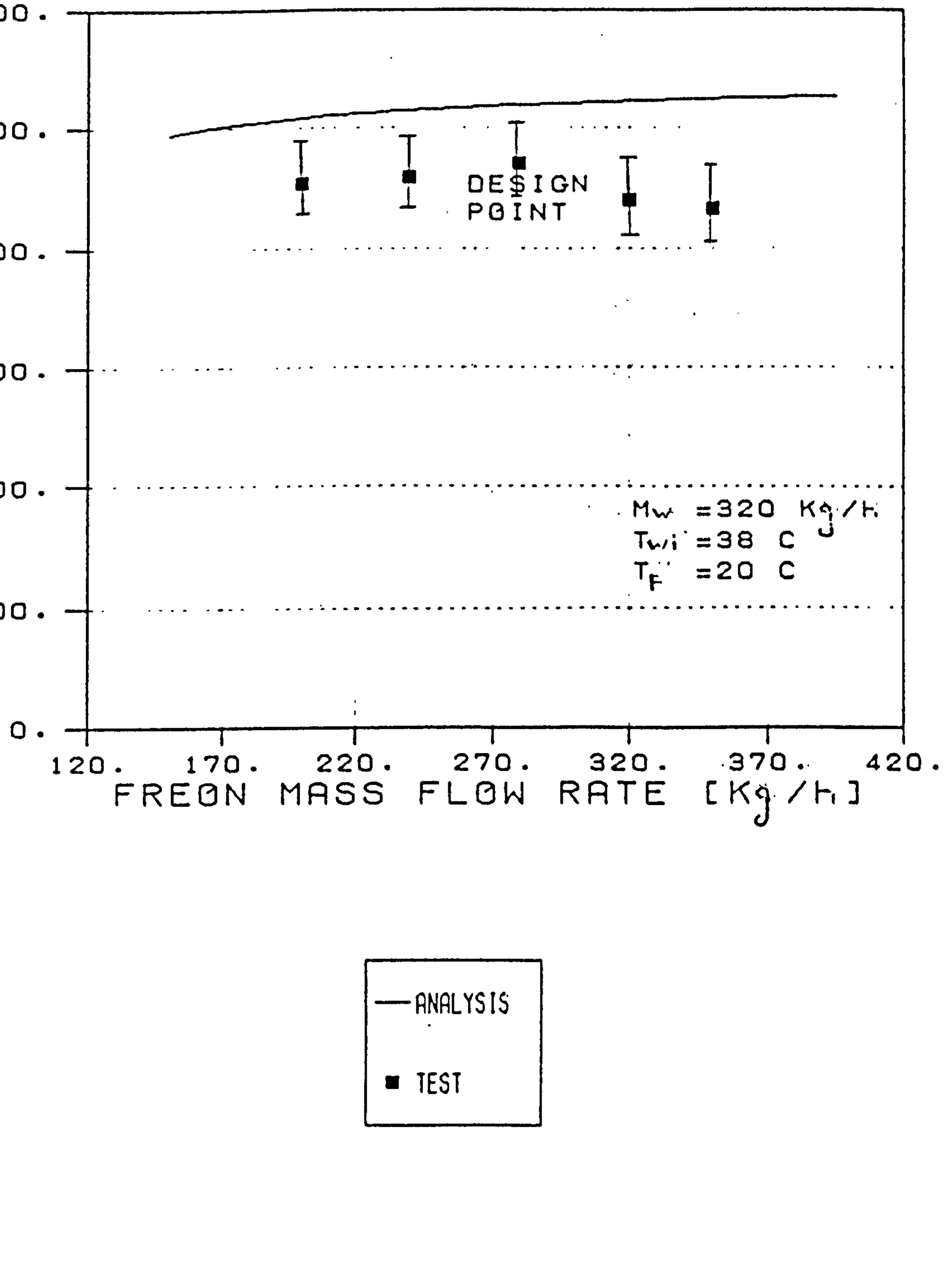

Figure 10.2 Variation of pressure drop with Freon mass flow rate (error bars indicated)

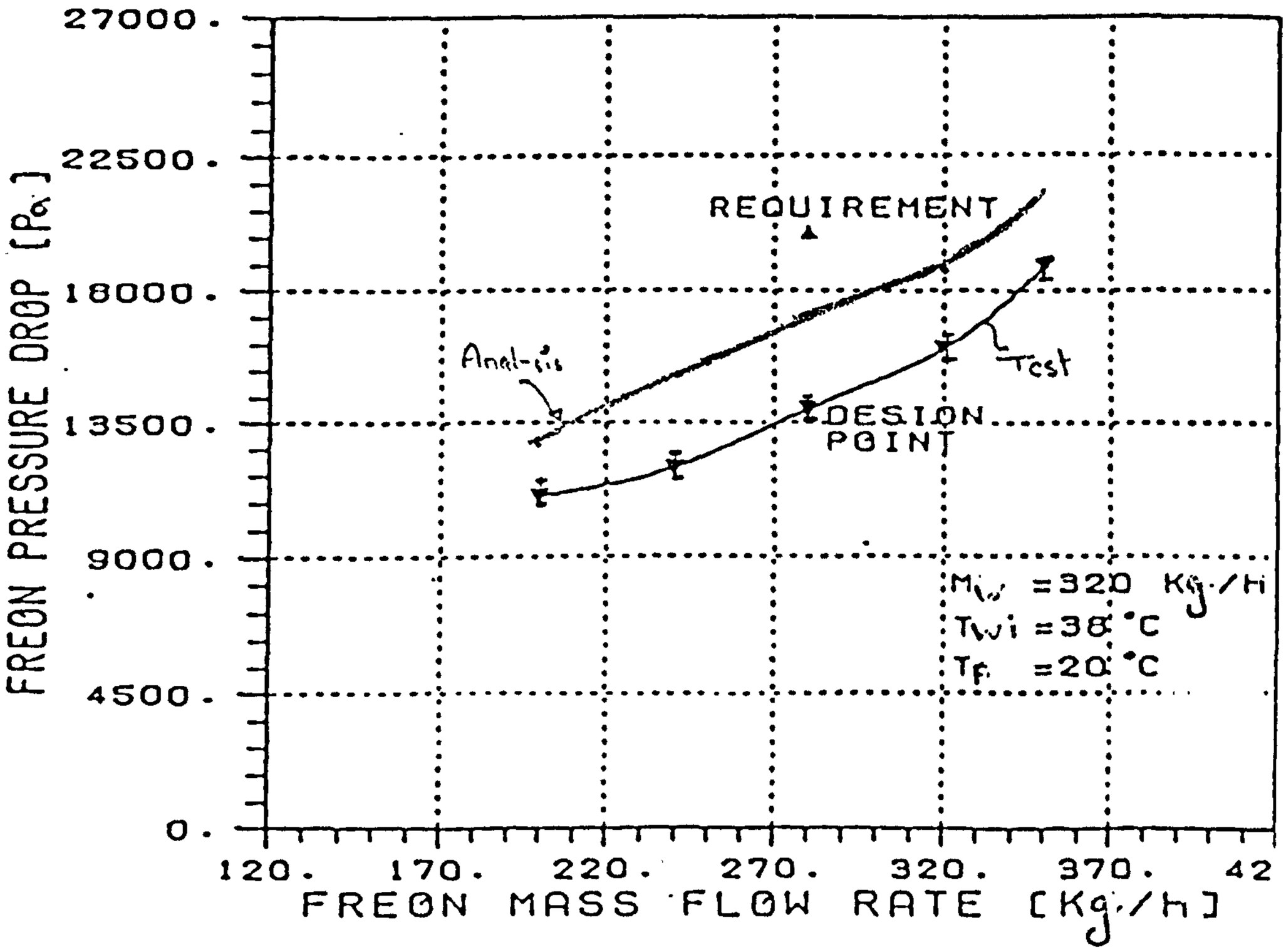

Figure 10.3 Variation of vapour quality with Freon mass flow rate (error bars indicated)

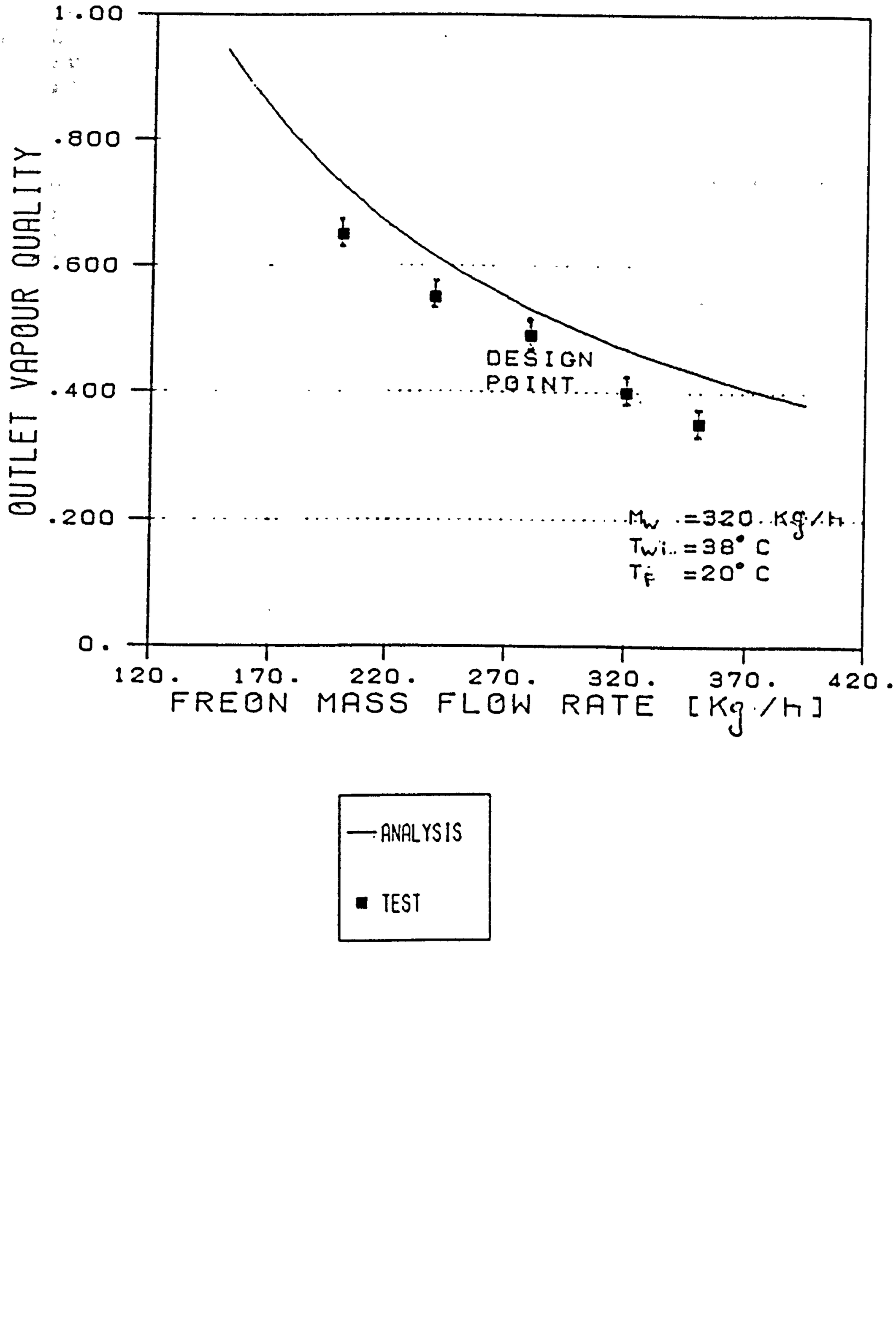

Transient Test Results

Water Inlet Temperature Step Change

The transient response of the exchanger based on a step variation in water inlet temperature (case 9 of Table 8.2), resulted in a a heat exchanger time constant of about 78s. A time delay from start of transient and resulting water outlet temperature change of about 30s.

Water Flow Rate Step Change

The transient response of the heat exchanger based on a step variation in water mass flow rate (case 10 in Table 8.2), gave a time constant (based on the water outlet temperature) of about 37 seconds. The profiles of the water outlet temperature against time and Freon outlet vapour quality are shown in Figs.9.1, and 9.2. respectively.

Freon Flow Rate Step Change

The profile of water outlet temperature for the cases regarding an input step change in Freon mass flow rate (see case 11 in Table 8.2) are shown in Fig.9.6. No appreciable change in water outlet temperature was discernible. The profile of Freon outlet vapour quality against time is shown in Fig.9.7.

ANALYSIS OF DEVIATIONS

The results of the test presented show the deviations between the test data and the predictions. In particular a maximum deviation of the heat transfer rate of 16% exists for the cases with saturated Freon conditions at the heat exchanger inlet.

Based on the analysis of the discrepancy in results between the test predictions and test measurements the following reasons for the differences can be made:

Firstly there was slightly different operating conditions for the set of tests compared to those predicted, and secondly local flow maldistribution could have occurred within the heat exchanger.
Each of the above contributing factors is discussed in the section below:

Different Operating Conditions

The heat transfer rate of the heat exchanger is proportional to the temperature profile of the fluids along their respective channel lengths. Therefore an increase in the Freon (coolant fluid) inlet pressure and hence of the operating saturation temperature yields a decrease of the heat exchanger performance, as the temperature difference across the water and Freon channels would reduce. This case occurred during the actual test, and in particular for the nominal case (see Table 8.2. The saturation temperature increase due to this effect was about 1°C.

Flow Maldistribution

In the heat transfer and pressure drop analysis of the evaporative heat exchanger, it was presumed that the fluids are uniformly distributed, through the core central part of the heat exchanger body without the headers. In particular the water flow was assumed to be symmetrically distributed between the water outer and inner channels. Contact temperature measurements on the external wall flowing in the channel close to the helix revealed temperatures lower, by 1°C, than the external section of the outer channel. This implies a slight maldistribution between the two water channels, thus reducing the temperature difference, and hence heat transfer. As the flow maldistribution is related to the size and shape of the water inlet and outlet passages, a better uniform flow distribution may be obtained by a re-design of the inlet and outlet headers.

In addition the Freon duct geometry differs from a circular section for which the possible mechanism was assessed.
A non-uniform distribution of of the liquid phase along the Freon channel section reduces the heat exchanger performance for the following reasons: firstly there is a net reduction of the effective contact area between the liquid phase flow and the Freon channel walls; secondly the asymmetric heat transfer from the two water channels. There were initially some concerns regarding the compatibility effects between aluminium and water which might have induced local corrosion internally to the exchanger which could have modified the flow distribution. A visual check of the heat exchanger inlet and outlet regions however removed this possibility. In any case the heat exchanger internal surfaces will need

to be periodically monitored in order to detect corrosion or surface coating degradation.

It is noted that during the heat exchanger transient tests were the water inlet temperature was subjected to a step response, after initial stability was reached, there was a momentary reduction in the warm water supply on the secondary side of the pre-heater heat exchanger (see Figs.9.1, 9.2, 9.3 and 1.4). The impact of this was a reduction in the Freon inlet temperature which was no longer at saturated liquid conditions. The effect of this was felt at the heat exchanger level where the Freon inlet temperature decreased and the Freon outlet temperature increased, behaving more like a single-phase heat exchanger, with a corresponding drop in Freon outlet vapour quality. As there was a drop in heat transfer coefficients, the water outlet temperature also increased.

At this stage the system controller began to take recovery actions (see Figs.9.1, 9.2 and 9.3), the heat load to the pre-heating heat exchanger (Fig.1.4) is increased, this is seen as an increase in the Freon inlet temperature (see Fig.9.3), rendering the Freon back in saturated conditions, with a corresponding drop in both Freon and water outlet temperatures.

The load on the pre-heater however continues to rise and conditions of the Freon at the inlet to the exchanger finds itself in the two-phase region. The heat exchange is reduced and the water outlet temperature begins to rise agian.
The situation is further complicated by the Freon flow control valves upstream of the heat exchanger, (see Fig.1.4) which begin to modulate the flow through them.

The interactions in terms of temperature and pressure fluctuations, vapour quality of two-phase systems are quite complex. Especially when different control logics are controlling different parts of the process. These invariably interact with one another; the situation is further complicated by the dynamics of the heat exchanger and other equipments in the loop as well as the effects of fluid propogation time delays.

A proposed way to correctly study these interactive effects is by means of a coupled thermo-hydraulic simulation of the heat exchanger incorporating appropriate control logics of the two-phase loop, (see ref.57).

11.0 HEAT EXCHANGER STEPWISE DESIGN GUIDELINES

There are many aspects which need to be considered in the design of a two-phase evaporative heat exchanger for space-based heat transport systems.
The heat exchanger must be lightweight, simple in design, compact, and have a good heat transfer performance in micro-gravity environment.
In this context a design guideline is a helpful tool in assuring that all aspects have been accounted for in the design of such space-borne hardware.

As a design aid for two-phase heat exchangers for space applications the following aspects listed below need to be considered:

1) **Identification of the gravity field.**

   This aspect is linked with the flight mission, and when the heat exchanger is required to perform. On-orbit 'micro-gravity' environment depends on altitude as well as other on-orbit perturbations such as thruster firing for attitude control on board the space-vehicle, or pump vibrations etc.

2) **Flow regime in micro-gravity environment.**

   The performance of a two-phase heat exchanger is influenced markedly with the two-phase fluid flow regime through the heat exchanger.
   The flow regimes inside a straight heated tube, where the working fluid evaporates, can be different on-ground compared to when on-orbit.
   As heat transfer and pressure drop data can be easily derived for annular two-phase flow regimes, the heat exchanger internal flow passages' should be designed as to enhance **annular flow** and promote a continuous wetting of the heated walls.

3) **Heat exchanger flow passages.**

   The design of two-phase evaporative heat exchangers should allow gravity independent flow-configurations to be achieved.
   The proposed design concept is one of

utilizing local centrifugal acceleration fields on the two-phase fluid to maintain a positive liquid-vapour phase separation.
Helical (or spiral) flow passages can be designed with small cross sectional areas to promote and maintain high heat transfer rates up to high vapour qualities.
The high heat transfer rates are maintained as the curvilinear flow path, inside the helical (or spiral) flow passages, keeps the heat exchanger walls wetted. This is assisted by a set of counter-rotating vortices set-up inside the flow passages, as a result of a secondary flow.

4) **Heat exchanger mass & pressure drops.**

In space-based systems there is a direct link between mass and pressure drop. The mass of the heat exchanger needs to be minimized as it translates directly into launch cost. Similarly the heat exchanger with a very small cross sectional area, results in a high pump power which detracts from the advantages of two-phase heat transport systems. The extra pump power needed will also require a higher electrical power supply to be taken onboard, which is an additional mass to be launched.

The computer program (see Appendix B) can be adapted for different flow passage configurations, and fluids to provide predictions of heat transfer rates and pressure drops inside the helically coiled evaporative heat exchanger. The heat exchanger geometry can then be optimised to reduce pressure drops, hence mass, for a heat exchanger with a given load to be transferred.

5) **Heat exchanger flow directions.**

Flow directions of the respective fluids effect the heat exchanger size and weight. The two types of flow are defined as counterflow (where the flows are opposite in direction) and parallel flow (where the

fluid flows in the same direction).
For two-phase evaporative heat exchanger designs (where one of the fluids is single-phase), parallel flow path is the preferred flow direction as it locates the highest temperature difference with the lowest heat transfer coefficients at the heat exchanger inlet. Similarly it locates the highest heat transfer coefficients with the lowest temperature difference at the exit of the heat exchanger.

6) **Correlations for helical flow passages.**

The correlations for heat transfer and pressure drops for the single and two-phase flows in helical flow passages to be used for the heat exchanger design definition are provided in Tables 4.2, 4.2, and 4.3.

7) **Selection of working fluid.**

In most space-based systems, water is commonly used as a single-phase heat transport fluid. Freon 114 is used as both a single and two-phase heat transport fluid as it has a low saturation pressure at 20°C, is relatively safe and belongs to a low toxicity class of Freons, and has a low freezing point, and therefore can be used in deep space radiators.
The production of the ChloroFluoroCarbons (Freon 114 being one of them) however is planned to be phased by the end of this decade and alternatives have to be found [see ref.56]
Ammonia however is another two-phase fluid intended to be used for the US Space-Station two-phase heat transportation system, taking advantage of its high latent heat of vapourization.

8) **Fluid and material compatibility.**

The choice of the heat exchanger materials is an important design consideration. For space-based thermal systems, materials with a high thermal conductivity, strength and low density are preferred. Compatibility of the fluid and heat exchanger material and parts is

important to avoid galvanic corrosion. For example if aluminium is selected for mass, and thermal reasons, the flow passages need to have protective surface treatments if water is the fluid used.

9) **Redundancy and safety.**

In most space-based systems redundancy and safety aspects are important, since in cases of failure there is no immediate repair or regular maintenance available (as would be on-ground).
In this context, any seals used in the heat exchanger design, need to be made redundant. In addition there is often a need to have a two-failure tolerant heat exchanger design. For example an overpressure of the fluid inside the passages (first failure) could lead to a rupture of the heat exchanger flow passages (second failure), leading to leakage of fluid across the flow passages, yet there may be a need for the heat exchanger to continue functioning as normal. In these cases an additional structural wall between the two fluids passages (though introduces an additional thermal barrier) can be considered in the design.

12.0 CONCLUSIONS

Helical flow passages to enhance annular flow in both micro 'g' and one 'g' environments can be employed in evaporative heat exchanger designs for space-based systems.

The flow regime similarity between micro'g' and one 'g' conditions allows on-ground predictions to be made, with a high level of confidence, of the heat exchanger performance in space environment.

A breadboard model of a 5kW helically coiled evaporative heat exchanger, for space-based systems, has been designed and manufactured. The heat exchanger design concept hinges on promoting annular flow regime, by the use of a concentric set of helical flow passages. Heat is transferred from a single-phase fluid (water) to a two-phase fluid (Freon 114), vapourizing it as it flows through the exchanger.

Ground tests gave results close to analytical predictions. Analytical predictions of the heat exchanger are based on a dedicated Fortran program incorporating correlations for two-phase heat transfer and pressure drops in helical flow passages.

13.0 RECOMMENDATIONS FOR FURTHER WORK

As regards to the choice of the two-phase fluid, the heat exchanger was designed for Freon 114, but as this fluid is planned to be phases before the end of this decade, other fluids need to be found. Ammonia is a candidate fluid currently considered for the two-phase loop of the U.S. space-station though the working pressures are much higher than Freon 114, the overall mass impact (for space utilisation) needs to be investigated.

The design of a two-phase evaporative heat exchanger with flow passages fully compliant with a two-failure tolerant requirement, needs to be investigated.

The heat exchanger computer simulation can be adapted for other fluids, however further areas of improvement are in the addition of facility to allow for the hydraulic simulation (coupled with the existing thermal simulation currently modelled). This would allow a more representative behaviour of the dynamics of the heat exchanger in transient conditions to be obtained.

Although the behaviour of the equipment, at unit level tests on-ground are encouraging, there is still a number of open areas connected with the heat exchanger behaviour, particularly in transient condition, when it is coupled with another two-phase equipment in parallel, such as a cold plate with different hydraulic characteristics.
Other hydraulic effects such as fluid propagation times through the equipment, as well as effects of operation of the exchanger in heat load sharing mode needs to be investigated.

Ultimately the exchanger needs to be tested in micro-graviry environment to verify its operational envelope.

14.0 APPENDICES

APPENDIX (A)

REFERENCES

1. **PETERSON G.P**, Thermal Control Systems for Spacecraft Instrumentation, J.SPACECRAFT, No.24,Jan-Feb, pp.7-13, 1987.

2. **DOBRAN F.** Super Heat Pipe Design Considerations to Space-Based Systems, Int. Symp. on Thermal Problems in Space-Based Systems, ASME HTD-Vol. 83, pp.1-12, 1987.

3. **GRODZKA P.G. and OWEN J.W.** Conjugating Binary Solutions for Spacecraft Thermal Control, Int. Symp. on Thermal Problems in Space-Based Systems, ASME HTD-Vol. 83, pp.109-117, 1987.

4. **DUNN P.D. and REAY D.A.**, HEAT PIPES, Pergammon Press, Oxford, 1976.

5. **McCABE M.E., KU J. and BENNER S**, Design and Testing of a High Power Spacecraft Thermal Management System, NASA Technical Memorandom 4051, June, 1988.

6. **TEGART J. and KIRKLAND Z**, On-Orbit propellant Re-supply Demonstration- Flight Results, AIAA paper No.85-1233, 1985.

7. **NAMKOONG D, BLOCK H.B, MACOSKO R.P. and CRABS C.C.**, Photographic Study of Condensing Mercury Flow in 0- and 1-G Environments, NASA TN D-4023, 1967.

8. **WILLIAMS J.L., KESHOCK E.G., WIGGINS C.L.**, Development of a Direct Condensing Radiator for use in a Spacecraft Vapour Compression Refrigeration System, ASME Journal of Engineering for Industry, Nov. pp.1053-1064, 1973.

9 **MARTINELLI R C., BOELTER L.M.K., TAYLOR T.H.M., THOMSON E.G., and MORRIN E.H.**, Isothermal Pressure Drop for Two-Phase Two-Component Flow in a Horizontal Pipe, TABS ASME, Feb, pp.139-151, 1944.

10. **KORSEMEYER R.B.** Medium-Power Reactor Experiment, Quaterly Prog. Report for Period Ending March 31, 1965, ORNL-3818, 1965.

11. **SIEGAL R. and USISKIN C.**, A Photographic study of boiling in the absence of gravity, TRANS ASME 81, Ser. C 230, 1959.

12. **WEINZIERI A. and STRAUB J.** Nucleate pool boiling in microgravity environment, PROC 7TH Int. HEAT TRANSFER Conf. 4, 1982.

13. **SIEGAL R.**, Effects Of Reduced Gravity On Heat Transfer, Advances In Heat Transfer, Academic Press, N.Y., pp.143-228, 1967.

14. **COCHRAN T.H.**, Forced-Convection Boiling Near Inception in Zero Gravity, NASA TN D-5612, 1970.

15. **OTSUJI T. and KUROSAWA A.**, Critical Heat Flux of Forced Convection Boiling in an Oscillating Acceleration Field- I. General Trends, Nuclear Engineering and Design, V71, pp.15-26.

16. **BERGLES A.E., COLLIER J.G., DELHAYE J.M., HEWITT G.F. and MAYINGER F.**, Two-Phase Flow and Heat Transfer in the Power and Process Industries, McGraw-Hill, New York, 1981.

17. **DUKLER A.E. and WICKS III, M. and CLEVELAND, R.G.**, Frictional Pressure Drop in Two-Phase Flow, American Institute Of Chemical Engineers Journal Vol. 10, pp.44-51, Jan.1964.

18. **ISBIN H.S., MOEN R.H., WICKEY R.O., MOSHER D.R. and LAESON H.C.**, Frictional Pressure Drop Correlations For Horizontal Pipe Flow, Chemical Engineering Progress Symposium Series, Vol.55 No. 23, pp.75-84, May 1959.

19. **HUGHMARK,G.H. and PRESSBURG B.S.**, Holdup and Pressure Drop With Gas.Liquid Flow in a Vertical Pipe, A.I.Ch,E. Journal, Vol.7, pp.677-682, Dec.1961.

20. **LEVY.S.**, Prediction of the Phase Pressure Drop and Density Distribution from Mixing Length Theory, Transactions of the American Society of Mechanical Engineers, pp.137-152, May 1962.

21. **LOCKHART R.W. and MARTINELLI R.C.**, Proposed Correlation Data for Isothermal Two-Phase, Two Component Flow in Pipes, Chemical Engineering Progress, Vol.45, No.1, pp.39-48, Jan.1949.

22. **SUO M. and GRIFFITH P.**, Two-Phase Flow Capilliary Tubes, Transactions of the American Society of Mechanical Engineers, pp.137-144, Sept. 1984

23. **BRAUN C.E., FREDLEY J.E., GILBERTI V.J. and HARTSHORN K.**, Applications Of Two-Phase Thermal

Transport Systems To Space Platforms, Int. Symp. on Thermal Problems in Space-Based Systems, ASME HTD-Vol. 83, pp.125-134, 1987.

24. **CHEN X., and ZHOU, F.**, The Two-Phase Flow in Helical Coiled Tube, Scientific Rept. 85-436, Xi'an Jiaotong University, China, 1985.

25. **KREEB H. and SIEPMANN R.**, Two-Phase Heat Transport System-Critical Component, Proc.3rd Eur. Symp. Space Thermal Control and Life Support Systems, Noordwijk, pp.75-82,1988.

26. **O'CALLAGHAN, P.W., and PROBERT S.D.**, Thermal resistance and directional index of pressed contacts between smooth non-wavy surfaces, I.MECH. ENG. Science, 16, 1, 41-55, 1974.

27. NIKANPOUR, D. Two-Phase Flow Technology Development Model Definition, BAe Tech. Note TN 4956, Aug. 1986 and June 1987.

28. **DUKLER A.E, WICKS M. and CLEVELAND R.G.**, Frictional Pressure Drop in Two-Phase Flow: A. A Comparison of Exsisting Correlation for Pressure Loss and B. An Approach Through Similarity Analysis, AIChE Jl, Vol.10, No.1, pp.38-51, 1964.

29. **HEPPNER D.B., KING C.D. and Littles J.W.**, Zero-G Experiments in Two-Phase Fluid Flow Regimes, ASME paper 75-ENAs-24, 1975.

30. **DUKLER A.E, FABRE J.A., McQUILLEN J.B. and VERNON R.**, Gas Liquid Flow at Micro-gravity Conditions: Flow Patterns and their Transitions, Int.Jl. Multiphase flow, Vol. 14, No.4,pp389-400, 1988.

31. **CRAIN B.Jr., and BELL K.J.**, Forced Convection Heat Transfer to a Two-Phase Mixture of Water and Steam in a Helical coil, AIChE Symp. Ser., Vol.69, No.131, pp.30-36, 1979.

32. **COLLIER N.G.**, Convective Boiling and Condensation, Mc.Graw Hill, N.Y., 1981.

33. **BANERJEE S., RHODES, E. and SCOTT D.S.**, Studies on cucurrent Gas Liquid Flow inHelically Coiled Tubes, Canadian J. Chem. Eng., 47, pp.445-517, 1969.

34. **OWHADI A.**, PhD. thesis, Oklahoma St. Univ., Stillwater (1966).

35. **ROHSENOW W.M., HARTNETT J.P., GANIC E.N.**, Handbook

of Heat Transfer Fundamentals, McGraw-Hill, N.Y.,1985.

36. **LOCKHART. R.W., and MARTINELLI R.C.,** Chem Eng. Prog., 45,39, 1949.

37. **KANDIKAR S.G.,** A General Correlation For Saturated Two-Phase Flow Boiling Heat Transfer Inside Horizontal and Vertical Tubes, Boiling and Condensation in Heat Transfer Equipment ASME HTD-Vol. 85, pp.9-19, 1987.

38. **WATTENDORF F.L.,** A study of the Effect of Curvature on Fully Developed Turbulent Flow, Proc. Royal Society, Vol. 148A, pp.565-598, 1935.

39. **LOVELL T.M.,** Liquid-Vapour Flow Regime Transitions for Use in Design of Heat Transfer Loops in Spacecraft: An In vestigation of Two-Phase Flow in Zero Gravity Conditions, AFWAL-TR-85-3021, 1985.

40. **THEOFANOUS, T.G.** Modelling Of Aerospace (Micro-gravity) Systems, Lecture Presented at short course on Two-Phase Flow Fundamentals for Industrial Applications, 23-27 March, 1987, ETH Zurich, 1987.

41. **COCHRANE P.H.,** Forced Convection Boiling near Inception in Zero Gravity, NASA-TN-D-5612, 1970.

42. **JANSSEN L.A.M. and HOOGENDOORN, C.J.,** Laminar Convective Heat Transfer in Helically Coiled Tubes, Int.J. Heat Mass Transfer, Vol.21,pp.1197-1206, 1978.

43. **WHITE C.N.,** Streamline Flow Through Curved Pipes, Proc. of the Royal Society, Vol. 123A, pp.645-663, 1929.

44. **SRINIVASAN P.S., NANDAPURKAR and HOLLAND F.A,** Pressure Drop and heat Transfer in Coils, Chem. Engr. No.218, 1968.

45. **KALB C.E. and SEADER J.D.,** Fully developed Viscous-Flow Heat Transfer in Curved Circular Tubes with Uniform Wall Temperature, AIChE Journal, VOL 20, pp.340-346, 1974.

46. **SEBAN R.A. and McLAUGHLIN E.F.,** Heat Transfer in Tube Coils with Laminar and Turbulent Flow, Int.Jl. Heat Mass Transfer, Vol 6,pp.387-395, 1963.

47. **PREMOLI A., FRANCESCO D. and PRINA,** A Dimensionless

Correlation for determining the Density of Two-Phase Mixtures, Termotecnica, 25,pp.17-26, 1979.

48. **CHEN J.C.**, A Correlation for Boiling Heat Transfer to Saturated fluids in Convective flow, ASME pre-prints 63-HT-34 presented at 6th National Heat Transfer Conference, Boston 11-14 Aug. 1963.

49. **HERD K.G., GROSS, W.P, CONNELL**, J.W, Correlation of Forced Flow Evaporation Heat Transfer Coefficients in Refrigeration Systems, Heat Exchangers for Two-Phase Applications, ASME Publications, HTD-27, pp.11-18, 1983.

50. **MERILO M.** Fluid-to-Fluid Modelling and Correlation of Flow Boiling Crisis inHorizontal Tubes, Int. J. Multiphase Flow, 5, pp.313-325, 1979.

51. **BADR O., PROBERT S.D., O,CALLAGHAN P.W.**, Selecting a Working Fluid for a Rankine-Cycle Engine, Applied Energy 21 pp.1-42, 1985.

52. **FREON fluorocarbon:** Properties and applications, Bulletin B-2E, du Pont de Nemoours Int. S.A., Geneva, Switzerland, 1982.

53 **STUMPEL D., CHALMERS D.**, Application of Uncertainty Philosophy to satellite Thermal Design, AIAA, 19th Thermophysics Conf., Snowmass, Colorado, June 25-28, 1984.

54 **DEAN W.R.**, Motion Of Fluid in Curved Pipe, Phil Mag. S7,4, pp 208-223, 1927.

55 **KOTHANDARAMAN C.P., SUBRAMANYAN S.**, Heat and Mass Transfer Data Book, Third Edition, 1977.

56 **BADR O., PROBERT S.D., O'CALLAGHAN P.W.**, Chlorofulorocarbons and the Environment: Scientific, Economic, Social and Political Issues. Applied Energy 37 pp 247-327, 1990.

57 NIKANPOUR D., CHAMPOLINI F., STANGERUP P., Thermo-Hydraulic Simulation and Regulation of Active Thermal Control Systems using ESACAP software, 4th European Symp. on Space Environmental Ccontrol Systems, Florence, Italy, Oct.1991.

APPENDIX (B) .

COMPUTER PROGRAM LISTING

The program reads input data from file TPEHX_% SUBS%.DAT where %SUBS% is the subscript identifying the run.

Card 1 : DENSAL, CONDAL, EPS

DENSAL	:	Aluminum density (kg/m^3)
CONDAL	:	Aluminum conductivity ($W/m°C$)
EPS	:	Aluminum roughness factor (mm) (presently not used)

Card 2 : DENSW, CPW, CONDW, VISCW

DENSW	:	Water density (kg/m^3)
CPW	:	Water specific heat capacity ($J/kg°C$)
CONDW	:	Water conductivity ($W/m°C$)
VISCW	:	Water viscosity (Ns/m^2)

Card 3 : DENSLF, CPLF, CONDLF, VISCLF, RLATENT

DENSLF	:	Liquid freon density (kg/m^3)
CPLF	:	Liquid freon specific heat capacity ($J/kg°C$)
CONDLF	:	Liquid freon conductivity ($W/m°C$)
VISCLF	:	Liquid freon viscosity (Ns/m^2)
RLATEN	:	Liquid freon vaporization latent heat (kJ/kg)

Card 4 : DENSVAP, VISCVAP, SIGMA

DENSVAP	:	Vapor freon density (kg/m^3)
VISCVAP	:	Vapor freon viscosity (Ns/m^2)
SIGMA	:	Surface tension (N/m)

Card 5 : TINW, TINF, PRESINF, QWATER, QFREON, XQUALI

TINW : Water inlet temperature (°C)
TINF : Freon inlet temperature (°C)
PRESINF : Freon inlet pressure (Pa), (presently not used)
QWATER : Water flow rate (kg/hr)
QFREON : Freon flow rate (kg/hr)
XQUALI : Freon inlet quality

An XQUALI value lower than zero may be used to take into account freon subcooling (the freon temperature is assumed to remain constant).

Card 6 : DWATER, DFREON, DCOIL, WALLTK, FINTK, NPW, NPF

DWATER : Water ducts hydraulic diameter (mm)
DFREON : Freon ducts hydraulic diameter (mm)
DCOIL : Medium coil diameter (mm)
WALLTK : Wall thickness (mm)
FINTK : Fin thickness (mm)
NPW : Water ducts number
NPF : Freon ducts number

Card 7 : BETA1, BETA, LCOIL, INTERV

BETA1 : Numerical parameters used in the
BETA2 evaluation of thermal resistence
RLCOIL : Coil length (m), (maximum duct length of freon)
INTERV : Number of intervals in which the coil length must be divided to obtain temperatures and pressure drops distributions

Card 8 : QTOT

QTOT : heat transfer rate required to the heat exchanger. It should be noted that the program stops when either the maximum duct length or the heat transfer rate are achieved

```
IBM Professional FORTRAN Compiler (V1.00) by Ryan-McFarland Corp
Source File: MAIN.FOR                    Options: /l

    1         PROGRAM MAIN
    2
    3 C       Program TPEHX solves the problem of a Two Phases Heat Exchanger.
    4
    5         INCLUDE 'INS.FOR'
    6         PARAMETER (NTEMP  =  26)
    7         PARAMETER (NPRES  =  26)
    8         COMMON /COM1R/ DENSW,CPW,CONDW,VISCW,DWATER,AWATER,QWATER,NPW
    9         COMMON /COM2R/ STEVIS,WATVIS,STEDEN,WATDEN
   10         COMMON /COM3R/ DENSAL,CONDAL,EPS
   11         COMMON /COM4A/ DENSLF,CPLF,CONDLF,VISCLF,RLATEN,QFREON,DFREON
   12        &,NPF,AFREON
   13         COMMON /COM5N/ WALLTK,FINTK,BETA1,BETA2,DCOIL,RLCOIL,INTERV
   14         COMMON /COM06/ TEMP(NTEMP),PRES(NPRES)
   15         COMMON /COM07/ DENSVA,VISCVA,SIGMA
   16         COMMON /COM08/ IFLOW,DPA,DPF,ALPHA,XCAP,XCAP1,FIQUAD,F,S,HC,HNCB,R
   17         COMMON /COM09/ TINW,TINF,PRESIN,XQUALI,QTOT
   18         COMMON /COM10/  NIN , NOUT , NPLOT , NTTY
   19         COMMON /COM11/ DPTOT
   20
   21
   22         OPEN(5,FILE='TPEHX.DAT')
   23         OPEN(6,FILE='TPEHX.OUT')
   24         OPEN(7,FILE='TPLOT.LST')
   25
   26         WRITE(0,*)'[ TPEHX rev 1.0 ]'
   27
   28         CALL INPUT
   29
   30         CALL TPEHX
   31
   32         WRITE(NOUT,'(///,10X,A)')'***** TPEHX COMPLETED OK *****'
   33
   34         WRITE(0,*)'***** TPEHX COMPLETED OK *****'
   35
   36         STOP
   37
   38         END
```

```
      BLOCK DATA TPINIT
      INCLUDE 'INS.FOR'
      DATA NIN / 5 / , NOUT / 6 / , NPLOT / 7 / , NTTY / 0 /
      DATA TEMP/0,2,4,6,8,10,12,14,16,18,20,22,24,26,28,30,32,34,36,38,
     &40,42,44,46,48,50/
      DATA PRES/0.08778,0.09496,0.10259,0.11069,0.11928,0.12837,
     &0.13799,0.14816,0.15890,0.17022,0.18215,0.19470,0.20791,
     &0.22178,0.23634,0.25161,0.26762,0.28438,0.30192,0.32026,
     &0.33941,0.35941,0.38028,0.40204,0.42471,0.44831/
      END
*****************************************************************************
      SUBROUTINE INPUT
C----- INPUT DATA  ---------------------------------------------------
      INCLUDE 'INS.FOR'
C----- INPUT & ECHO  -------------------------------------------------
      WRITE(NOUT,900)
  900 FORMAT( 1H1,/,1X,132('*') )
      WRITE(NOUT,910)
  910 FORMAT(///,10X,' P R O G R A M    T P E H X')
      WRITE(NOUT,920)
  920 FORMAT(///,10X,
     &' CALCULATION OF HEAT FLOW FOR WATER TO' ,
     &' FREON HELICOIDAL HEAT EXCHANGER')
      WRITE(NOUT,930)
  930 FORMAT( ///,1X,132('*') )
      WRITE(NOUT,1000)
 1000 FORMAT (1H1,/,10X,'***** INPUT ECHO *****',//)
      READ(NIN,*) DENSAL,CONDAL,EPS
      WRITE(NOUT,1001) DENSAL,CONDAL,EPS
 1001 FORMAT(/,10X,'Aluminum properties',//,5X,'Density (Kg/m3) =',
     &F10.4,12X,'Conductivity (W/M*C) =',F10.4,
     &21X,'Roughness Factor (mm) =',F10.4,//)
      READ(NIN,*) DENSW,CPW,CONDW,VISCW
      WRITE(NOUT,1002) DENSW,CPW,CONDW,VISCW
 1002 FORMAT(/,10X,'Water properties',//,5X,'Density (Kg/m3)    =',
     &F10.4,10X,'Specific Heat Capacity (J/Kg*C) =',F10.4,
     &10X,'Conductivity (W/m*C) =',F10.4,/,
     &5X,'Viscosity (Ns/m2) =',E10.4,//)
      READ(NIN,*) DENSLF,CPLF,CONDLF,VISCLF,RLATEN
      WRITE(NOUT,1003) DENSLF,CPLF,CONDLF,VISCLF,RLATEN
 1003 FORMAT(/,10X,'Liquid Freon properties',//,5X,
     &'Density (Kg/m3)    =',F10.4,10X,
     &'Specific Heat Capacity (J/Kg*C) ='
     &,F10.4,10X,'Conductivity (W/m*C) =',F10.4,/,5X,
     &'Viscosity (Ns/m2) =',E10.4,10X,'Latent Heat (kJ/Kg) =',F10.4,//)
      READ(NIN,*) DENSVA,VISCVA,SIGMA
      WRITE(NOUT,1004) DENSVA,VISCVA,SIGMA
 1004 FORMAT(/,10X,'Freon Vapor properties',//,5X,
     &'Density (Kg/m3)    =',F10.4,/,5X,
```

```
      READ(NIN,*) TINW,TINF,PRESIN,QWATER,QFREON,XQUALI
      WRITE(NOUT,1005) TINW,TINF,PRESIN,QWATER,QFREON,XQUALI
1005 FORMAT(/,10X,'Initial Conditions',//,5X,
     &'Water Inlet Temperature (C) =',F10.4,10X,
     &'Freon Inlet Temperature (C) =',F10.4,10X,/
     &,5X,'Freon Inlet Pressure (Pa)   =',E10.4,/
     &,5X,'Water Flow (Kg/h)           ='
     &,F10.4,10X,'Freon Flow (Kg/h)=',F10.4,10X,
     &'Initial Vapor Quality =',F8.4,//)

      READ(NIN,*) DWATER,DFREON,DCOIL,WALLTK,FINTK,NPW,NPF
      READ(NIN,*) BETA1,BETA2,RLCOIL,INTERV
      WRITE(NOUT,1006) DWATER,DFREON,DCOIL,WALLTK,FINTK,RLCOIL,NPW,NPF
     &,BETA1,BETA2,INTERV
1006 FORMAT(/,10X,'System Parameters',//,5X,
     &'Water Equivalent Diameter (mm) =',F8.3,7X,
     &'Freon Equivalent Diameter (mm) =',F8.3,7X,
     &'Coil Diameter (mm) =',F10.4,/,5X,
     &'Wall Thickness (mm)            =',F8.3,7X,
     &'Fin Thickness (mm)             =',F10.4,7X,
     &'Coil length (m)  =',F10.4,/,5X,
     &'Water Ducts Number             =',I3,10X,
     &'Freon Ducts Number =',I3,/,5X,
     &'Beta1 =',F8.4,5X,'Beta2 =',F8.4,5X,
     &'Intervals Number =',I10,//)

      READ(NIN,*) QTOT
      WRITE(NOUT,1007) QTOT
1007 FORMAT(/,10X,'Requested total heat exchanged (W) =',F10.4,//)

      STEVIS=16.25E-06
      WATVIS=125.2E-06
      STEDEN=10.6
      WATDEN=847.
      WRITE(NOUT,1009) STEVIS,WATVIS,STEDEN,WATDEN
 1009 FORMAT(/,10X,'Steam and water properties satisfying property
     & index:',//,10X,'Steam viscosity (Ns/m2) = ',E10.4,5X,
     &'Water viscosity (Ns/m2) = ',E10.4,
     &/,10X,'Steam density (Kg/m3)   = '
     &,E10.4,5X,'Water density (Kg/m3)   = ',E10.4,/)

C----- PROPERTY INDEX EVALUATION AND PRINTING ------------------------------

      PINDEX=((VISCLF/VISCVA)**0.2)*DENSVA/DENSLF
      WRITE(NOUT,1008) PINDEX
 1008 FORMAT(/,10X,'Freon property index =',F10.4,/)
      PINDWA=((WATVIS/STEVIS)**0.2)*STEDEN/WATDEN
      WRITE(NOUT,1010) PINDWA
 1010 FORMAT(10X,'Water property index =',F10.4,/)

      WRITE(NOUT,1077)
 1077 FORMAT (///,10X,'***** END OF INPUT ECHO *****',//)

C----- UNITS HOMOGENEIZATION -----------------------------------------------

      DWATER=DWATER/1000.
      DFREON=DFREON/1000.
      DCOIL=DCOIL/1000.
      WALLTK=WALLTK/1000.
      FINTK=FINTK/1000.
      EPS=EPS/1000.
      QWATER=QWATER/3600.
      QFREON=QFREON/3600.
```

```
**********************************************************************
      SUBROUTINE TPEHX

      INCLUDE 'INS.FOR'

      DIMENSION FLAG(2)
      CHARACTER FLAG*10
      DATA FLAG/'Turbulent ',' Laminar '/

C----- COMPUTATION OF GENERAL PARAMETERS ------------------------------

      WRITE(NOUT,1005)
 1005 FORMAT ( 1H1,10X,///,10X,
     &'***** COMPUTATION OF GENERAL PARAMETERS *****' , /// )

      AWATER=DWATER**2
      AFREON=DFREON**2
      PI=3.14159265
      WATVEL=QWATER/(DENSW*AWATER*NPW)
      FRVEL=QFREON/(DENSLF*AFREON*NPF)
      WRITE(NOUT,1011) WATVEL
 1011 FORMAT(10X,'Water velocity (m/s) = ',F10.4)

C----- EVALUATION OF HWATER AND DP WATER ------------------------------

      CALL WATER(HW,DPW)

      DPW=DPW*2*(DFREON+FINTK)*NPF/((DWATER+FINTK)*NPW)

      WRITE(NOUT,1014) HW
 1014 FORMAT(/,10X,'Water Film Coefficient (W/m2*C) = ',E10.4)
      WRITE(NOUT,1015) DPW
 1015 FORMAT(/,10X,'Pressure Drop per Flow Length (Pa/m) = ',E10.4)
      WRITE(NOUT,1012) FRVEL
 1012 FORMAT(/,10X,'Freon velocity (m/s) = ',F10.4)

C----- SET INITIAL VALUES   -------------------------------------------

      DZ=RLCOIL/INTERV
      WRITE(NOUT,1016) DZ
 1016 FORMAT(/,10X,'Dz (m) = ',F10.4)
      WRITE(NOUT,1017)
 1017 FORMAT ( ///,10X,'***** END OF PRELIMINARY COMPUTATIONS *****' )
      WRITE(NOUT,1018)
 1018 FORMAT ( 1H1,10X,'***** RUNTIME RESULTS *****',/// )
      DPTOT=0.
      TW1=TINW
      TW2=TINW
      XQ1=XQUALI
      DXOLD=0.8/INTERV
      QSUM=0.
      ZERO=0.
      I=0
      R2 = RESIST(XQUALI,HW,HF,TW1,TINF)

      WRITE(NOUT,1020)  I,ZERO,XQUALI,TINW,ZERO,ZERO,ZERO
      WRITE(NOUT,1019)                HF,HC,HNCB,ZERO,R2
      WRITE(NOUT,1030)  F,S,ZERO,ZERO,ZERO,      ZERO
      WRITE(NPLOT,2000) ZERO,QTOT,XQUALI,TW2,HF,ZERO,ZERO,ZERO


C----- MAIN ROUTINE ---------------------------------------------------
```

```
      CALL BALANCE(DXOLD,DZ,XQ1,XQ2,TW1,TW2,HW,HF,TINF,INTERV)
      DX=XQ2-XQ1

      CALL DPFREON(DZ,DP,XQ1,XQ2)
      DPTOT=DPTOT+DP
      Q=(XQ2-XQUALI)*RLATEN*QFREON

      CALL PAGE (I,NOUT)
      WRITE(0,1029)I,Z1,Q
 1029 FORMAT (5X,'I = ',I4,5X,'Z1 = ',F12.3,5X,'q = ',F12.3)

       WRITE(NOUT,1020) I,Z1,XQ2,TW2,Q,DPTOT/1.0E5,DPW*Z1/1.0E5
 1020 FORMAT(/,5X,'I = ',I3,2X,'Z1 =',F8.4,2X,'x =',F9.6,2X,
     &'Tw =',F8.4,2X,' qtot =',F12.3,2X,
     &'dpfreon(bar) =',F8.4,2X,'dpwater(bar) =',F8.4)

       WRITE(NOUT,1019)                    HF,HC,HNCB,XCAP1,R2
 1019 FORMAT(/,5X,                              'HF =',F12.3,2X,
     &'Hc =',F12.3,2X,'HNcb =',F12.3,2X,'Xtt =',F6.3,2X,
     &'RESIST = ',F12.6)

       WRITE(NOUT,1030) F,S,ALPHA,DPA,DPF,      FIQUAD
 1030 FORMAT(/,5X,'F =',F10.4,2X,'S =',F6.4,2X,
     &'Alpha =',F6.4,2X,'Dpa(Pa) =',F12.3,2X,'Dpf(Pa) =',F12.3,2X,
     &                          'Fiquad =',F12.3,//)
       WRITE(NPLOT,2000) Z1,QTOT,XQ2,TW2,HF,Q,DPTOT,DPW*Z1

       QLAST=(TW1-TW2)*CPW*QWATER
       QSUM=QSUM+QLAST
       IF(QSUM.GE.QTOT) GO TO 2
       DXOLD=XQ2-XQ1
       XQ1=XQ2
       TW1=TW2
     1 CONTINUE
       HTOT=Z1*NPF*(DFREON+FINTK)/(PI*DCOIL)
       WRITE(NOUT,1022) HTOT,QSUM,Z1
       DPWAT=DPW*Z1
       WRITE(NOUT,1023) DPTOT/1.E5,DPWAT/1.E5
       WRITE(NOUT,1021)

       WRITE(0,2022) HTOT,QSUM,Z1
       WRITE(0,2023) DPTOT/1.E5,DPWAT/1.E5
       WRITE(0,1021)
 1021 FORMAT(/,10X,'Warning: effectiveness not respected')
       RETURN
     2 CONTINUE
       QDIFF=QSUM-QTOT
       DZLAST=DZ*(1-(QDIFF/QLAST))
       DPLAST=DP*DZLAST/DZ
       DPTOT=DPTOT-DP+DPLAST
       Z1=Z1-DZ+DZLAST
       DPWAT=DPW*Z1
       HTOT=Z1*NPF*(DFREON+FINTK)/(PI*DCOIL)
       WRITE(NOUT,1022) HTOT,QSUM,Z1
       WRITE(NOUT,1023) DPTOT/1.E5,DPWAT/1.E5

       WRITE(0,2022) HTOT,QSUM,Z1
       WRITE(0,2023) DPTOT/1.E5,DPWAT/1.E5

 1022 FORMAT(/,10X,'HTOT = ',F10.4,5X,'QSUM = ',F10.4,5X,
     & 'TOTAL LENGTH = ',F10.4)
 1023 FORMAT(/,10X,'Total freon pressure drop (bar) =',E10.4,10X
     &,'Total water pressure drop (bar) =',E10.4)
 2022 FORMAT(/,1X,'HTOT = ',F8.4,2X,'QSUM = ',F10.4,2X,
```

```
     &,'Water pressure drop (bar) =',F10.4)
2000  FORMAT ( 8F15.3 )

      END

*****************************************************************************

      SUBROUTINE WATER(HW,DPW)

C----- This subroutine computes film coefficient and pressure drop for
C----- the water duct

      INCLUDE 'INS.FOR'

      WATVEL=QWATER/(DENSW*AWATER*NPW)
      REYNLD=DENSW*WATVEL*DWATER/VISCW
      RECRIT=2100*(1.+12*((DWATER/DCOIL)**0.5))
      PRANDW=CPW*VISCW/CONDW
      WRITE (NOUT,1009) REYNLD,RECRIT
 1009 FORMAT(/,10X,'Water Reynolds number =',E10.4,//,
     &10X,'Water Critical Reynolds number =',E10.4)
      HW=H1PHASE(REYNLD,PRANDW,DWATER,DCOIL,CONDW,IDUM)

      EFFE = FRIC(REYNLD,DWATER,DCOIL)
      IF(REYNLD.GE.RECRIT) THEN
C ----------------------------  Water turbulent flow  ------------------
      WRITE(NOUT,1010)
 1010 FORMAT(/,10X,'Water turbulent flow')
      WRITE(NOUT,1011) EFFE
 1011 FORMAT(/,10X,'Friction Factor for curved Pipes (f)=',E10.4)

      ELSE
C ----------------------------  Water laminar flow  --------------------
      WRITE(NOUT,1012)
 1012 FORMAT(//,10X,'Water laminar Flow')

      WRITE(NOUT,1011) EFFE
      END IF

      DPW=0.5*DENSW*(WATVEL**2)*EFFE/DWATER
      RETURN
      END

*****************************************************************************

      FUNCTION COLEBROOK(EPS,DWATER,REYNLD)

C----- This function provides the friction factor for straight pipes
C----- computed according to Colebrook equation (ASHRAE,1985)

      A=64./REYNLD
      B=4*A
      ERR=1.E-4
      X1=A
      X2=B
    1 CONTINUE
      F1=COLEB(X1,EPS,DWATER,REYNLD)
      F2=COLEB(X2,EPS,DWATER,REYNLD)
      DERIV=(F2-F1)/(X2-X1)
      DELT=-F1/DERIV
      TEMP=X2
      X2=X1+DELT
      DELT1=ABS(TEMP-X2)
```

```
      COLEBROOK=X2
      RETURN
      END

*****************************************************************************

      FUNCTION COLEB(X,EPS,D,RE)

C----- Colebrook equation (ASHRAE,1985) ----------------------------

      IF ( X .LT. 1.0E-6 ) THEN
         COLEB = 1.0E5
         RETURN
      END IF
      A1=EPS/(3.7*D)
      A2=2.51/(RE*SQRT(X))
      COLEB=1./(SQRT(X))+2*ALOG10(A1+A2)
      RETURN
      END

*****************************************************************************

      SUBROUTINE BALANCE(DXOLD,DZ,XQ1,XQ2,TW1,TW2,HW,HF,TF,INTERV)

C----- This subroutine performs a series of iterations using a Modified
C----- Newton Technique. Convergence is achieved when the heat absorbed
C----- by the freon results equal to the heat transmitted (HNET=0.).

      A=DXOLD
      B=DXOLD*1.05
      IF(B.LE.A) STOP 'ERROR IN SUBROUTINE BALANCE'
      ERR=1.E-3/INTERV
      X1=A
      X2=B
    1 CONTINUE
      F1=HNET(X1,XQ1,TW1,TW2,TF,DZ,HW,HF)
      F2=HNET(X2,XQ1,TW1,TW2,TF,DZ,HW,HF)
      DERIV=(F2-F1)/(X2-X1)
      DELT=-F1/DERIV
      TEMP=X2
      X2=X1+DELT
      DELT1=ABS(TEMP-X2)
      F3=HNET(X2,XQ1,TW1,TW2,TF,DZ,HW,HF)
      IF((F1*F3).GT.0)X1=TEMP
      IF(ABS(DELT).GT.ERR.AND.DELT1.GT.ERR) GO TO 1
      XQ2=XQ1+X2
      RETURN
      END

*****************************************************************************

      FUNCTION HNET(DX,XQ1,TW1,TW2,TF,DZ,HW,HF)

C----- This subroutine computes the net heat produced ( or dissipated)
C----- by the system as the difference between the heat released by
C----- the water and the heat absorbed by the freon.

      INCLUDE 'INS.FOR'

      DELQ1=RLATEN*QFREON*DX
      R1=RESIST(XQ1,HW,HF,TW1,TF)
      R2=RESIST(XQ1+DX,HW,HF,TW2,TF)
      R=(R1+R2)/2
```

```
      ELSE
      TW2=(TW1-TF)*EXP(-DZ/(R*QWATER*CPW))+TF
      END IF
      DELQ2=(TW1-TW2)*CPW*QWATER
      HNET=DELQ2-DELQ1
   15 FORMAT(5X,'DELQ1=',F10.4,5X,'R1=',F10.4,5X,'R2=',F10.4,/,
     &5X,'TW2=',F10.4,5X,'HNET=',F10.4,/)
      RETURN
      END
```

****

```
      FUNCTION RESIST(X,HW,HF,TW,TF)

C----- This subroutine computes the thermal resistance per unit length
C----- of the freon duct.

      INCLUDE 'INS.FOR'

      ELLE=DFREON+FINTK
      CALL FREON(HF,X,TW,TF)
      RFREON=BETA1/(4*HF*DFREON)
      RALUM=WALLTK/(2*CONDAL*ELLE)
      RWATER=BETA2*(DWATER+FINTK)/(8*HW*DWATER*ELLE)
      RESIST=(RFREON+RALUM+RWATER)/NPF

      END
```

****

```
      SUBROUTINE FREON(HF,X,TW,TF)

C----- This subroutine computes the film coefficient for freon.

      INCLUDE 'INS.FOR'

      FRVEL = QFREON/(DENSLF*AFREON*NPF)
      PRANDF= CPLF*VISCLF/CONDLF
      G     = QFREON / (AFREON*NPF)
      IF(X.LT.-0.001) THEN
C------------------------------- SUBCOOLED FLOW ----------------------
      REYNLF=DENSLF*FRVEL*DFREON/VISCLF
      HC=H1PHASE(REY  NLF,PRANDF,DFREON,DCOIL,CONDLF,IFLOW)
      HNCB = 0.
C     IF(REY1.LT.RECRITF) WRITE(NOUT,100)
  100 FORMAT(10X,'Warning: laminar freon flow')
      XCAP1=0.
      F = 0.
      S = 0.
      ELSE
C------------------------------------ TWO-PHASE FLOW --------------
      XCAP1=XTT(X,VISCLF,VISCVA,DENSLF,DENSVA,G,DFREON,DCOIL)
      F    = 2.35*((1./XCAP1+0.213)**0.736)
      REYNLF=DENSLF*FRVEL*DFREON*(1-X)/VISCLF
      HFC = (0.023*(REYNLF**0.8)*(PRANDF**0.4)*
     & (REYNLF*(DFREON/DCOIL)**2)**0.05)*CONDLF / DFREON
      IFLOW=1
      HC=F*HFC
      S=1./(1.+(REYNLF**1.17)*2.53E-06)
      DELTSAT=(TW-TF)/2.
      TWALL=(TW+TF)/2.
      DELPSAT=PSAT(TF,TWALL)
      A4=(CONDLF**0.79)*(CPLF**0.45)*(DENSLF**0.49)
```

```
      HF=HC+HNCB

      RETURN
      END

*****************************************************************************

      FUNCTION PSAT(T1,T2)

C----- This function computes DPSAT which appears in the film
C----- coefficient due to nucleate boiling. The coefficient 1000000
C----- accounts for the fact that pressure are input in Mpa.

      INCLUDE 'INS.FOR'

      P1=BILIN(T1,TEMP,NTEMP,PRES,NPRES)
      P2=BILIN(T2,TEMP,NTEMP,PRES,NPRES)
      PSAT= (P2 - P1) * 1000000
      RETURN

      END

*****************************************************************************

      FUNCTION BILIN(T,TEMP,NTEMP,PRES,NPRES)

C----- This function performs linear interpolation of a set of data.

      DIMENSION TEMP(NTEMP),PRES(NPRES)
       DO 1 I=1,NTEMP
       IF(TEMP(I).GE.T) GO TO 2
    1  CONTINUE
    2  CONTINUE
      BILIN=PRES(I-1)+(PRES(I)-PRES(I-1))*(T-TEMP(I-1))/(TEMP(I)-
     &TEMP(I-1))

       RETURN

       END

*****************************************************************************

      SUBROUTINE DPFREON(DZ,DP,XQ1,XQ2)

C----- This subroutine computes pressure drops for freon ------------

      INCLUDE 'INS.FOR'

      DX=XQ2-XQ1
      IF(DX.LT.0) WRITE(NOUT,15)
   15 FORMAT(/,10X,'DELTAX<0 IN SUBROUTINE DPFREON - ERROR')
      X=(XQ1+XQ2)/2.
      FRVEL=QFREON/(DENSLF*AFREON*NPF)
      REYNLF=DENSLF*FRVEL*DFREON/VISCLF
      IF(X.LE.0) THEN
C------------------------- SUBCOOLED FLOW ----------------------------

      EFFE=FRIC(REYNLF,DFREON,DCOIL)
      DPF=0.5*(DENSLF*(FRVEL**2)*EFFE/DFREON)*DZ
      DPA=0.
      XCAP=0.
      XCAP2=0.
      ELSE
```

```
      IF(G.GT.1500.) STOP 'WARNING: G>G*'
      ALPHA  = VOIDF(X,G)
      ALPHA1 = VOIDF(XQ1,G)
      ALPHA2 = VOIDF(XQ2,G)
      DPA    = G**2 * (DPACC(XQ2,ALPHA2,DENSVA,DENSLF) -
     &         DPACC(XQ1,ALPHA1,DENSVA,DENSLF))
      EFFE   = FRIC(REYNLF,DFREON,DCOIL)
      DPFRF  = 0.5*EFFE*(G**2)/(DFREON*DENSLF)
      REVAP  = G * DFREON / VISCVA
      EFFEGO = FRIC(REVAP,DFREON,DCOIL)
      E      = (1.-X)**2+X**2 * (DENSLF*EFFEGO)/(DENSVA*EFFE)
      FF     = X**0.78 * (1.-X)**0.24
      H      = (DENSLF/DENSVA)**0.91*(VISCVA/VISCLF)**0.19
      H      = H * (1.- VISCVA/VISCLF)**0.7
      ROTP   = 1./(X/DENSVA+(1.-X)/DENSLF)
      FR     = G**2/(9.81*DFREON*ROTP**2)
      WE     = G**2*DFREON/(SIGMA*ROTP)
      FIQUAD = E + 3.24*FF*H / ((FR**0.045)*(WE**0.035))
      DPF    = DPFRF*FIQUAD*DZ
      IF(DPA.LT.0.) DPA = 0.
      END IF
      DP=DPF+DPA

      RETURN
      END

*****************************************************************************

      FUNCTION XTT(X,RMUF,RMUG,DENF,DENG,G,DDUCT,DCOIL)

      IF(X.GT.0.999) STOP 'Warning: superheated flow'
      IF(X.LE.0.) THEN
C        THE VALUE 9.9793 IS SUCH THAT F = 1 IN SUBROUTINE FREON
         XTT = 9.9793
         RETURN
      END IF

      REL    = G*DDUCT*(1.-X)/RMUF
      REG    = G*DDUCT*X/RMUG
      EFFEL = FRIC(REL,DDUCT,DCOIL)
      EFFEG = FRIC(REG,DDUCT,DCOIL)

      XTT = ((1.-X)/X)*((DENG*EFFEL/(DENF*EFFEG))**0.5)

      END

*****************************************************************************

      FUNCTION H1PHASE(RE,PR,DDUCT,DCOIL,COND,IFLOW)

      RATIO=DDUCT/DCOIL
      RECRIT=2100*(1.+12*(RATIO**0.5))

      IF(RE.GE.RECRIT) THEN
C------------------------------------ TURBULENT FLOW ---------------------
      RNUSSL=0.023*(RE**0.8)*(PR**0.4)*(RE*RATIO**2)**0.05
      IFLOW=1
      ELSE
C------------------------------------ LAMINAR FLOW -----------------------

      IFLOW=2
      DEAN=RE*RATIO**0.5
```

```
RNUSSL=0.836*(DEAN**0.5)*(PR**0.1)
END IF

H1PHASE=RNUSSL*COND/DDUCT

RETURN
END
```

```
*****************************************************************************

      FUNCTION FRIC(REYNLD,DDUCT,DCOIL)

      RECRIT = 2100.*(1.+12.*((DDUCT/DCOIL)**0.5))

      IF(REYNLD.GE.RECRIT) THEN
      IF(((DDUCT/DCOIL)**2).GT.700) STOP 'WARNING : DW/DC TOO LARGE'
      EFFES=0.
      EFFE=0.336*(REYNLD*((DDUCT/DCOIL)**2))**(-0.2)
      EFFE=EFFE*((DDUCT/DCOIL)**0.5)

      ELSE
C ------------------------  Water laminar flow  ---------------------

      DEAN=REYNLD*SQRT(DDUCT/DCOIL)
      EFFES=64./REYNLD
      IF(DEAN.LT.11.6) THEN
      EFFE=EFFES
      ELSE IF(DEAN.GT.2000) THEN
      EFFE=EFFES*0.1064*DEAN**0.5
      ELSE
      V2=(11.6/DEAN)**0.45
      EFFE=EFFES/(1-((1-V2)**2.22))
      END IF

      END IF

      FRIC = EFFE
      END

*****************************************************************************

      FUNCTION VOIDF(X,G)

      INCLUDE 'INS.FOR'

      IF (X.LT.0.0001) THEN
        VOIDF = 0.
        RETURN
      END IF

      BETA = X*DENSLF/((1.-X)*DENSVA+X*DENSLF)
      Y    = BETA / (1 - BETA)
      RE   = G * DFREON / VISCLF
      WE   = DFREON * (G**2) / (SIGMA * DENSLF)
      E1   = 1.578*(RE**(-0.19))*((DENSLF/DENSVA)**0.22)
      E2   = 0.0273*WE*(RE**(-0.51))*((DENSLF/DENSVA)**(-0.08))
      ESSE = 1. + E1 * ((Y/(1.+Y*E2)) - Y*E2)**0.5
      VOIDF= X/(X+ESSE*(1.-X)*DENSVA/DENSLF)

      END

*****************************************************************************
```

```
      DPACC = 0.
      RETURN
      END IF
      DPACC = X**2/(ALPHA*ROG) + (1.-X)**2/((1.-ALPHA)*ROF)-1./ROF

      END

*****************************************************************************

      SUBROUTINE PAGE(I,NOUT)

      DO 1 K = 7 , 10000 , 6
         IF(K.GT.I) RETURN
         IF(K.EQ.I) WRITE(NOUT,'(1H1)')
    1 CONTINUE

      END



      PROGRAM MAIN

C     Program TPEHX solves the problem of a Two Phases Heat Exchanger.

      INCLUDE 'INS.FOR'

      OPEN(5,FILE='TPEHX.DAT')
      OPEN(6,FILE='TPEHX.OUT')
      OPEN(7,FILE='TPLOT.LST')

      WRITE(0,*)'[ TPEHX rev 1.0 ]'

      CALL INPUT

      CALL TPEHX

      WRITE(NOUT,'(///,10X,A)')'***** TPEHX COMPLETED OK *****'

      WRITE(0,*)'***** TPEHX COMPLETED OK *****'

      STOP

      END
*****************************************************************************
```

APPENDIX (C)

Leakage Problems & Recovery Steps

Analyzing the first leakage test results, the following conclusions were made:

1) The seal redundancy between the two sides was assured by means of both O-rings and a NEOPRENE flat gasket in all points except the two critical areas below the cover plate where the water and Freon channels come close together (see Fig. 7.2)

2) Distance between the water and Freon side in the above critical areas were only a few millimeters apart and the use of the flat gasket alone was inadequate to assure leak tightness.

3) The used flathead screws did not provide sufficient contact pressure between cover and flat gasket so as to assure internal tightness of the evaporative heat exchanger. This is particularly true as the flathead screw provides less axial force on the screw stem in comparison with cheese-headed screw with the same tightening torque.

The following corrective actions were envisaged:

1. change of the M4 screws with a larger diameter one.

2. change of the screws with ones of high resistance material so as to increase torque.

3. Re-manufacture the ends of the cylinders in order to obtain a flat surface for the assembly-gasket contact area.

4. Use a local reinforcement (working as a pressure plate) on the critical areas. This reinforcement could be made of an external equipment with two bases, drilled in five points for housing five thread sticks connecting both bases. In this way, the cover plates are clamped between the bases of the equipment, and the base is provided with support points situated over the cover plate channels in order to exert pressure locally over the critical areas.

5. Re-design of the inlet and outlet manifold or change of the flat gasket and cover design locally, in order to increase the distance between the two sides in the critical area.

6. Increase of the thickness of the cover plates in order to increase the stiffness and reduce plate bowing.

Closer investigation of the first option revealed that it was not possible to introduce M8 cheese headed screws on the cover and that M6 bolts could be applied to the screws positioned in the middle of the water channels.

The recovery measure which was selected prior to execution of the helium and water tests are detailed below:

a) Grinding of the top and bottom of the heat exchanger body in order to flatten the surface formed by the four cylinders (co-planarity < 0.05mm) and to eliminate the two steps forming the seat of the flat gasket.

b) grind the bottom surfaces of the covers (co-planarity < 0.05mm).

c) add four M6 bolts on each cover in the area of the external water channel.

d) manufacture an external local reinforcement to be used as a backup in case the leakage results did not prove to be adequate) so as to externally increase the pressure between the cover plate and flat gasket.

After carrying out these recovery measures, a helium leak test was performed (for calibration curves and measurement points see Figs.C2 and Fig.C3) on the heat exchanger and the results are as follows:

- internal leakage rate from water side to Freon side with a pressure difference of 2.1 bar between the two sides was 4.1×10^{-5} Standard cc/s.

- internal leakage rate from Freon side to water side with a pressure difference of 3.4 bar between the two sides was 1.2×10^{-4} Standard cc/s.

A water leakage test was also performed with a pressure difference between the two sides (water and Freon) of 2 bar for 1 hour duration.
The water leak test was performed with the following procedure:

- the heat exchanger leak test setup was configured as shown on Fig C1.
- the heat exchanger Freon side inlet was

connected to the gaseous nitrogen supply and the Freon side to the shut off valve (D) upstream of the moisture meter and gas flowmeter.

- gaseous nitrogen was flowed through the Freon side at a volume flow rate of 5 l/min.
- maintaining the gaseous nitrogen at 5 l/min, the heat exchanger, water side was pressurised until a 2 bar pressure difference between the two sides was established.
- the moisture level (dew point temperature) at 5 minute intervals for about 1 hour was recorded. In all the dew point temperatures recorded there was no increase in the gas moisture content as indicated in Table C.1.

Figure C1 Water leakage test set-up from water to Freon side

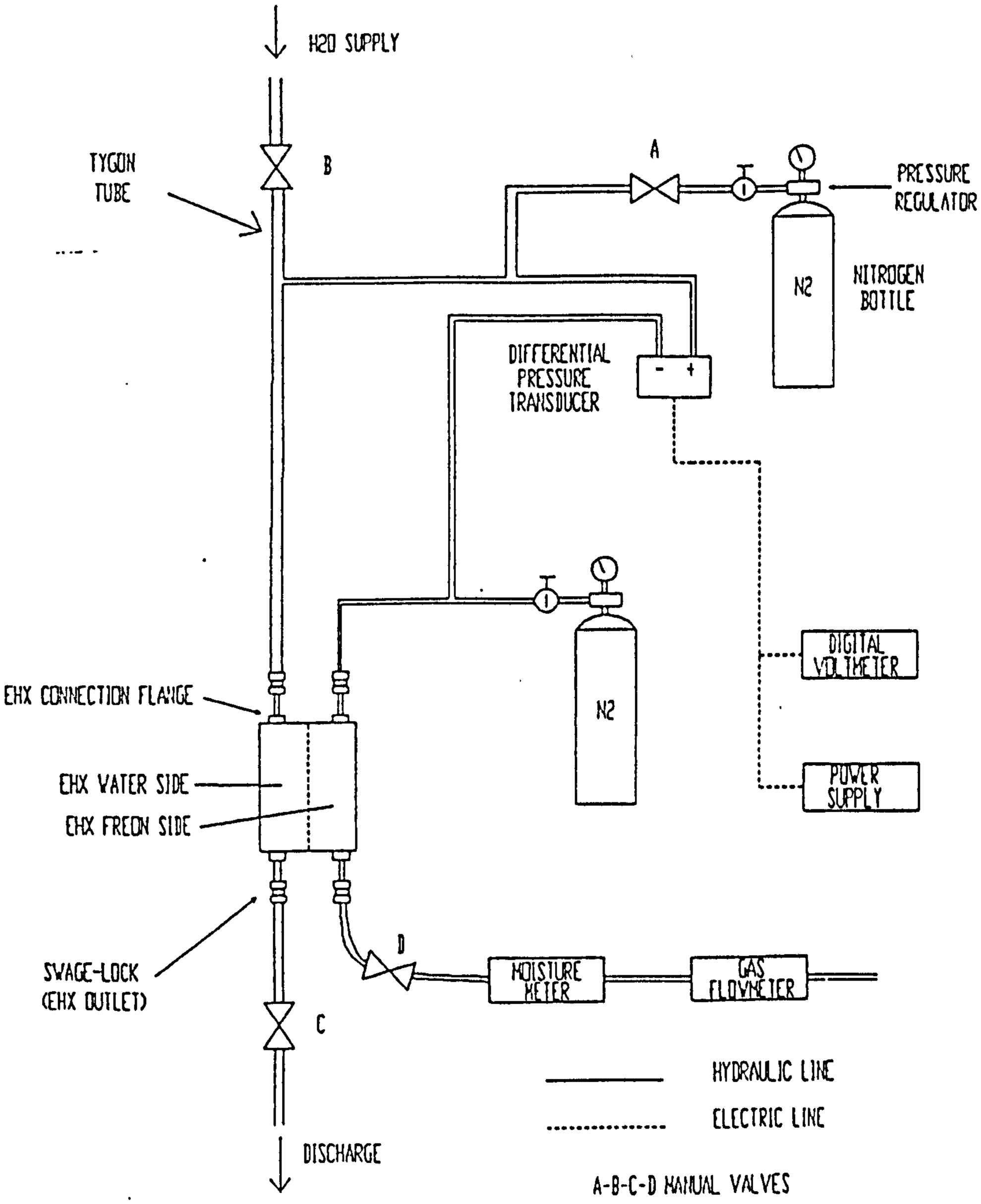

Figure C2 Internal Leakage test results (water to Freon) and calibration curves

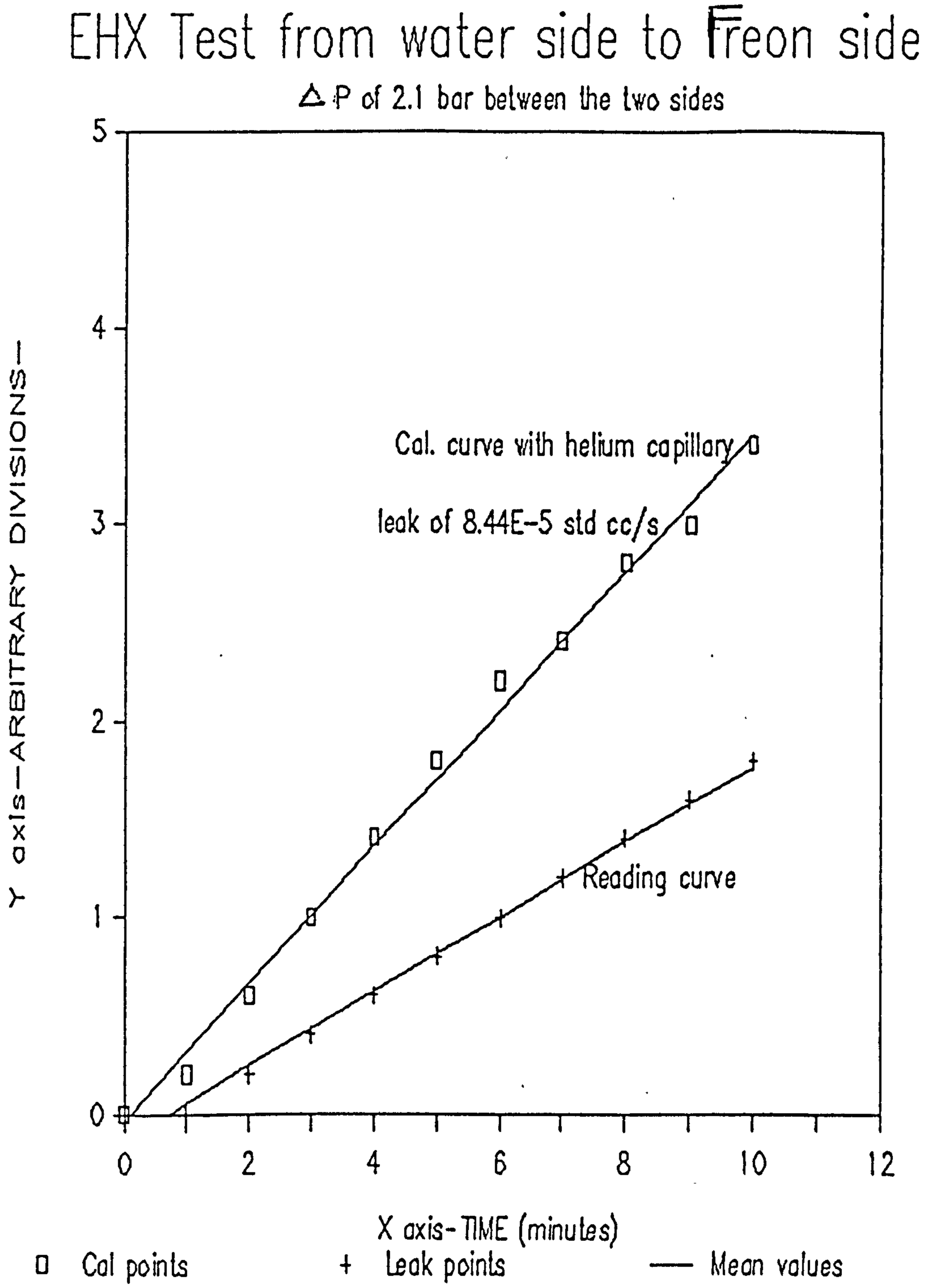

Figure C3 Internal Leakage test results (Freon to water) and calibration curves

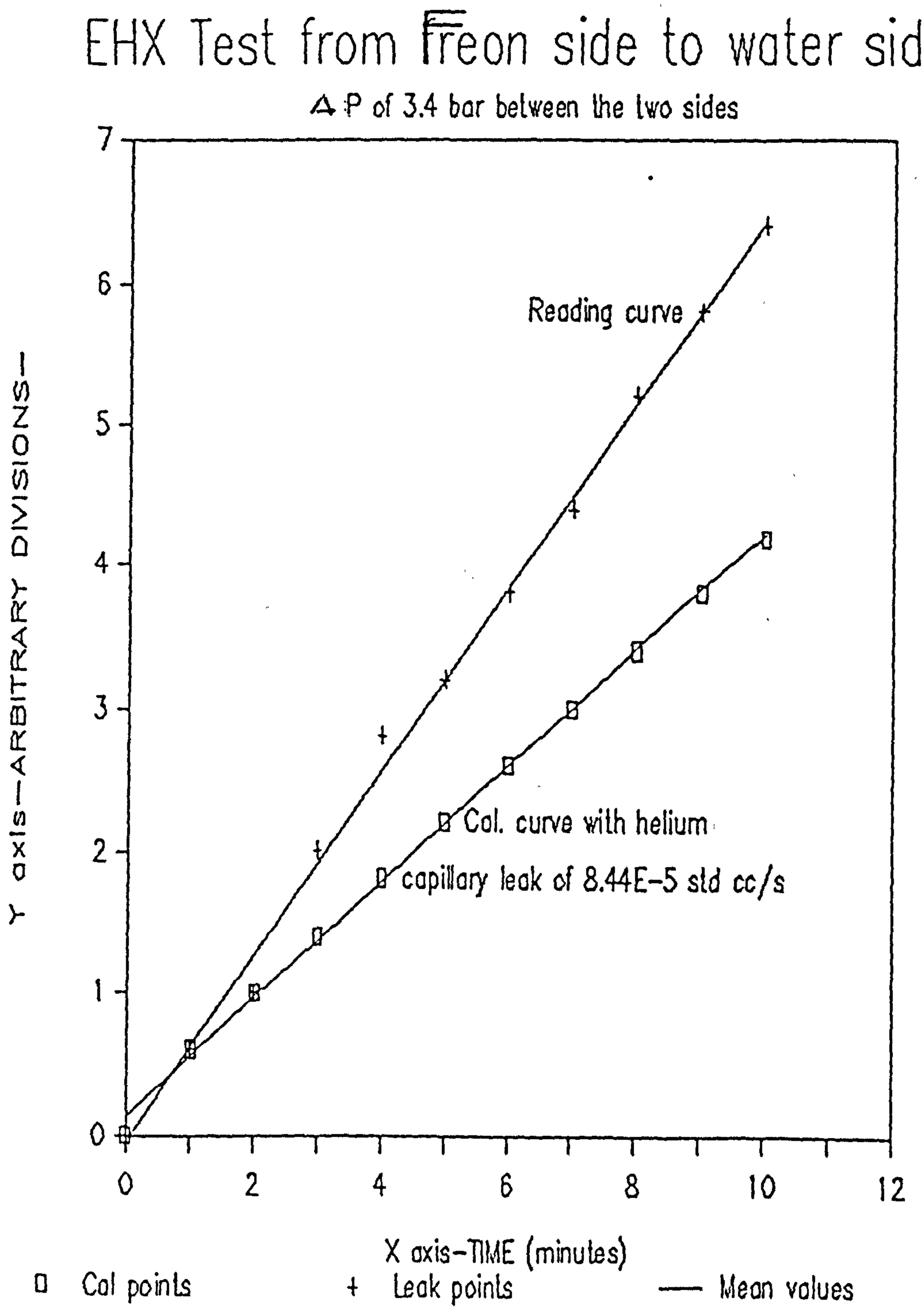

Table C1 Moisture meter measurement indicating leakage levels

Measurement No.	Time (h)	Dew Point Temperature °C	Pressure Difference bar	Gas Volume Flow Rate l/min
1->13	1	-57	2.02->2.05	5

A dew point temperature variation less than 0.5°C was measured during the test. This value is equal to half the resolution of the dew point temperature meter. The gas moisture content in terms of parts per million (ppm) by volume is 1 ppmv using the meter conversion chart. The corresponding moisture content value in terms of milligram per litre can also be evaluated (more accurately than the conversion chart by means of a correlation, taking into account the molecular weight of the working nitrogen gas. The correlation is obtained through the definition of the ppmv moisture content (i.e. the ratio between water-vapour partial pressure and the total gas pressure) using the perfect-gas law.

The moisture mass flow rate for the gas flow at 5 /min resulted in a mass leakage rate of 3.7×10^{-3} mg/min.

APPENDIX (D)

MAIN TECHNICAL CHARATERISTICS OF OTHER CRITICAL COMPONENTS IN THE TWO-PHASE LOOP

A schematic of an evaporative cold plate is given in Fig. D-1. A summary of the technical characteristics of the capilliary assisted cold plate is given below:

Maximum Heat Load:	5kW
Maximim Heat Flux Density:	15KW/m^2
Overall Length:	840mm
Overall height of outlet:	43mm
Overall thickness:	25mm
Mass:	19kg

Figure D-1 Schematic of evaporative cold plate

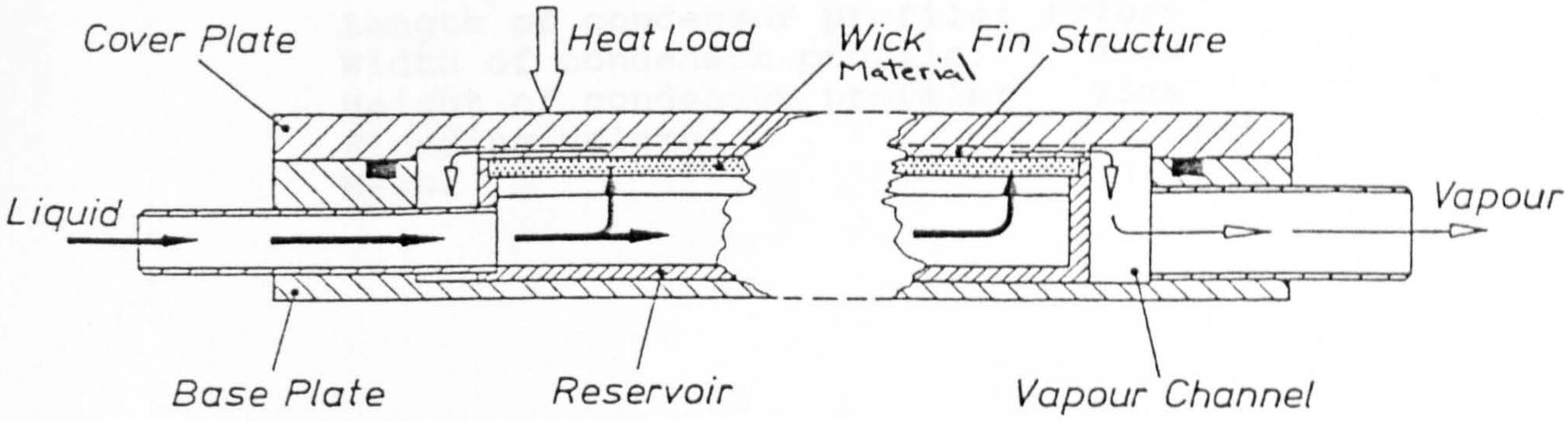

A schematic of a condenser is given in Fig. D-2. A summary of the technical characteristics of the condenser is given below:

Heat Rejection Capability: per condensor	1KW
Overall length:	1920mm
Overall Width:	255mm
Length of condensor profile:	1770mm
Width of condensor profile:	25mm
Height of condensor profile:	15mm
Flooding volume:	< 0.31dm^3
Mass:	3kg

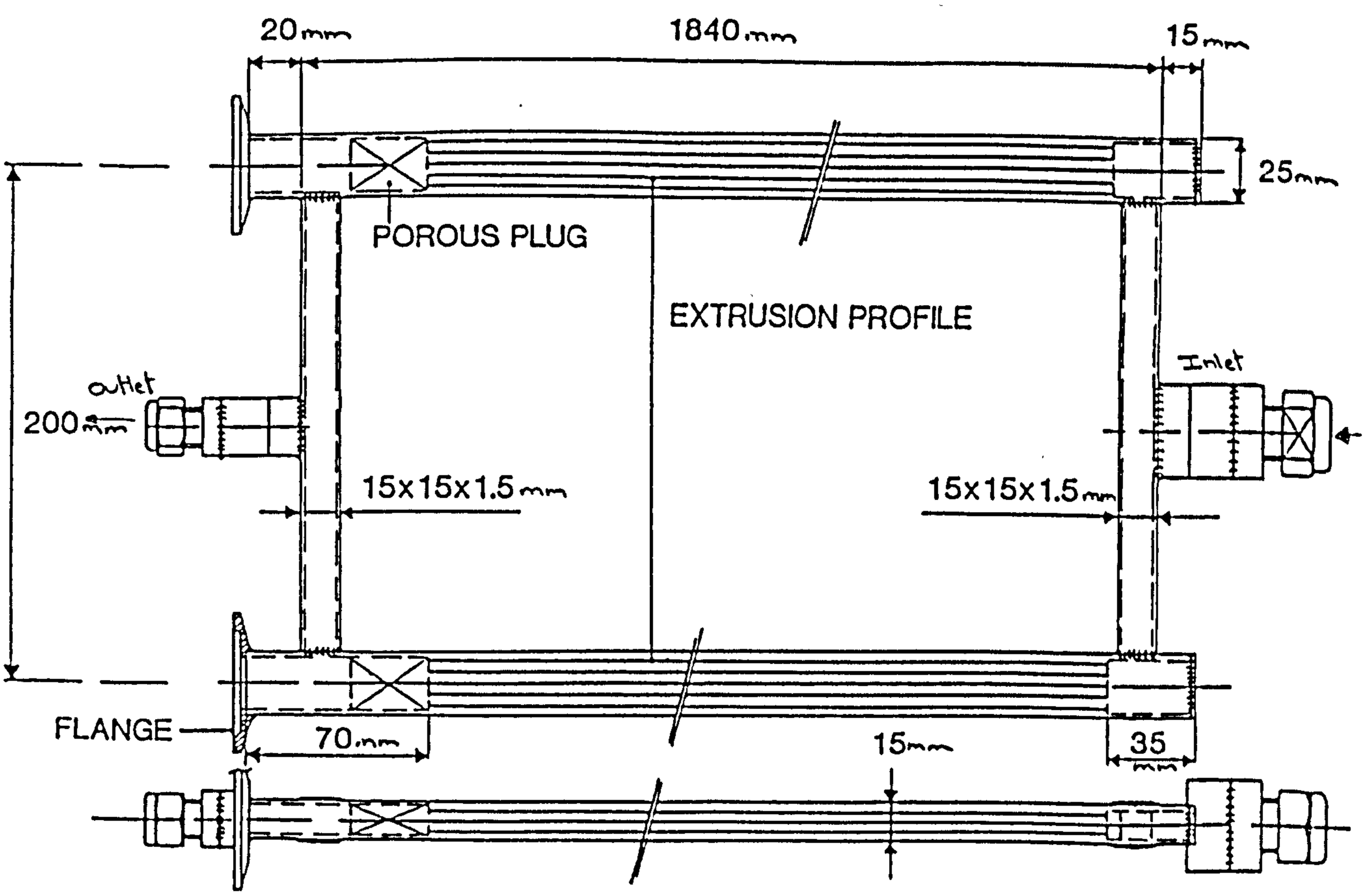

A
he

PAGE
MISSING

155

Fig D.2.

A schematic of an accumulator is given in Fig. D-3. A summary of the technical characteristics of the accumulator is given below:

Overall Length:	450mm
Outer Diameter:	266mm
Range of volume change;	0-6dm^3
Maximum stroke of bellows:	135mm
Maximum flow rate:	5dm^3 /min
Power consumption:	< 70W
Mass:	13kg

Figure D-3 Schematic of accumulator

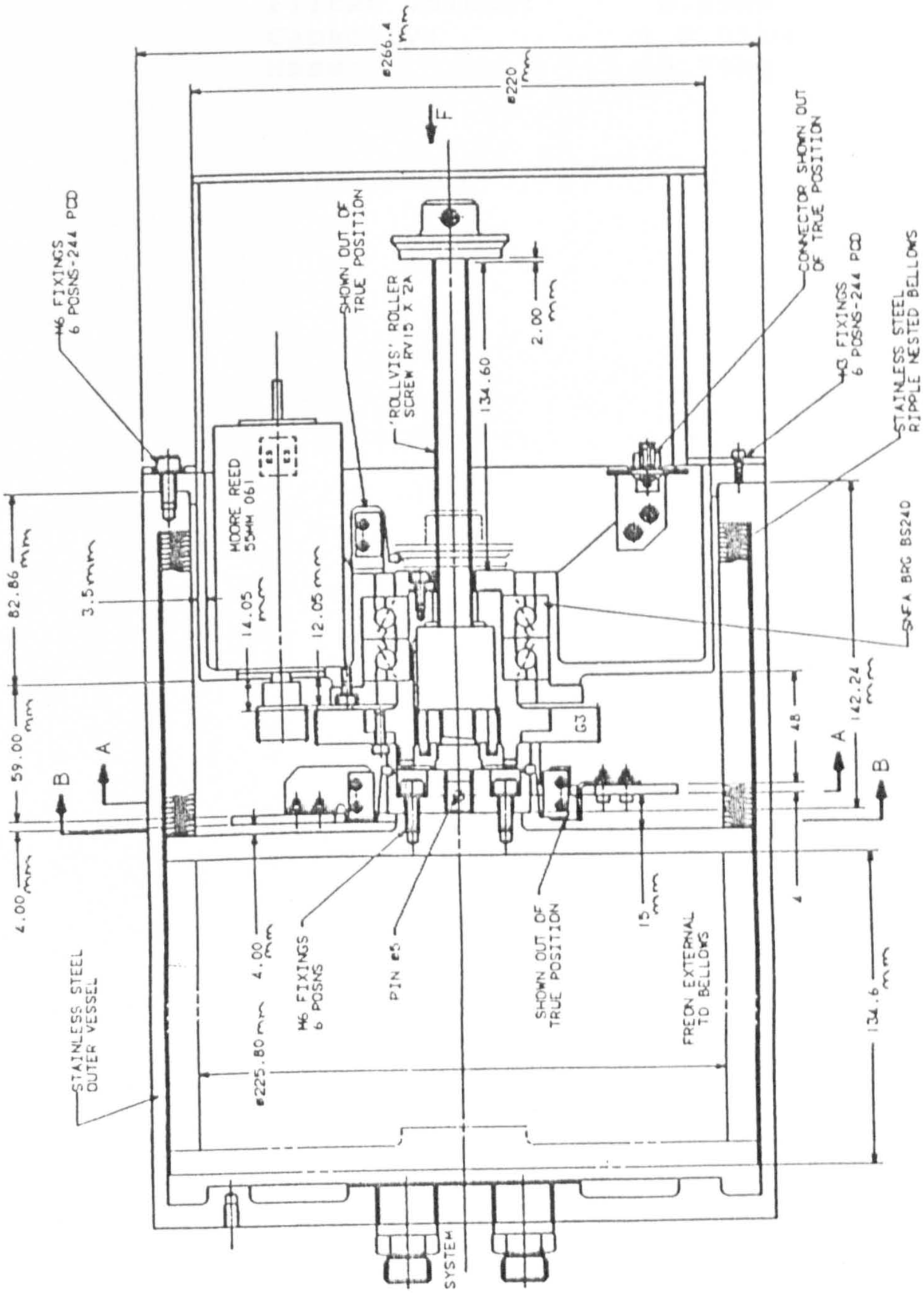

A schematic of a gas trap is given in Fig. D-4. A summary of the technical characteristics of the gas trap is given below:

Overall length:	188mm
Outer Diameter:	77.5mm,
Filter Volume:	0.55dm³
Capacity:	> 0.01kg
Mass:	0.73kg

Figure D-4 Schematic of gas trap

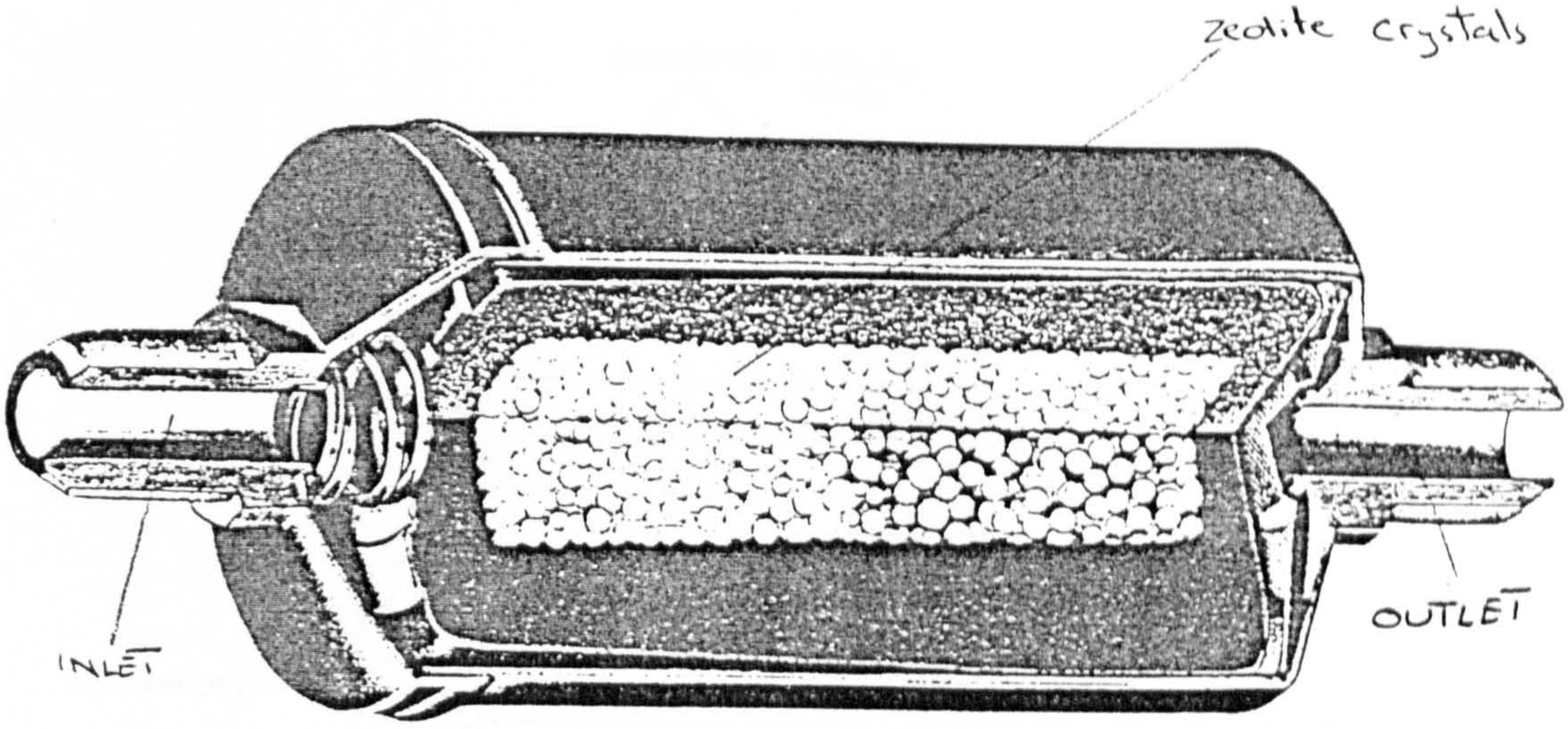

Figure D-5 Schematic of vapour quality sensor.

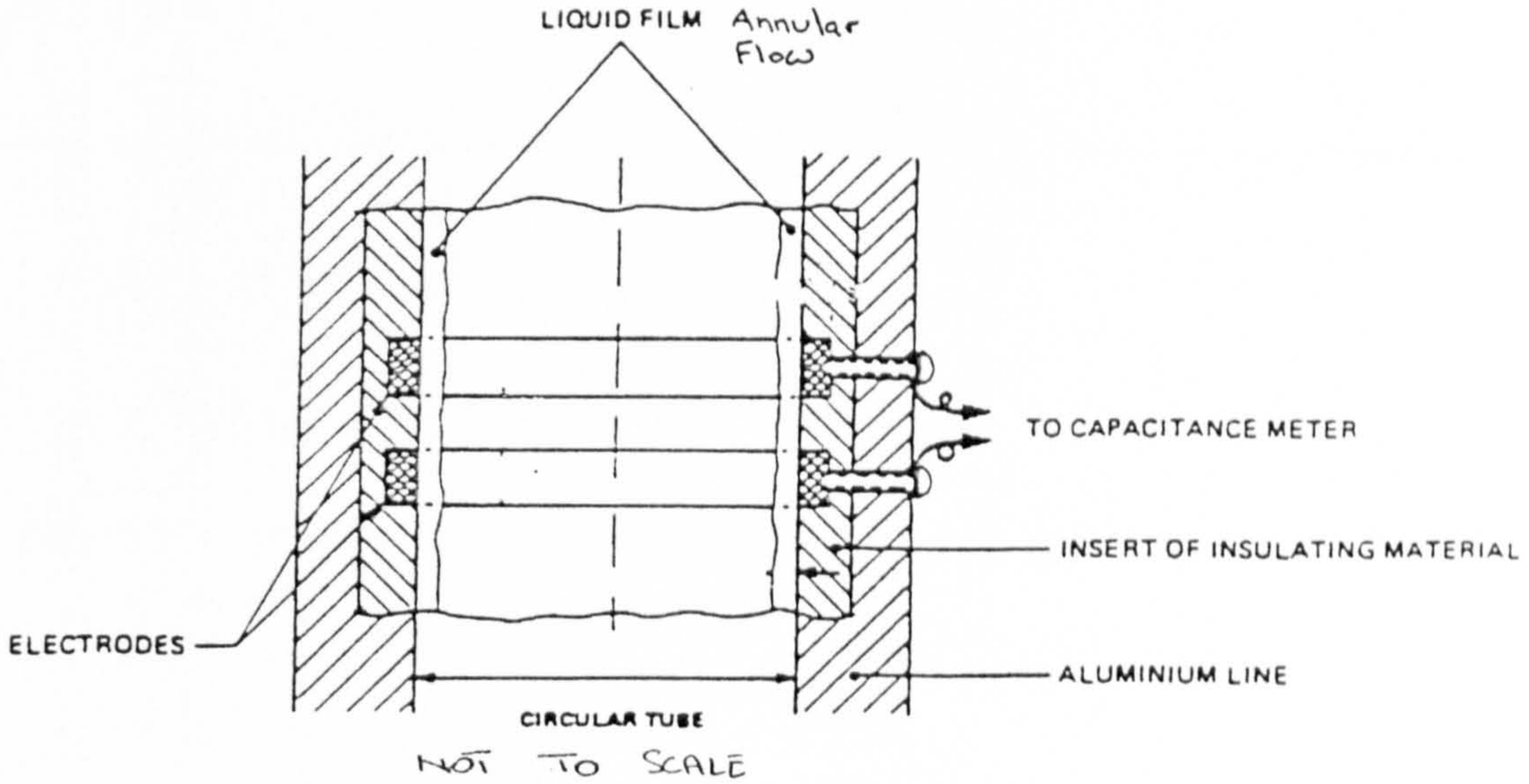

APPENDIX (E)

DAMAGED TEXT IN ORIGINAL

HEAT EXCHANGER PERFORMANCE COMPUTER OUTPUT

P R O G R A M T P E H X

CALCULATION OF HEAT FLOW FOR WATER TO FREON HELICOIDAL HEAT EXCHANGER

***** INPUT ECHO *****

Aluminum properties

Density (Kg/m3) = 2770.0000 Conductivity (W/M*C) = 121.4000 Roughness Factor (mm) = .0300

Water properties

Density (Kg/m3) = 997.0000 Specific Heat Capacity (J/Kg*C) = 4176.0000 Conductivity (W/m*C) = .6000
Viscosity (Ns/m2) = .8300E-03

Liquid Freon properties

Density (Kg/m3) = 1463.0000 Specific Heat Capacity (J/Kg*C) = 993.0000 Conductivity (W/m*C) = .0567
Viscosity (Ns/m2) = .3800E-03 Latent Heat (kJ/Kg) = 125.6000

Freon Vapor properties

Density (Kg/m3) = 13.7000
Viscosity (Ns/m2) = .1150E-04 Surface Tension (N/m) = .1200E-01

Initial Conditions

Water Inlet Temperature (C) = 38.0000 Freon Inlet Temperature (C) = 20.0000
Freon Inlet Pressure (Pa) = .1800E+06
Water Flow (Kg/h) = 320.0000 Freon Flow (Kg/h)= 240.0000 Initial Vapor Quality = .0000

System Parameters

Water Equivalent Diameter.(mm) = 9.000 Freon Equivalent Diameter (mm) = 13.000 Coil Diameter (mm) = 250.0000
Wall Thickness (mm) = 3.000 Fin Thickness (mm) = 1.5000 Coil length (m) = 5.5000

```
Water Ducts Number          = 2          Freon Ducts Number = 2
Beta1 = 1.0310    Beta2 = 2.4960    Intervals Number =      25


 Requested total heat exchanged (W) = 9000.0000


 Steam and water properties satisfying property      index:

 Steam viscosity (Ns/m2) = .1625E-04    Water viscosity (Ns/m2) = .1252E-03
 Steam density (Kg/m3)   = .1060E+02    Water density (Kg/m3)   = .8470E+03


 Freon property index =    .0188

 Water property index =    .0188



***** END OF INPUT ECHO *****

1

 ***** COMPUTATION OF GENERAL PARAMETERS *****


 Water velocity (m/s) =      .5503

 Water Reynolds number = .5950E+04

 Water Critical Reynolds number = .6801E+04

 Water laminar Flow

 Friction Factor for curved Pipes (f)= .4119E-01

 Water Film Coefficient (W/m2*C) =  .2232E+04

 Pressure Drop per Flow Length (Pa/m) =  .1909E+04

      Freon velocity (m/s) =      .1348

      Dz (m) =      .2200


      ***** END OF PRELIMINARY COMPUTATIONS *****
1      ***** RUNTIME RESULTS *****
```

I = 0 Z1 = .0000 x = .000000 Tw = 38.0000 qtot = .000 dpfreon(bar) = .0000 dpwater(bar) = .0000

HF = 2325.447 Hc = 315.742 HNcb = 2009.675 Xtt = .000 RESIST = .010314

F = 1.0000 S = .9290 Alpha = .0000 Dpa(Pa) = .000 Dpf(Pa) = .000 Fiquad = .000

I = 1 Z1 = .2200 x = .044968 Tw = 36.9857 qtot = 376.534 dpfreon(bar) = .0010 dpwater(bar) = .0042

HF = 2434.088 Hc = 538.995 HNcb = 1895.093 Xtt = 2.127 RESIST = .010314

F = 1.7752 S = .9325 Alpha = .5185 Dpa(Pa) = 49.892 Dpf(Pa) = 54.822 Fiquad = 5.898

I = 2 Z1 = .4400 x = .088078 Tw = 36.0132 qtot = 737.509 dpfreon(bar) = .0025 dpwater(bar) = .0094

HF = 2521.458 Hc = 737.149 HNcb = 1784.307 Xtt = 1.124 RESIST = .010314

F = 2.5250 S = .9358 Alpha = .7027 Dpa(Pa) = 89.255 Dpf(Pa) = 104.847 Fiquad = 11.281

I = 3 Z1 = .6600 x = .129163 Tw = 35.0864 qtot = 1081.526 dpfreon(bar) = .0047 dpwater(bar) = .0126

HF = 2575.256 Hc = 893.489 HNcb = 1681.866 Xtt = .771 RESIST = .010314

F = 3.1828 S = .9390 Alpha = .7713 Dpa(Pa) = 41.503 Dpf(Pa) = 143.052 Fiquad = 15.391

I = 4 Z1 = .8800 x = .168113 Tw = 34.2078 qtot = 1407.657 dpfreon(bar) = .0065 dpwater(bar) = .0168

HF = 2606.244 Hc = 1022.193 HNcb = 1584.051 Xtt = .595 RESIST = .010314

F = 3.7857 S = .9420 Alpha = .8101 Dpa(Pa) = 44.945 Dpf(Pa) = 175.920 Fiquad = 19.927

I = 5 Z1 = 1.1000 x = .204917 Tw = 33.2776 qtot = 1715.834 dpfreon(bar) = .0081 dpwater(bar) = .0210

HF = 2521.223 Hc = 1130.278 HNcb = 1490.945 Xtt = .477 RESIST = .010314

F = 4.3501 S = .9448 Alpha = .8361 Dpa(Pa) = 48.119 Dpf(Pa) = 205.425 Fiquad = 22.102

I = 6 Z1 = 1.3200 x = .239615 Tw = 32.5949 qtot = 2006.375 dpfreon(bar) = .0119 dpwater(bar) = .0252

HF = 2624.620 Hc = 1222.066 HNcb = 1402.554 Xtt = .402 RESIST = .010314

F = 4.8852 S = .9474 Alpha = .8550 Dpa(Pa) = 50.747 Dpf(Pa) = 232.475 Fiquad = 25.012

I = 7 Z1 = 1.5400 x = .272080 Tw = 31.8581 qtot = 2279.893 dpfreon(bar) = .0150 dpwater(bar) = .0294

HF = 2615.959 Hc = 1300.545 HNcb = 1319.414 Xtt = .347 RESIST = .010314

F = 5.3966 S = .9499 Alpha = .8695 Dpa(Pa) = 52.717 Dpf(Pa) = 257.569 Fiquad = 27.712

I = 8 Z1 = 1.7600 x = .303005 Tw = 31.1650 qtot = 2537.161 dpfreon(bar) = .0184 dpwater(bar) = .0336

HF = 2611.118 Hc = 1367.939 HNcb = 1243.180 Xtt = .306 RESIST = .010314

F = 5.8883 S = .9523 Alpha = .8812 Dpa(Pa) = 54.058 Dpf(Pa) = 281.010 Fiquad = 30.234

I = 9 Z1 = 1.9800 x = .331886 Tw = 30.5135 qtot = 2778.995 dpfreon(bar) = .0219 dpwater(bar) = .0379

HF = 2597.068 Hc = 1425.962 HNcb = 1171.106 Xtt = .273 RESIST = .010314

F = 6.3629 S = .9545 Alpha = .8909 Dpa(Pa) = 54.826 Dpf(Pa) = 303.004 Fiquad = 32.600

I = 10 Z1 = 2.2000 x = .359019 Tw = 29.9314 qtot = 3006.190 dpfreon(bar) = .0257 dpwater(bar) = .0420

HF = 2579.005 Hc = 1475.979 HNcb = 1103.027 Xtt = .247 RESIST = .010314

F = 6.8223 S = .9566 Alpha = .8990 Dpa(Pa) = 55.082 Dpf(Pa) = 323.689 Fiquad = 34.826

I = 11 Z1 = 2.4200 x = .384500 Tw = 29.3267 qtot = 3219.545 dpfreon(bar) = .0297 dpwater(bar) = .0462

HF = 2557.870 Hc = 1519.101 HNcb = 1038.768 Xtt = .226 RESIST = .010314

F = 7.2679 S = .9585 Alpha = .9059 Dpa(Pa) = 54.902 Dpf(Pa) = 343.172 Fiquad = 36.922

I = 12 Z1 = 2.6400 x = .408422 Tw = 28.7870 qtot = 3419.852 dpfreon(bar) = .0339 dpwater(bar) = .0504

HF = 2534.411 Hc = 1556.263 HNcb = 978.148 Xtt = .208 RESIST = .010314

F = 7.7009 S = .9603 Alpha = .9120 Dpa(Pa) = 54.357 Dpf(Pa) = 361.534 Fiquad = 38.898

I = 13 Z1 = 2.8600 x = .430877 Tw = 28.2805 qtot = 3607.981 dpfreon(bar) = .0382 dpwater(bar) = .0546

HF = 2509.232 Hc = 1588.247 HNcb = 920.985 Xtt = .193 RESIST = .010314

F = 8.1220 S = .9620 Alpha = .9172 Dpa(Pa) = 53.512 Dpf(Pa) = 378.845 Fiquad = 40.760

I = 14 Z1 = 3.0800 x = .451957 Tw = 27.8050 qtot = 3784.384 dpfreon(bar) = .0427 dpwater(bar) = .0586

HF = 2483.653 Hc = 1615.724 HNcb = 367.929 Xtt = .180 RESIST = .010314

F = 8.5318 S = .9636 Alpha = .9219 Dpa(Pa) = 52.429 Dpf(Pa) = 395.168 Fiquad = 42.516

I = 15 Z1 = 3.3000 x = .471747 Tw = 27.3586 qtot = 3950.095 dpfreon(bar) = .0473 dpwater(bar) = .0530

HF = 2458.317 Hc = 1639.271 HNcb = 619.047 Xtt = .169 RESIST = .010314

F = 8.9311 S = .9550 Alpha = .9261 Dpa(Pa) = 51.163 Dpf(Pa) = 410.557 Fiquad = 44.172

I = 16 Z1 = 3.5200 x = .490330 Tw = 26.9394 qtot = 4105.697 dpfreon(bar) = .0520 dpwater(bar) = .0672

HF = 2432.356 Hc = 1659.384 HNcb = 772.973 Xtt = .159 RESIST = .010314

F = 9.3201 S = .9564 Alpha = .9298 Dpa(Pa) = 49.753 Dpf(Pa) = 425.066 Fiquad = 45.733

I = 17 Z1 = 3.7400 x = .507781 Tw = 26.5458 qtot = 4251.919 dpfreon(bar) = .0569 dpwater(bar) = .0714

HF = 2406.943 Hc = 1676.490 HNcb = 729.553 Xtt = .150 RESIST = .010314

F = 9.6992 S = .9677 Alpha = .9332 Dpa(Pa) = 48.233 Dpf(Pa) = 438.740 Fiquad = 47.204

I = 18 Z1 = 3.9600 x = .524171 Tw = 26.1760 qtot = 4389.059 dpfreon(bar) = .0619 dpwater(bar) = .0756

HF = 2379.599 Hc = 1690.963 HNcb = 688.636 Xtt = .143 RESIST = .010314

F = 10.0586 S = .9669 Alpha = .9363 Dpa(Pa) = 46.634 Dpf(Pa) = 451.626 Fiquad = 48.591

I = 19 Z1 = 4.1800 x = .539568 Tw = 25.8287 qtot = 4517.979 dpfreon(bar) = .0670 dpwater(bar) = .0798

HF = 2353.205 Hc = 1703.129 HNcb = 650.077 Xtt = .136 RESIST = .010314

F = 10.4285 S = .9701 Alpha = .9390 Dpa(Pa) = 44.982 Dpf(Pa) = 463.765 Fiquad = 49.897

I = 20 Z1 = 4.4000 x = .554034 Tw = 25.5024 qtot = 4639.109 dpfreon(bar) = .0722 dpwater(bar) = .0840

HF = 2327.014 Hc = 1713.274 HNcb = 613.740 Xtt = .130 RESIST = .010314

F = 10.7792 S = .9711 Alpha = .9416 Dpa(Pa) = 43.302 Dpf(Pa) = 475.196 Fiquad = 51.127

I = 21 Z1 = 4.6200 x = .567629 Tw = 25.1957 qtot = 4752.945 dpfreon(bar) = .0774 dpwater(bar) = .0902

HF = 2201.143 Hc = 1721.650 HNcb = 579.493 Xtt = .124 RESIST = .010314

F = 11.1208 S = .9721 Alpha = .9439 Dpa(Pa) = 41.611 Dpf(Pa) = 495.960 Fiquad = 52.285

I = 22 Z1 = 4.9400 x = .580408 Tw = 24.9075 qtot = 4859.954 dpfreon(bar) = .0828 dpwater(bar) = .0924

HF = 2275.692 Hc = 1729.478 HNcb = 547.213 Xtt = .119 RESIST = .010314

F = 11.4532 S = .9731 Alpha = .9460 Dpa(Pa) = 39.925 Dpf(Pa) = 496.093 Fiquad = 53.275

I = 23 Z1 = 5.0500 x = .592425 Tw = 24.6364 qtot = 4960.571 dpfreon(bar) = .0882 dpwater(bar) = .0965

HF = 2250.738 Hc = 1733.954 HNcb = 516.784 Xtt = .115 RESIST = .010314

F = 11.7768 S = .9740 Alpha = .9480 Dpa(Pa) = 39.255 Dpf(Pa) = 535.910 Fiquad = 54.401

I = 24 Z1 = 5.2800 x = .603727 Tw = 24.3815 qtot = 5055.205 dpfreon(bar) = .0937 dpwater(bar) = .1009

HF = 2226.243 Hc = 1738.248 HNcb = 488.095 Xtt = .111 RESIST = .010314

F = 12.0916 S = .9748 Alpha = .9499 Dpa(Pa) = 38.613 Dpf(Pa) = 574.606 Fiquad = 55.367

I = 25 Z1 = 5.5000 x = .614359 Tw = 24.1416 qtot = 5144.237 dpfreon(bar) = .0993 dpwater(bar) = .1050

HF = 2202.554 Hc = 1741.513 HNcb = 461.041 Xtt = .107 RESIST = .010314

F = 12.3976 S = .9755 Alpha = .9515 Dpa(Pa) = 38.005 Dpf(Pa) = 523.053 Fiquad = 56.276

HTOT = .2031 QSUM = 5144.2340 TOTAL LENGTH = 5.5000

Total freon pressure drop (bar) = .9933E-01 Total water pressure drop (bar) = .1050E+00

***** TPEHX COMPLETED OK *****

APPENDIX (F)

PUBLICATIONS

The list below are papers and technical notes published during the period of study.

(1) NIKANPOUR D., Two-Phase Flow Technology Development Model Definition. British Aerospace Technical Note TN 4956 ISSUE A & 1, Stevenage Aug. 1986 & June 1987.

(2) NIKANPOUR D., KREEB H., SILL K., Orbital Replaceable Unit-Cold Plate Dry Thermal Interface Concept and Test Measurements, International SYMP. on Thermal Problems in Space-Based Systems,ASME, Boston, USA,Dec 13-18,1987.

(3) NIKANPOUR D., PETRUZZIELLO M., Cryogenic Fluid Sink Device for Thermal Control of a Spaceplane during Ascent and Re-entry Phases, 3rd. European Symposium on Space Thermal Control & Life Support Systems, Noordwijk, The Netherlands, Oct.3-6, 1988.

(4) BARBAGALLO G., NIKANPOUR D., A helically Coiled Evaporative Heat Exchanger for Space-Based Heat Transport Systems. Int. Heat Pipe Conf., Minsk, USSR, May 21-25 1990.

(5) NIKANPOUR D., CHAMPOLINI F., STANGERUP P., Thermo-Hydraulic Simulation and Regulation of Active Thermal Control Systems using ESACAP Software. 4th. European Symp. on Space Environment Control Systems. Florence, Italy, Oct.1991.